PETROPHYSICS – LOG ANALYSIS

AQUISITION AND INTERPRETATION OF WIRELINE LOGS

Dr. Peter Fitch

Department of Earth Science and Engineering

Imperial College London, SW7 2AZ

(p.fitch@imperial.ac.uk)

CONTENTS

INTRODUCTION

Petrophysics is the study of rock properties and their interactions with fluids, such as gas, liquid hydrocarbon, and aqueous solutions (Tiab & Donaldson, 1996). The main goal of petrophysical analysis is to gain an understanding of the volume and distribution of hydrocarbon and water within a subsurface reservoir. Fluids within a reservoir rock are usually contained in the space between or within grains or crystals; the *pore space*. Pore space is typically saturated by water at the time of deposition or formation of the reservoir rock. Hydrocarbons can be produced as organic-rich material is buried and heated under pressure in the subsurface. As hydrocarbons have a lighter density than water, oil and gas will migrate upwards through the subsurface until they reach a barrier that prevents further movement, for example a mudstone or shale. Pore space in the upper section of a reservoir will typically be filled with gas (light hydrocarbon), pores in the mid section will be dominated by oil, and the lower section will comprise only water. In oil and gas-rich sections of a reservoir water can fill up to 30 % of the pore space, trapped in small pores, along grain boundaries or within the chemical structure of minerals (such as clays). The contact between water and oil, or oil and gas, zones are not the sharp changes in fluid type traditionally depicted on cross-sections and maps. The transition from one fluid zone to another can occur over centimetre, metres, or 10s to 100s of metres depending on rock properties such as pore size, capillary pressures, and wettability. Consequently measurements of reservoir rock properties will be a result of rock or grain chemistry, mineralogy, facies, lithology, fluid type(s) and any unfilled pores (or voids) in the sample volume. Petrophysical analysis uses a variety of empirical and more complex statistical relationships to analyse and interpret the volume and distribution of pore space and the reservoir fluids which occupy this space.

The volume of hydrocarbon initially in place (HCIIP, or stock tank oil initially in place - STOIIP) in a reservoir is a function of the gross rock volume (GRV), volume of pore space (Ø), the proportion of reservoir to non-reservoir rock (net-to-gross, NTG), the proportion of pore space occupied by hydrocarbon (saturation, 1-Sw), and the formation volume factor (FVF), as show in Equation 1 (Tiab & Donaldson, 1996).

$$HCIIP = GRV \times Ø \times (NTG) \times (1-S_w) / FVF \qquad \text{(Equation 1)}$$

Estimates of gross rock volume can be derived from seismic data, while pore space, net-to-gross, and saturation can be measured from core samples or estimated from wireline log measurements.

This module focusses on the interpretation of openhole wireline log measurements. Before describing the various tools and interpretation techniques used in standard wireline log analysis, we will review key background terminology.

PETROPHYSICAL "ROCK"

In petrophysical analysis a reservoir rock is divided into three key components, (1) the rock matrix, (2) clay or shale, and (3) pore space filled with fluid (Figure 1).

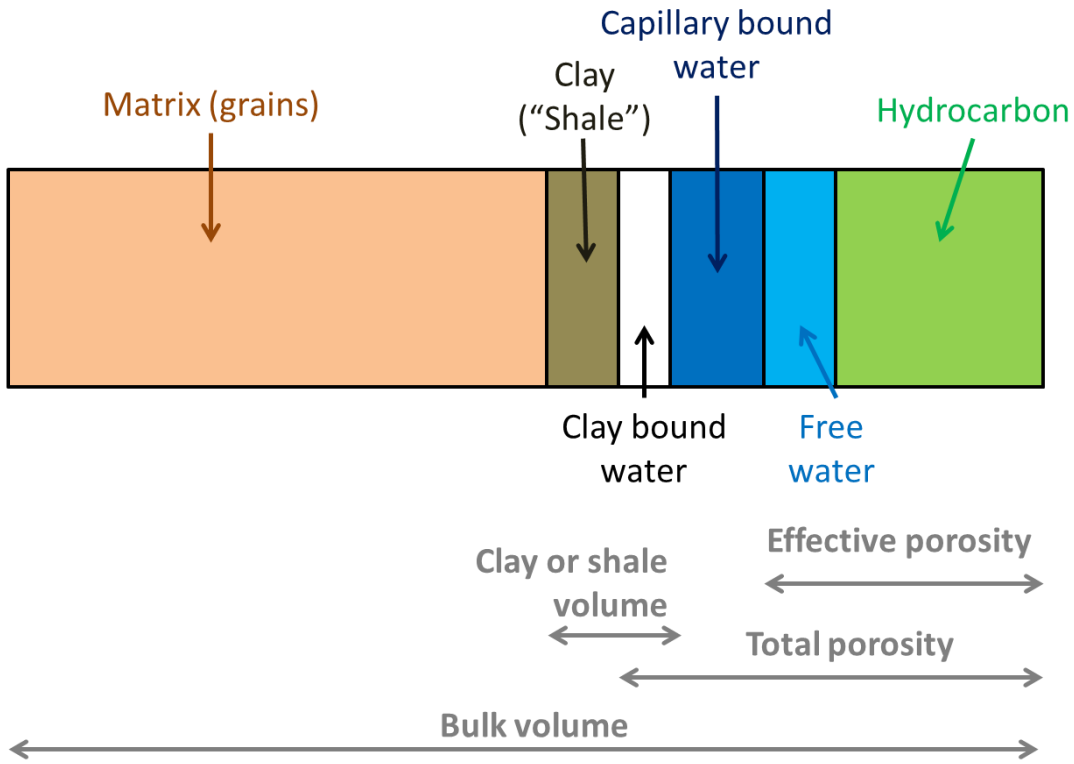

Figure 1. Schematic representation of the constituents of a petrophysics "rock".

In petrophysics, the solid material of a reservoir rock can be either matrix or clay ("shale"). *Matrix* refers to the grains or crystals of a rock, for example a sandstone might be composed of only quartz grains, while a limestone can be composed of calcite grains. The grain shape, size and packing will dictate the space between grains, the pore space. Clays (or "*shale*") can refer to (a) fine-grained detrital material with diameter less than 4 microns (clay, silt or mud sized grains), and/or (b) a loosely defined group of hydrous silicate minerals (e.g., kaolinite, smectite and illite). Clays can fill the gaps between the matrix, decreasing the pore space. Clay minerals contain fluids (electrolytes) within their mineral structure.

POROSITY (Ø)

Porosity is the total fractional volume of pore space per unit volume of a rock, or formation (Equation 2).

$$\emptyset = \frac{volume\ pore\ space}{total\ volume\ of\ rock} \qquad \text{(Equation 2)}$$

Porosity can range from 0 to 1 (0 to 100 % - *porosity can be stated as a percentage, but the fractional form is always used in calculations*). A dense uniform material, such as glass or evaporites, can have zero porosity. Well-consolidated sandstones can have a porosity of 0.1 – 0.2 (10 – 20 %), and unconsolidated sands may have a porosity greater than 0.3 (30 %). The maximum theoretical porosity, for material made of perfectly spherical beads, is 0.47 (47 %). A shale can have porosity greater than 0.4 (40 %), however individual pores are so small that they do not allow fluid movement.

Porosity is controlled by grain (or crystal) size, shape and packing. If the pore space exists only between matrix material (e.g., sand grains) the porosity is called *intergranular porosity*. If pore space exists within the matrix material then the porosity is called intragranular porosity. *Primary porosity* was formed at time of sediment deposition, or formation. If porosity has been created post-deposition by processes such as diagenesis (e.g., dissolution) or tectonics (e.g., fracturing) then the porosity is referred to as *secondary porosity*.

Total porosity ($Ø_t$) refers to the total pore space, whether it is connected or isolated. Total porosity includes interstitial water within clay grains (clay bound water, CBW). Changes in grain size and the presence of clay minerals may result in small or occluded pore throats, so that the total pore space is not interconnected. *Effective porosity* ($Ø_e$) is the fractional volume of connected pore space, excluding clay and capillary bound water (water contained in small, tight pore space which is unable to move). It is the effective porosity which contains moveable, or "free", fluids.

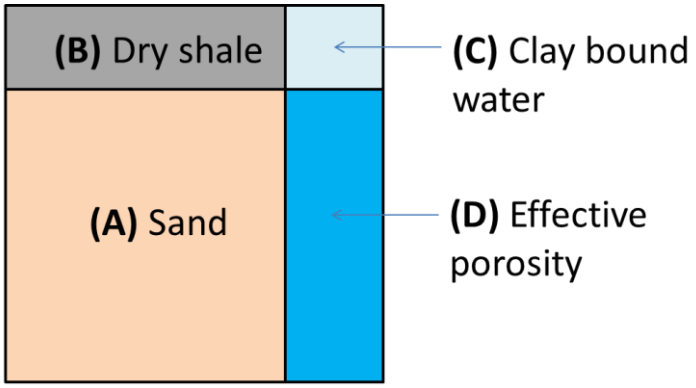

$$\emptyset_t = \frac{D + C}{A + B + C + D} \qquad \emptyset_e = \frac{D}{A + B + C + D}$$

Figure 2. Sketch illustrating the proportions of a reservoir rock in terms of total porosity ($Ø_t$) and effective porosity ($Ø_e$).

PERMEABILITY

Permeability (k) is the ease with which a fluid moves through a porous material. As such, permeability is related to the effective porosity. There is a general relationship between increasing porosity and permeability, but this is not always the case. Grain size is a key control on permeability. Typically smaller grain size results in smaller pores and therefore a lower permeability. Equation 3 illustrates that permeability is a complex parameter with many controls, such as flow rate and fluid viscosity. If more than one fluid type is present, the permeability of the rock to a given fluid will be reduced, referred to as the effective permeability (k_e).

$$Q = \frac{kA\Delta P}{\mu L} \qquad \text{(Equation 3)}$$

Where: Q – volumetric flow rate, A – cross sectional area, ΔP/L – pressure drop, and μ – viscosity of the fluid.

The darcy (D) is the measurement unit for permeability. The darcy is typically too large a value for the permeability of most common reservoirs. Permeability is therefore more typically expressed in *millidarcys (mD)*, or in the case of tight rocks microdarcys (μD). In general, a rock with permeability greater the 1 mD is considered a reservoir rock – 10 to 100 mD are high, and 100 to 1000 mD are very high permeability values.

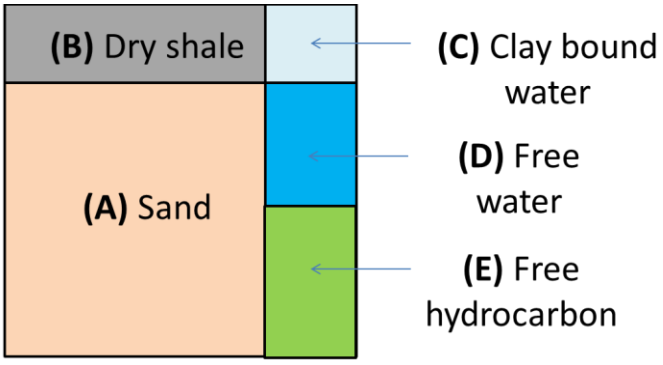

$$S_w = \frac{D + C}{C + D + E} \qquad S_h = \frac{E}{C + D + E}$$

Figure 3. Sketch illustrating the proportions of a rock in terms of water saturation (S_w) and hydrocarbon saturation (S_h).

SATURATION

The saturation of a rock refers to the fraction of its pore space that is occupied by a particular fluid. *Water saturation* (S_w) is the fraction of the porosity that contains water, if the reservoir only contains

water then water saturation is 1 (100 %). Hydrocarbon, oil or gas, saturation (S_h, S_o, or S_g, respectively) is the fraction of the porosity containing hydrocarbon. As mentioned above, a small volume of water will be present as clay or capillary bound water, even in oil and gas-rich sections of a reservoir. Therefore, water saturation will rarely, if ever, be zero. The minimum S_w value is referred to as the irreducible water saturation (S_{wi}).

INVASION

To prevent the risk of "blow outs" caused by over pressured reservoir formation, the hydrostatic pressure of the column of drilling mud (in the upper section of the borehole) is traditionally set to be greater than the pore pressure of the formations. This means that under normal circumstances the pressure difference between the mud column and formation forces drilling mud into porous and permeable reservoir rocks (Figure 4). This process is referred to as *invasion*.

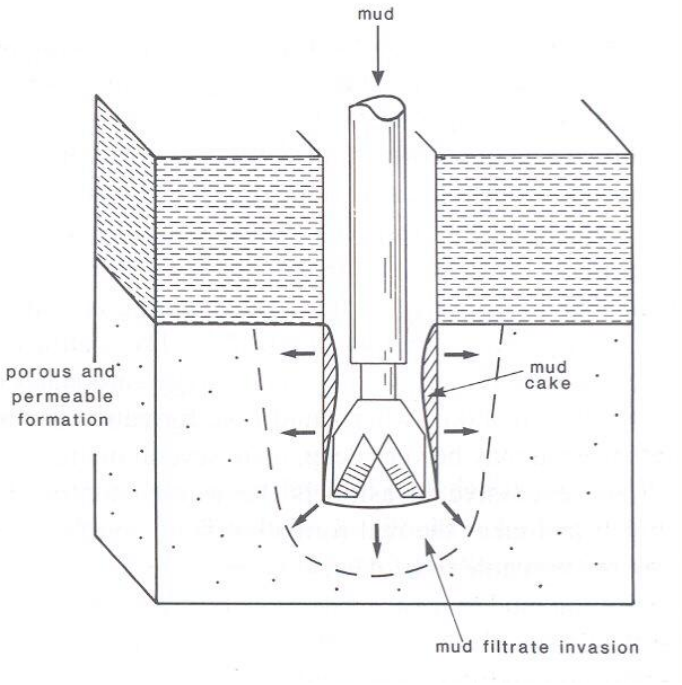

Figure 4. Schematic representation of the invasion of drilling mud into a porous and permeable formation (Rider, 1996).

As drilling mud is forced into the formation the porous rock acts as a filter, separating the mud into solid and liquid components. The liquid components of the drilling mud are able to move further into the formation (forming "*mud filtrate*"), while the solid components form a deposit on the borehole wall known as "*mudcake*". Over time the mudcake forms a thick skin between the formation and the borehole. Mudcake typically has a very low permeability that, therefore, reduces the rate of further mud filtrate invasion into the formation, until flow of mud filtrate into the formation is effectively prevented (Figure 5, left).

In the area closest to the borehole wall most of the original formation fluids have been displaced, or flushed, by the mud filtrate. This is the *flushed zone* (Figure 5, right). Typically the formation in the flushed zone will only contain mud filtrate, with no formation fluids. As we move further away from the borehole wall the mud filtrate has displaced progressively less of the formation fluids, resulting in a *transition zone* (Figure 5, right). The flushed and transitions zones may be referred to as the *invaded zone*. The extent or diameter of the invaded zone depends on the type of drilling mud, the pressure differential, the porosity and permeability of the formation, and the time since drilling.

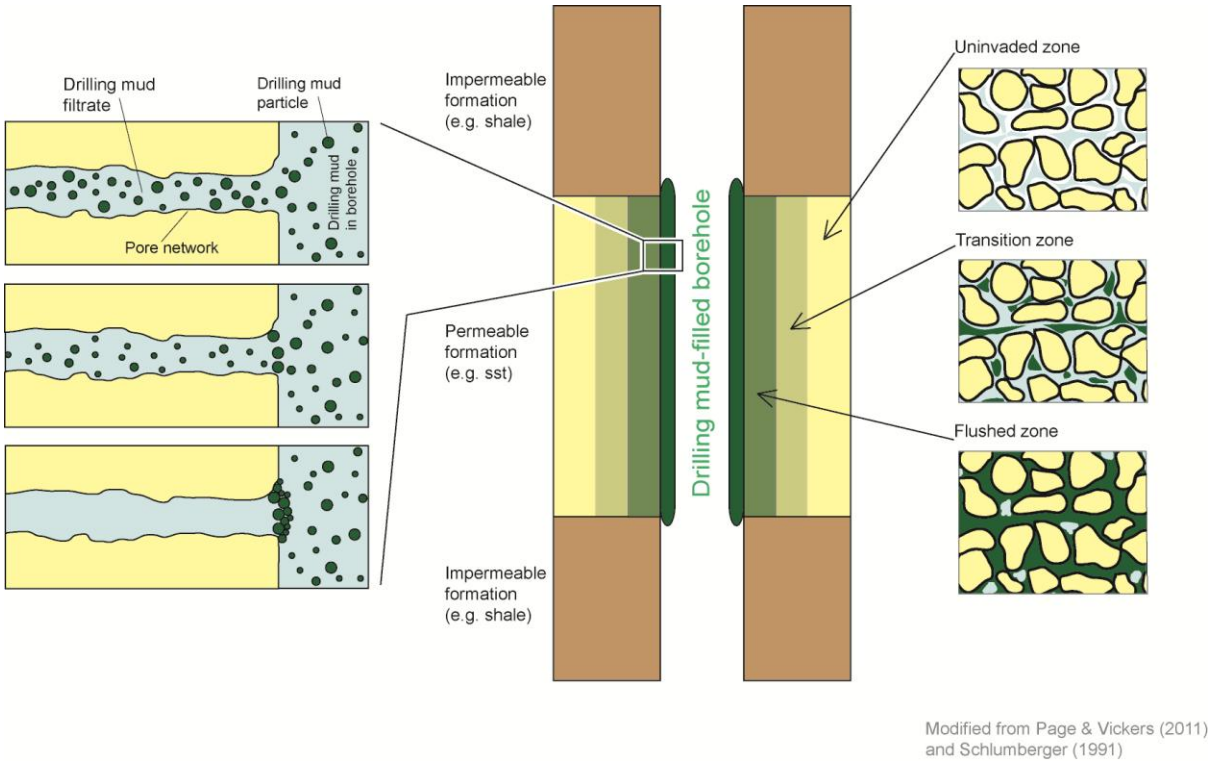

Figure 5. Schematic illustration of the invasion and the development of a mudcake (Modified from Schlumberger, 1991, and Page & Vickers, 2011).

Unless the formation is particularly tight or of low permeability (e.g., a mudstone or shale), the same volume of mud filtrate will invade the formation in a given time period regardless of porosity or permeability. Therefore, in a highly porous and permeable formation the depth of invasion will be small as there is more space to accommodate a set volume of filtrate, leading to rapid formation of a mudcake. Whereas in a less porous and permeable formation the same volume of fluid moves further into the formation before a thick enough mudcake has developed to stop invasion (e.g., Figure 6).

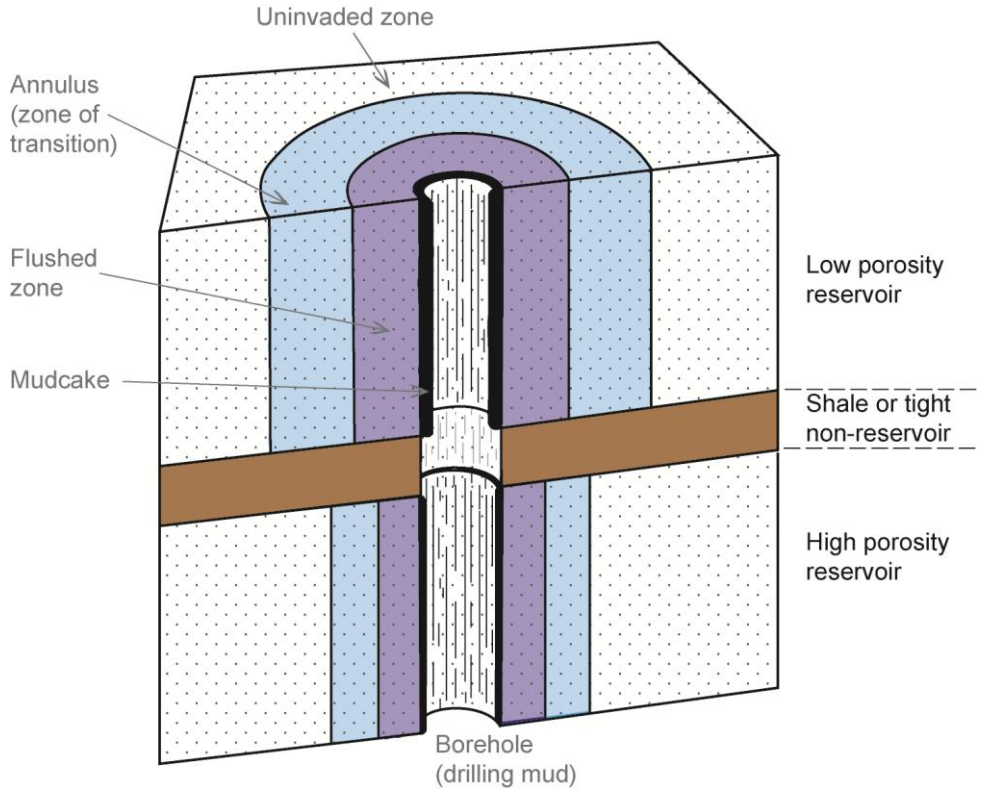

Figure 6. Schematic representation of the depth of invasion into a low and high porosity formation (Modified from Rider, 1996).

WELL LOGS

A well log is the graphical representation of a continuous geophysical measurement against depth down a borehole. The first well log was produced by Henri Doll in 1927 to show variations in electrical resistivity from a borehole in Pechelbronn oil field, north-eastern France (Figure 7). The measurement instrument was lowered down a borehole and stopped periodically to allow measurements to be made. Calculations of electrical resistivity were plotted by hand on a graph. In modern times, a variety of tools and methods of acquisition are used to generate a suite of well log data.

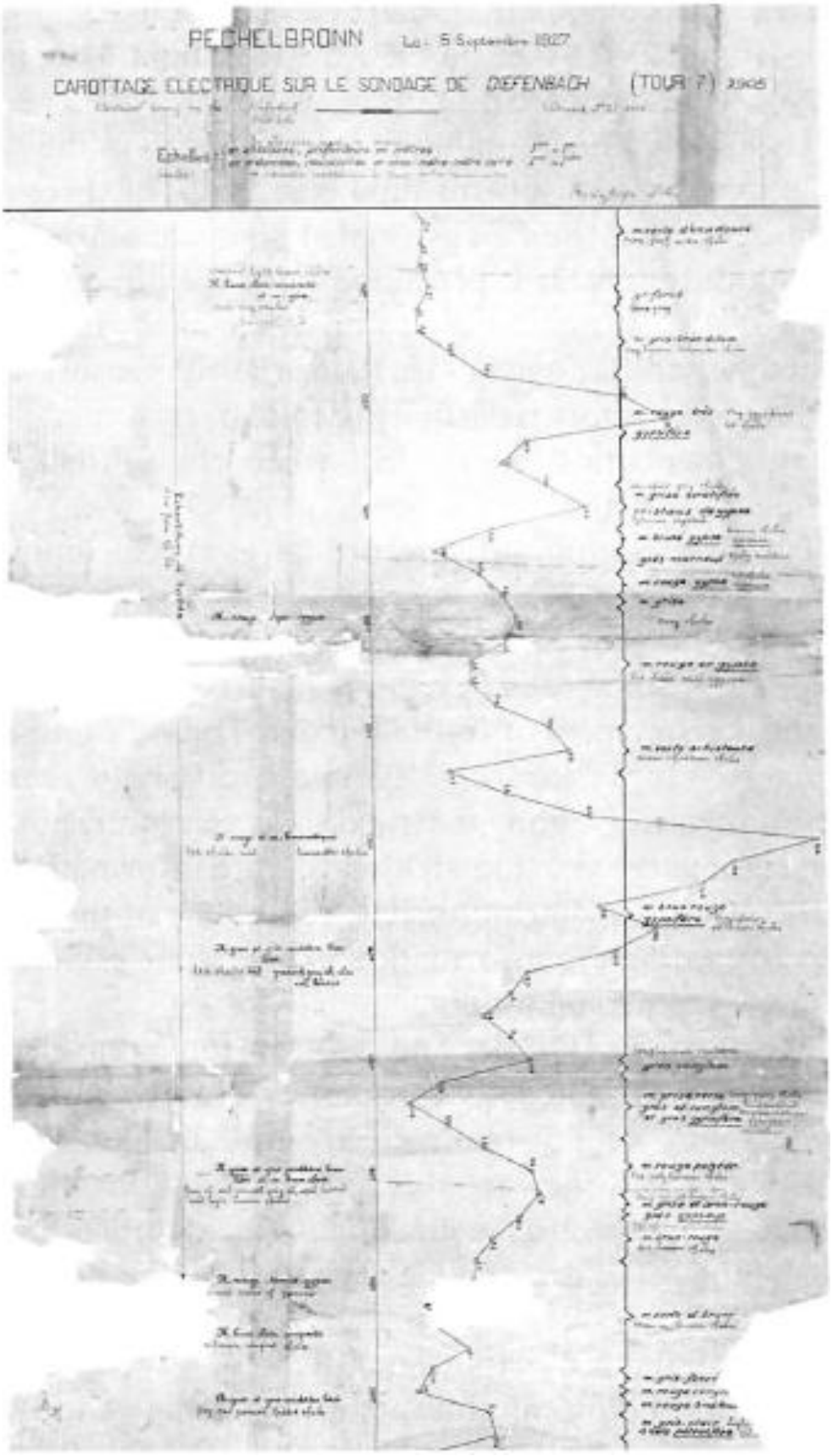

Figure 7. The first well log plot by Henri Doll in 1927 (Schlumberger, 1991).

DATA ACQUISITION

1) Wireline logging

Measurement instruments ("downhole tools", e.g., Figure 8) are lowered down the borehole on a cable which supplies power, and carries transmits signals from the tool to computational equipment on the surface.

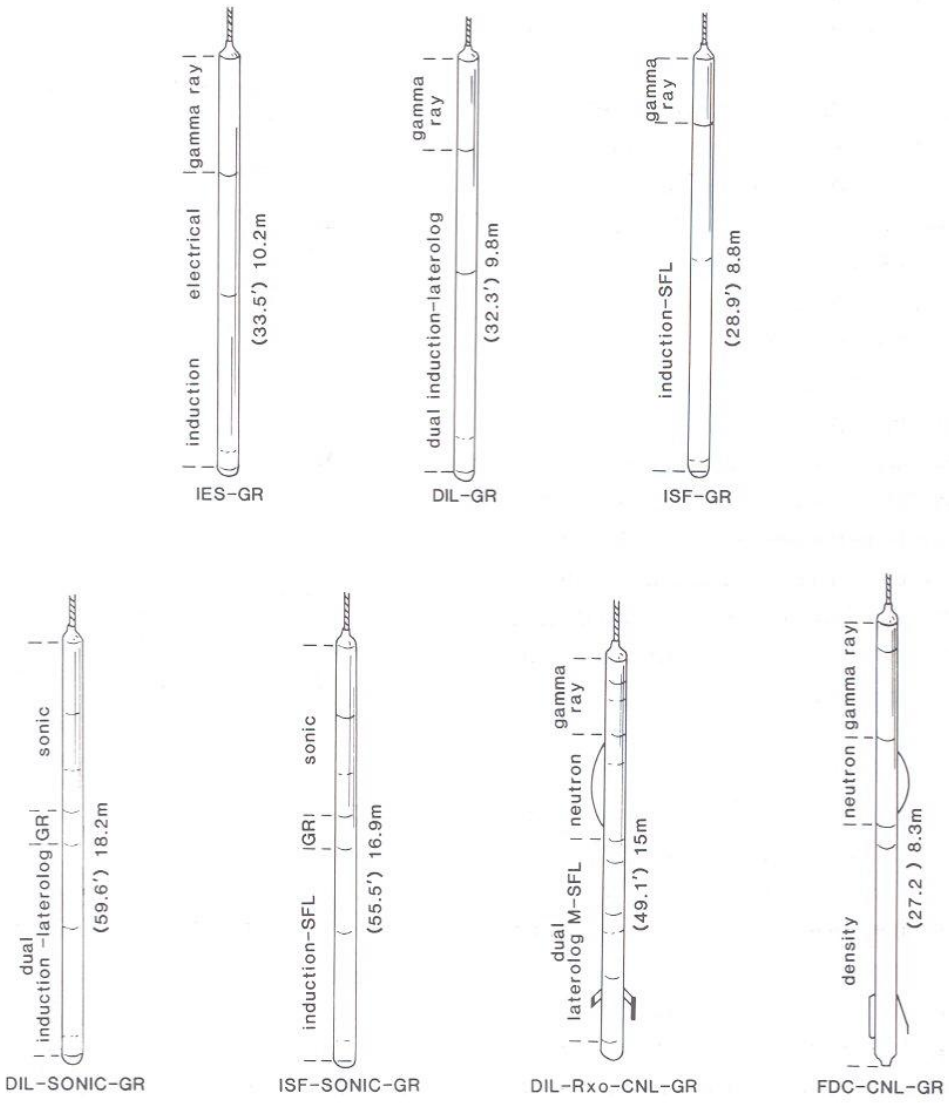

Figure 8. Typical combination of logging tools. Lengths as shown, tool diameter *c.* 3 inches (Rider, 1996).

A winch pulls the measurement instruments to the surface, providing a continuous record of measured properties through the borehole. Traditional wireline measurements are taken every 15 cm (6 inches), at a logging speed of 300 to 1800 m/hour (1000 – 6000 ft/hour). To save time and expense, more than one measurement instrument will typically be run at a time, connecting to form a tool string. Logging

speed varies for each measurement device, and is usual set by the maximum speed of the "slowest" tool. Wireline logs can be acquired in *open-hole* (the reservoir formation rock forms the wall of the borehole), or in *cased-hole* where a tube of metal casing lines the borehole. This course focusses on the interpretation of open-hole wireline logs.

Where horizontal, or deviated, wells are drilled the wireline tool string will not simply "fall" down the borehole under its own weight. Instead, the tool must be pushed down the deviated hole before being pulled back to the surface in the traditional way. The tool string can be pushed by *drillpipe conveyed logging* or *coiled tubing* techniques (Figure 9).

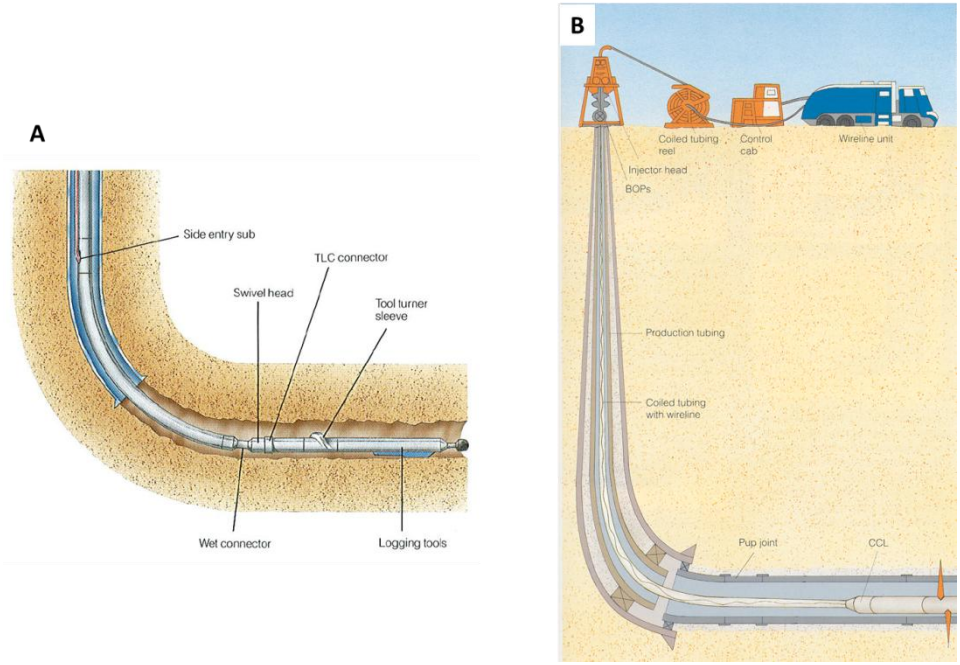

Figure 9. Illustration of (A) drillpipe conveyed logging, and (B) coiled tubing conveyed tool in a horizontal well (*after Schlumberger*).

Wireline logs can be grouped into four main classes;

a) Passive measurements – natural gamma radiation, spontaneous potential

b) Porosity measurements – density, neutron porosity, and sonic or acoustic

c) Resistivity measurements – conventional, focussed or induction

d) "Advanced" measurements – borehole image logs, nuclear magnetic resonance, dielectrics…

2) Measurements While Drilling (MWD)

Measurements While Drilling (MWD) are drilling measurements acquired during the borehole drilling process by a nonmagnetic collar located near the drill bit. MWD measurements include the depth, azimuth, inclination and tool facing direction – giving an indication of the borehole deviation from vertical. MWD measurement are typically supplemented by drilling measurements of drilling depth, true vertical depth and the rate of penetration of the drill bit. MWD measurements may also include basic, low resolution measurements of electrical resistivity and natural gamma radiation.

3) Logging While Drilling (LWD)

Logging While Drilling (LWD) measurements are acquired at the same time as drilling of the borehole, in comparison to wireline measurements which are acquired after drilling has been completed. LWD tools consist of a range of measurement devices, directly following the drill bit in specialised drill collars (reinforced drill string). Logging sensors continually measure parameters during drilling and transmit signals back to the surface in real-time, or can be stored in memory chips onboard the tool for collection once the tool has returned to the surface. LWD measurements are logged directly after drilling, in the order of minutes or hours (depending upon the drilling rate). A suite of log measurements, comparable to that of wireline, is provided by service companies, and are generally comparable in accuracy to wireline counterparts.

Wireline (Open hole)	***LWD (logging-while-drilling)***
Full range of measurements	Limited / full range
Repeat runs	One chance
Good spatial resolution	Noise
No azimuthal data	Utilises rotation – azimuthal information
Core possible	*Core?*
Invasion effects	Data transmission rates poor
Good for near vertical good quality holes	Good for inclined holes
	Geosteering / Directional Drilling

Table 1. Comparison of wireline and LWD measurements.

LWD tools are of great use in deviated and horizontal drilling, avoiding the need for additional drillpipe conveyed and coiled tubing, while also providing the opportunity of acquiring measurements of the formation at times of minimal invasion. Other benefits include reduced rig time costs, and real

time data to allow optimised drilling operations. Additional comparison of wireline and LWD measurements are provided in Table 1.

PRESENTATION OF LOGGING DATA

Well logs are traditionally presented as simple graphs, with the measured property on the x-axis and depth on the y-axis. In the petroleum industry, the standard suite of log data is typically reported on an American Petroleum Institute (API) grid that is divided into three graphs (or tracks) with a narrow column recording depth (e.g., Figure 10).

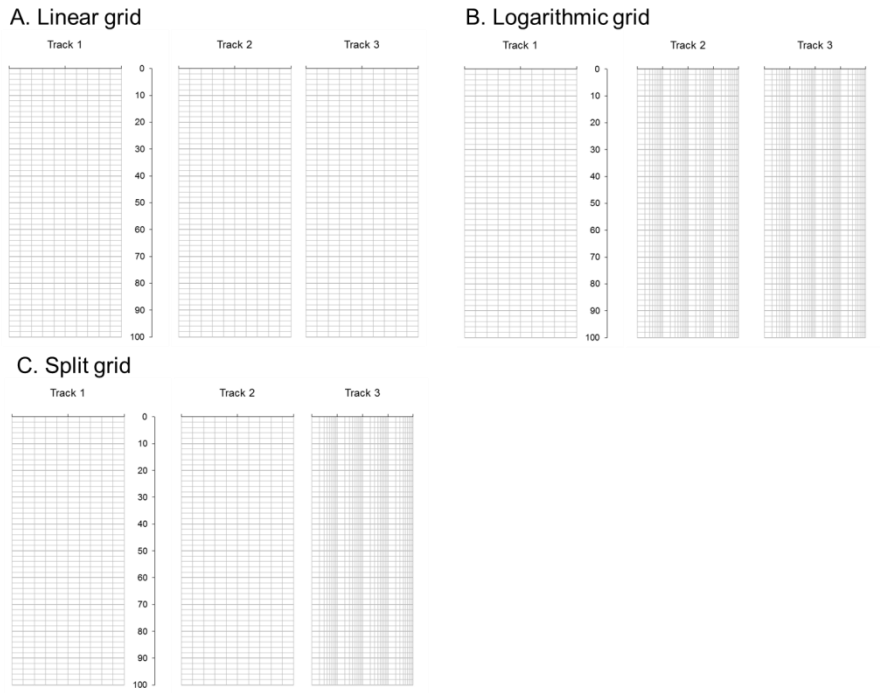

Figure 10. Illustration of the traditional American Petroleum Institute grids for well log presentation.

Each of the tracks will have a specific scale division, depending on the measurement being presented, for example the gamma ray track may exist from 0 to 200 API and bulk density may exist from 1.95 to 2.95 g/cm^3 on a linear grid scale (from left to right). Neutron porosity is typically displayed decreasing from left to right (e.g., from 0.45 to -0.15 p.u.) Measurements that record large variations in the magnitude of values, such as resistivity, are traditionally displayed on a logarithmic scale from 0.2 to 2000 ohm.m. When first looking at a log presentation it is essential that you check the measurement displayed on each track, and the scales used to ensure that the log value is read correctly.

Depending on the vintage of the well log dataset you may be presented with a range from hard copies acquired at the time of drilling, to full digital recording which can be displayed as simple text files, in computer software packages, or in high end log interpretation software packages provided by major

service, operator and consulting companies. These software packages provide a fantastic tool for time efficient, advanced multi-well analysis, and allow integration with other subsurface datasets (e.g., seismic sections). However, all experience petrophysical log analysts are competent in completing a detail analysis and interpretation by hand – important for quality control, and ensuring we understand the techniques used.

OBJECTIVES OF WIRELINE LOG INTERPRETATION

1. QUALITATIVE INTERPRETATION

A "quick look" visual inspection of the log data

- Porous and permeable beds
- Fluid contacts
- Correlation – between individual wells, and to seismic sections
- General facies analysis – trends, grain size profiles, key geological environments…

2. QUANTITATIVE INTERPRETATION

Estimation of values for key reservoir properties, input for calculation of STOIIP and its uncertainties.

- Shale volume
- Porosity (and permeability)
- Water and/or hydrocarbon saturation
    - In the uninvaded or flushed zones (S_w and S_{xo}, respectively)
    - Irreducible water or residual oil saturations
    - Moveable oil saturation index

1. CALIPER LOGS

One of the primary controls on the quality of wireline logging data is the quality of the borehole itself. Each logging tool will measure a specific volume of rock (related to the depth of investigation and tool resolution). We assume that the tool responds only to the reservoir rocks, with minor correction being made for the borehole. Therefore, anything that is not part of the reservoir will influence log measurements, and may bias our interpretations. Typical features which may impact on measurement quality are *bad hole conditions* such as shale sloughing and enlarged borehole (cave in or collapse), although mudcake and invasion will also influence logging measurements. Borehole *rugosity* provides an understanding of how the drilled borehole diameter differs from the size of the drill bit (is it "on gauge").

All wireline tools will have a mechanical *caliper* that measures variations in borehole size with depth. There are a range of calipers used on different wireline tools, by different service companies; ranging from simple one armed pads, to two / armed devices, and bowstrings (Figure 1.1).

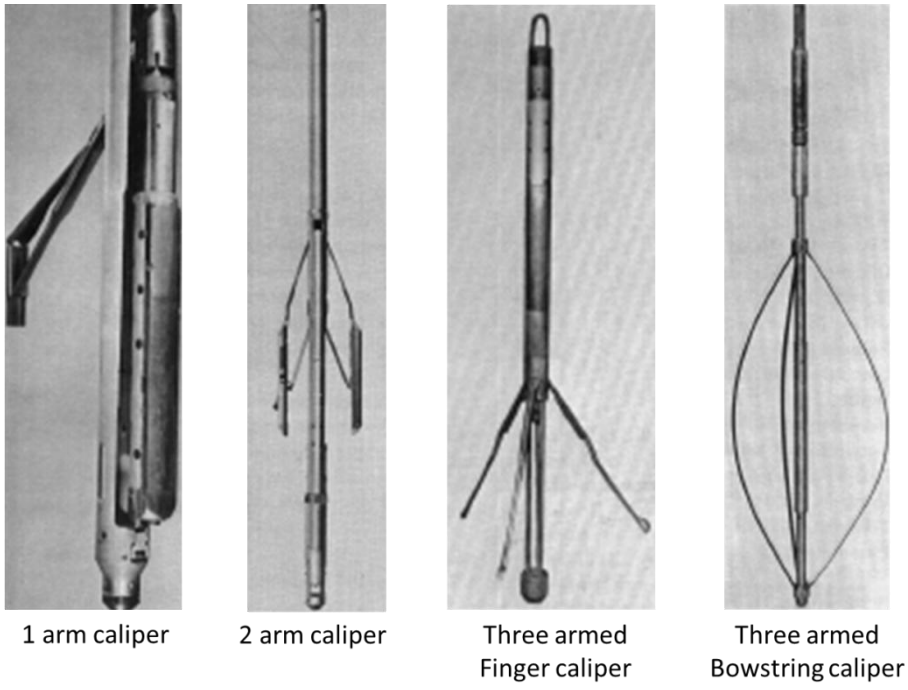

Figure 1.1. Examples of caliper devices (Modified from Hilchie, 1968).

The traditional caliper arm is articulated away from the wireline tool to push against the borehole wall. As the tool is pulled up the borehole the caliper arm will move closer toward the tool in that case of obstructions or a smaller borehole diameter, and will move away from the tool in enlarged borehole

sections. This movement generates an electrical output which is recorded and can be displayed with the other well log measurements.

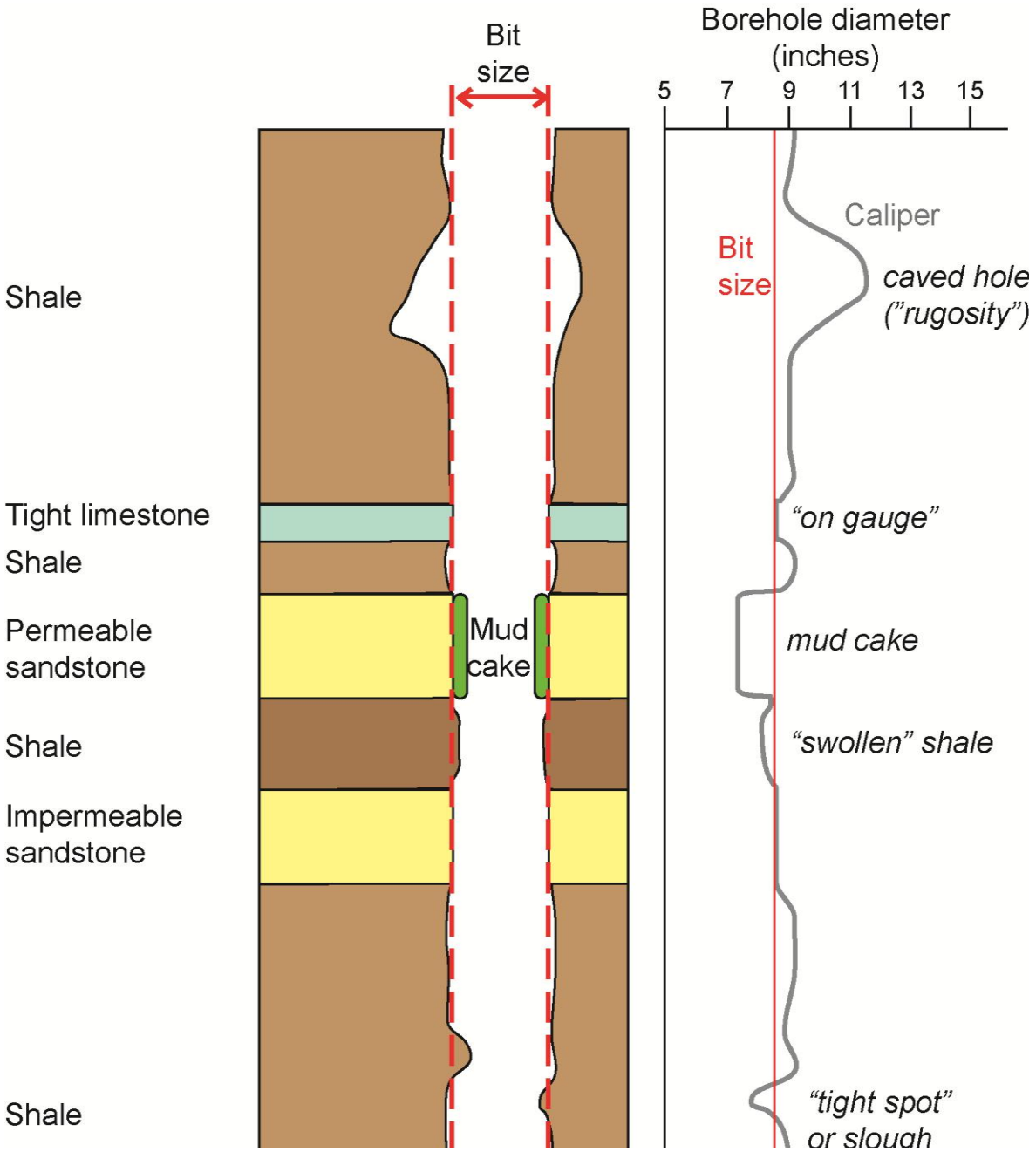

Figure 1.2. Schematic illustration of how the caliper log responds to borehole diameter (Modified from Rider, 1996).

If the caliper is on gauge then the borehole diameter is comparable to the size of the drill bit. This is the ideal situation, and is common in well consolidate, and low permeability formations. The caliper log may show the borehole diameter is larger than bit size indicating cave in in weak unconsolidated sands and brittle shale (Figure 1.2), or dissolved salt carbonate formations by fresh drilling fluids. If

the caliper shows a smaller borehole diameter than the bit size this could be the result of pronounced mudcake development on highly porous and permeable formations, or of hole sloughing caused by swollen shales (Figure 1.2). If not identified and corrected for, the presence of caving will lead to an underestimation of bulk density or an overestimation of sonic (acoustic) travel time – both of which might lead to an overestimation of formation porosity.

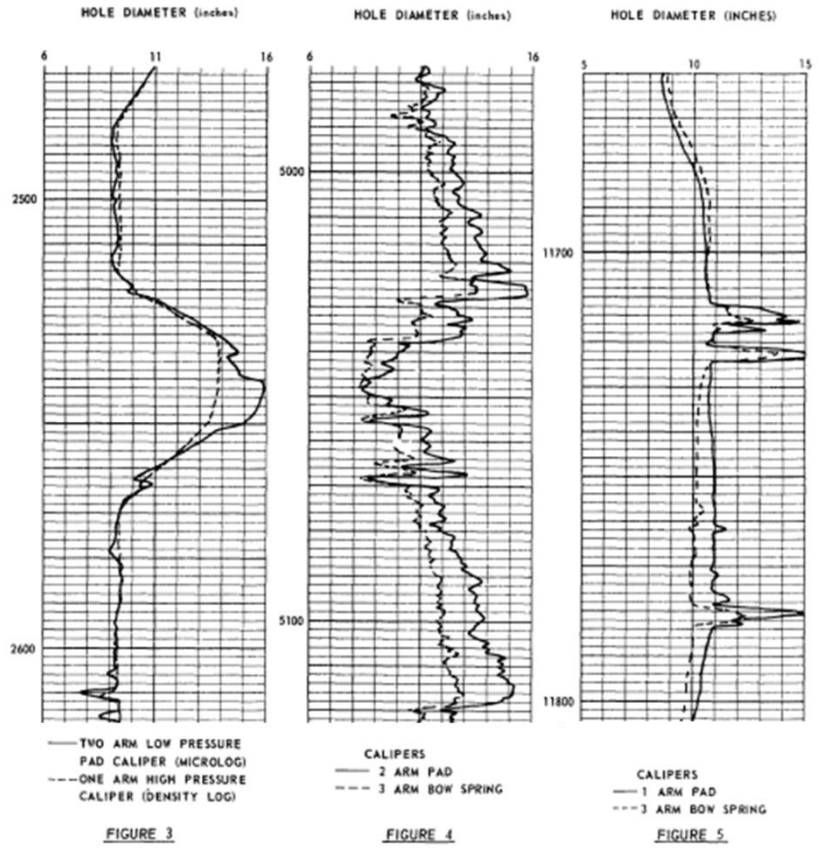

Figure 1.3. Examples of caliper measurements (Hilchie, 1968).

Calipers are also used to align the tool in the borehole. For example, in that case of measurement device with shallow depth of investigation (such as for micro-resistivity or density) a one arm caliper will push the tool against the borehole wall. Multi-arm or bowstring calipers can be used to centre the tool in the borehole in a similar way.

2. GAMMA RAY LOGS

One method by which unstable isotope can gain stability is by losing energy through the emission of gamma rays. Gamma rays (γ) are high energy photons that have no mass or charge, and are effectively they are electro-magnetic waves (similar to x-rays).

Most elements in reservoir are stable and do not emit natural radiation. The most common unstable elements are potassium (K^{40}), thorium (Th), and uranium (U). These elements continuously emit gamma rays, the number and energy of the gamma rays is specific to each individual element (Figure 2.1). The gamma rays are able to penetrate through several 10s cm of formation, depending on the density of the rock. As the gamma rays collide with other atoms they lose energy until the gamma ray is weak and absorbed by an atom (Compton-scattering), a denser the rock will lead to more collisions.

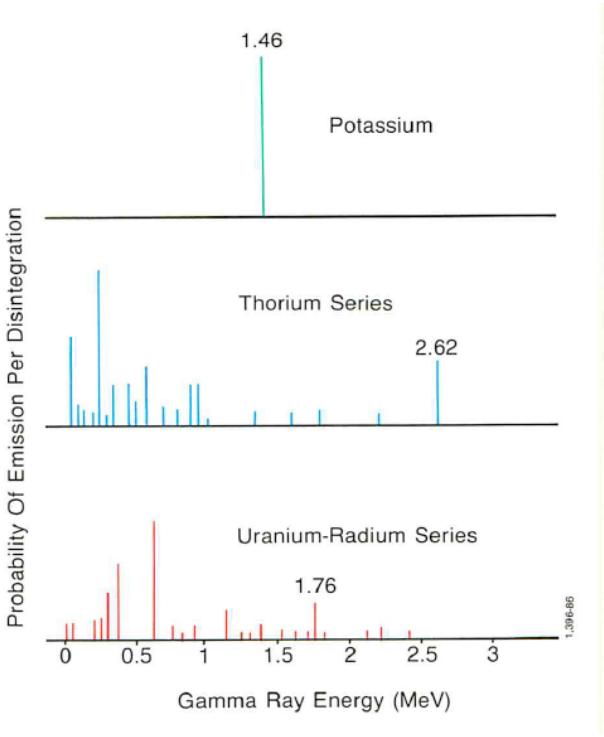

Figure 2.1. Gamma ray emission spectra for the radioactive elements potassium, thorium and uranium (Schlumberger, 1991).

There are two main types of gamma ray log, (1) Total Gamma Ray, GR, and (2) Natural Gamma Ray Spectroscopy, NGS.

1. TOTAL GAMMA RAY LOG (GR)

Gamma rays that move from the formation and into the borehole can be measured by a Gamma Ray (GR) logging tool, or sonde. The GR sonde uses a scintillation counter to measure gamma radiation from the surrounding rock, Geiger-Mueller counters have been used in the past. The detector

generates a discrete electrical pulse for each gamma ray detected, this is recorded over time. Gamma Ray log measurements are calibrated to API units, and arbitrary scale produced by the American Petroleum Institute. The total amount of gamma rays measured in the borehole is proportional to the concentration of radioactive elements in the formation.

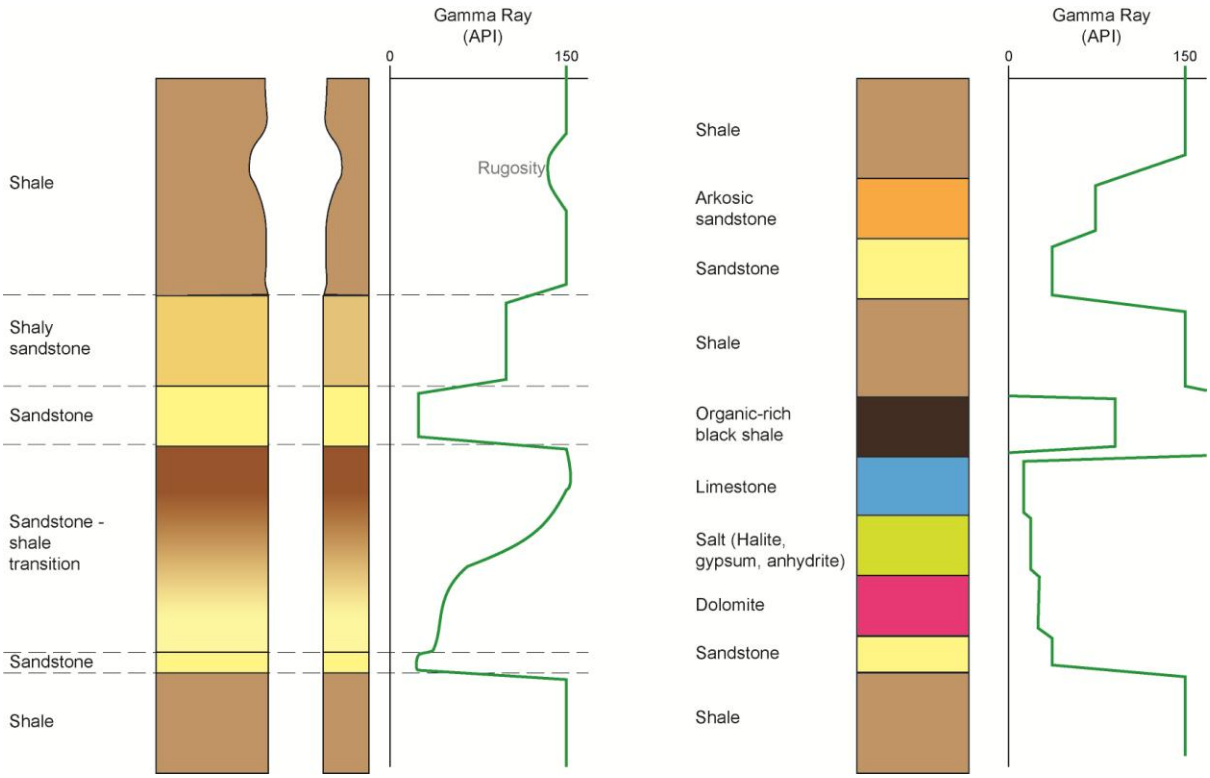

Figure 2.2. Schematic illustration of the Gamma Ray log in common reservoir rock types.

Shales, and mudstone, typically contain a larger concentration of radioactive elements than any other sedimentary rock. Consequently, shales will have high GR measurements of 80 API units, and above (Figure 2.2). A *clean* sandstone, limestone or dolomite will typically contain low, to negligible, concentration of radioactive elements. GR measurements of less than 30 API (5-30 API, Figure 2.2) are common for clean reservoir rock types. As the proportion of shale in a reservoir rock increases, i.e., it becomes more shaly, the measured GR values will increase from the clean to shale values (e.g., Figure 2.2, left). The presence of volcanic ash or potassium-rich feldspars can lead to an increase in the GR values of some arkosic sandstone (e.g., Figure 2.2, right).

PRESENTATION OF THE GAMMA RAY LOG

The Gamma Ray log is traditionally displayed in track one with the caliper, to the left of the log plot. Gamma Ray is plotted in API units, increasing from left to right (e.g., Figure 2.3). The scale will vary depending on the maximum radioactivity measured in the formation – typically from 0 – 150, 0 – 200, or 0 – 250.

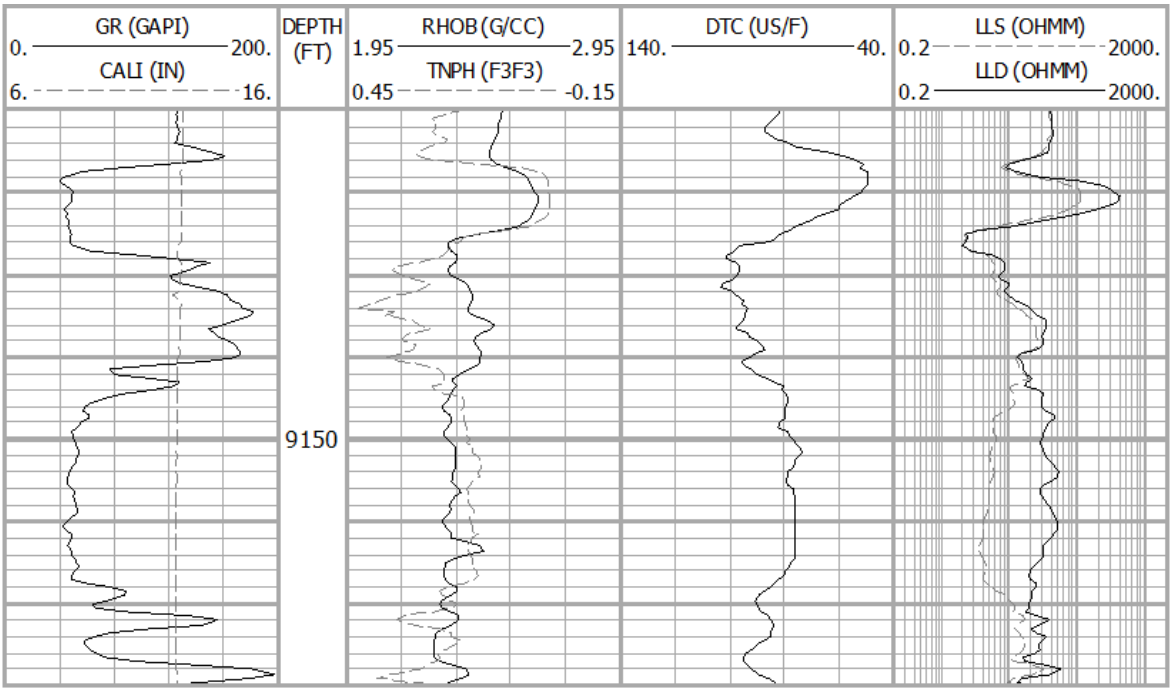

Figure 2.3. Example well log plot through a North Sea reservoir. Note Gamma Ray log displayed in track one (*CALI – caliper, GR – gamma ray, RHOB – bulk density, TNPH – neutron porosity, DTC – compressional sonic, LLS and LLD – shallow and deep resistivity*).

QUALITATIVE USE OF THE GAMMA RAY LOG.

- Location of shale beds ("impermeable beds")
- Well correlation
- Locating bed boundaries
- Identification of sharp and transitional contacts
- Identification of coals – exceptionally low GR values

QUANTITATIVE USE OF THE GAMMA RAY LOG.

Quantitative interpretation of the Gamma Ray log provides a simple method to estimate the percentage volume of shale in a reservoir formation. To do this the log section must include a thick shale bed, typically with high Gamma Ray values. We assume that the reservoir (sandstone, limestone, or dolomite) is clean or shaly, that is to say that any radioactive elements are only associated with the presence of shale – not arkosic sandstone or uranium enriched limestone.

Figure 2.4 illustrates the procedure for estimating the volume of shale from the GR log.

1) Record the Gamma Ray value for the zone or depth of interest (GR_{log})

2) Select a section of 100 % shale, typically the highest GR measurements. This gives the *shale line* and GR_{shale} value
3) Select a clean, shale free section (lowest GR measurement). This gives the *clean line* and the GR_{clean} value
4) Use the following equation to calculate the fractional volume of shale, this can be multiplied by 100 to gain a percentage shale volume

$$V_{sh} = \frac{(GR_{log} - GR_{clean})}{(GR_{shale} - GR_{clean})} \qquad \text{(Equation 2.1)}$$

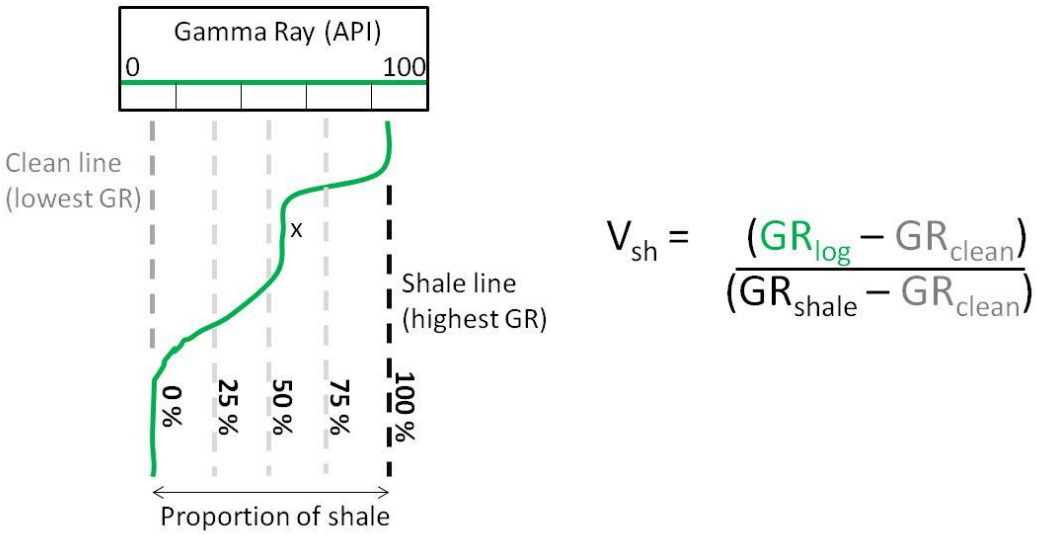

Depth	GR_{log}	GR_{clean}	GR_{shale}	V_{sh}
x	50	10	85	0.53 (53 %)

Figure 2.4. Schematic illustration of how shale volume can be estimated from the Gamma Ray log.

This simple linear relationship between GR measurements and shale volume is used widely in petrophysical analysis. Non-linear, empirical relationships may also be used – for example those provided by Larionov, Clavier, and Steiber. These non-linear relationships typically reduce the volume of shale estimated from the GR log. Shale volume will be discussed again in section 7, using the neutron-density method.

2. NATURAL GAMMA RAY SPECTROMETRY (NGS)

As with the Total Gamma Ray logging tool, the Natural Gamma Ray Spectrometry (NGS) tool measures natural radioactivity being emitted from the reservoir formation. NGS not only measured the number of gamma rays detected, it also measures the energy level of each individual gamma ray.

The NGS tool uses a sodium iodide scintillation detector to measure gamma ray levels and generates a smeared spectra of gamma ray energy levels (e.g., Figure 2.5). Each of the main radioactive elements emits gamma rays with a characteristic energy signature (Figure 2.1); Potassium (K^{40}) at 1.46 MeV, Thorium has a sequential decay series characterised by a peak at 2.62 MeV (decay of Ti^{208}), and Uranium also has a long sequential decay series characterised by a peak at 1.76 MeV (decay of Bi^{214}). The spectra of gamma ray energies generate by the NGS tool can therefore be used to determine the amounts of potassium, thorium, and uranium in the formation.

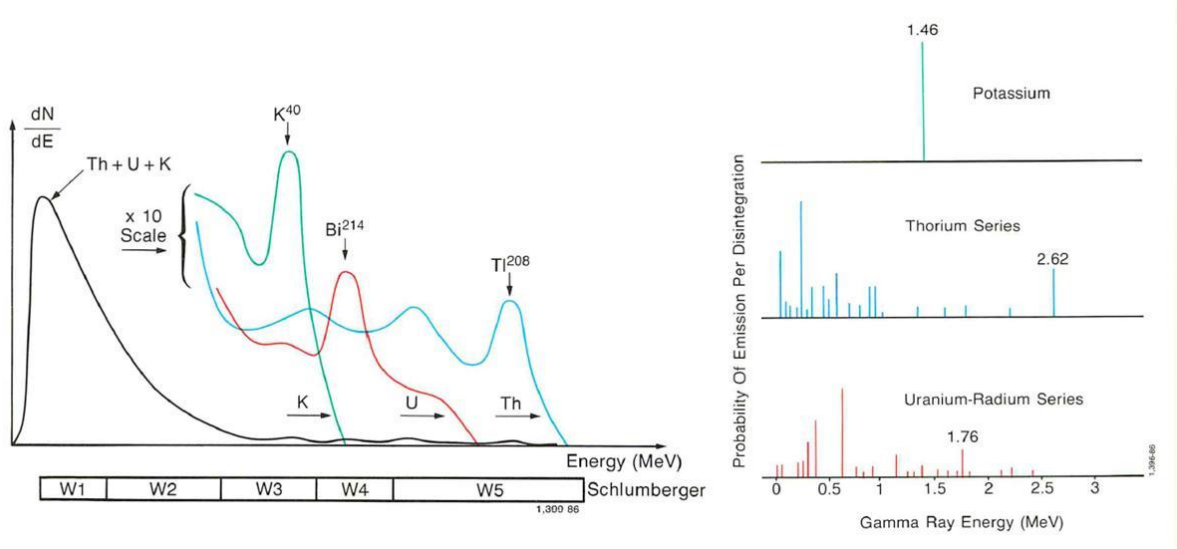

Figure 2.5. Example of a gamma ray emission spectra measured by the NGS tool. Note the smearing of the individual spectra for potassium, thorium and uranium (Schlumberger, 1991).

PRESENTATION OF THE NATURAL GAMMA RAY SPECTROMETRY LOG

Five logs (*curves*) are produced by the NGS tool; a standard total GR log in API units (SGR), the concentration of potassium in percent (POTA), thorium in parts per million (THOR), uranium in parts per million (URAN), and a computed gamma ray log (CGR). The computer gamma ray log is a sum of the gamma rays detected for thorium and potassium only, removing the effect of uranium. Figure 2.6 provides an example of the log presentation for NGS measurements, here the total gamma ray log (SGR) is shown to be dominated by high uranium content between 9600 – 9550ft.

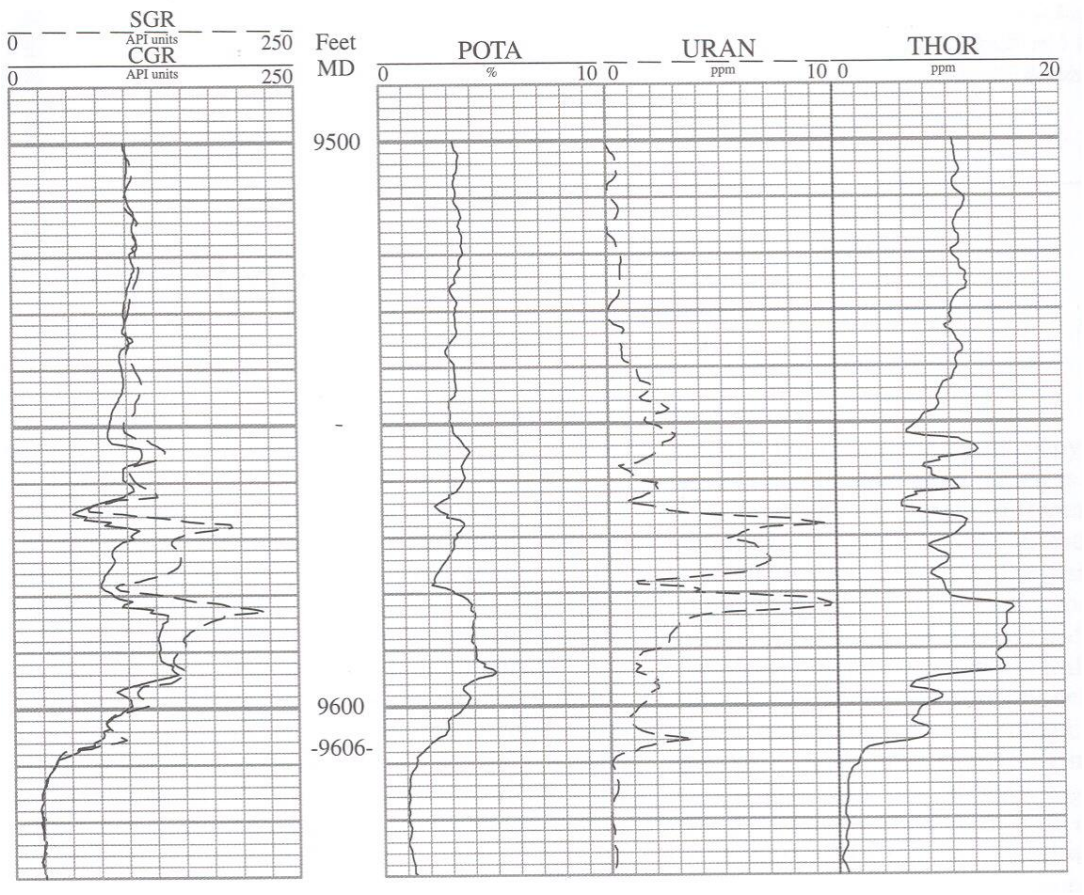

Figure 2.6. Example of a suite of NGS log data from the Lower Carboniferous Barnett Shale, West Texas. At 9606 ft there is a contact between shale and underlying clean limestone (Asquith & Krygowsky, 2004).

APPLICATION OF THE NATURAL GAMMA RAY SPECTROMETRY LOG

The main uses of the NGS log data are in identifying controls on the Gamma Ray log measurement, distinguishing between different clay minerals, and therefore calculating an improved value of shale volume.

Potassium occurs in micas and micaceous clay minerals (e.g. Illite), feldspar (e.g. Orthoclase), and less commonly in evaporates. *Thorium* is a stable element that rarely goes into solution, consequently it is generally transported and deposited with fine-grained clay and silt material (shales and mudstone), or heavy mineral deposits. Thorium is commonly associated with bauxites, and kaolinite. *Uranium* is typically linked with the presence of organic matter (black shales), and phosphates (e.g. Sylite and Langbeinite).

Clay mineral identification

The concentration of potassium and thorium can be used to identify the clay minerals present in a shale, mudstone, or shaly sandstone. A chart, such as Figure 2.7, can be used for this purpose.

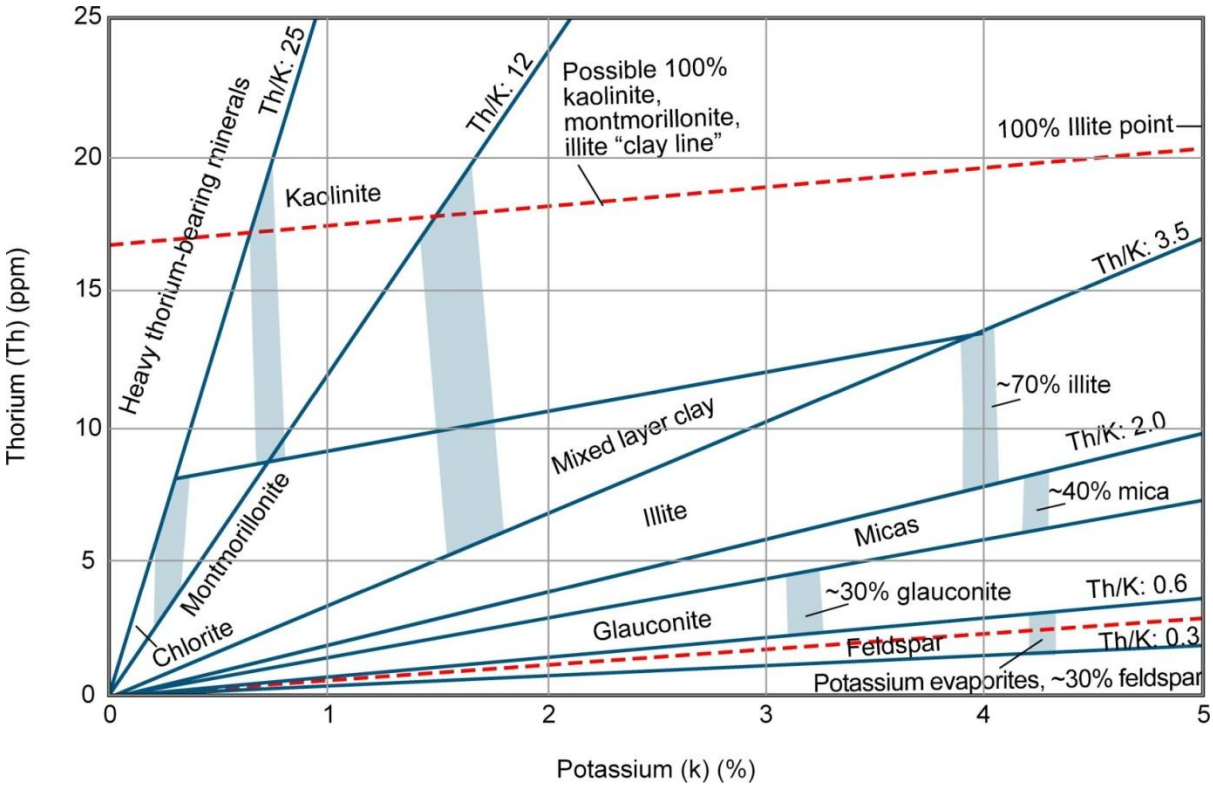

Figure 2.7. Clay mineral identification using the Natural Gamma Ray Spectrometry tool (Schlumberger, 2009).

Radioactivity in sandstones

A clean sandstone, composed only of quartz grains will typically show low GR values. However, the presence of a variety of additional detrital minerals can increase a sandstones radioactivity and the corresponding GR log measurements. The most common radioactive sandstones are those rich in orthoclase feldspar. Arkose sandstones contains more than 10 % feldspar (e.g. the Sherwood Sandstone of the Wytch Farm field). Arkose sandstones typically have a low Th/K ratio of less than 1 ppm/%. Clay bearing, micaceous, sandstones, graywackes and greensands will have high thorium content (Th/K ratios of 1 – 2.5 ppm/%, e.g. the mica sands of the North Sea). Heavy mineral bearing sandstone are often rich in thorium and uranium, resulting in high Th/K and U/K ratio greater than 20-25 ppm/%. Clearly it is important to identify the sandstones rich in feldspar, mica or heavy minerals as the use of GR as an indicator of shale volume is not suitable in such cases. In cases of feldspar-rich

sandstones, thorium content may be used as a shale volume indicator instead of the total gamma ray response.

Radioactivity in carbonates

Pure, clean, limestones and dolomites are typically not radioactive. This aids their identification from the GR log. However, there are some cases where radioactive elements are contained within intervals of carbonate rock types. Radioactive carbonate rocks are generally associated with the presence of uranium. Organic-rich mater may be deposited with carbonate material. As describe previously, organic matter is often linked with uranium enrichment. Uranium and organic-rich material may be concentrated in stylolites, for example in the Eocene Limestones of Tunisia. Thin layers of carbonate sediment associated with times of slow deposition, such as karst, palaeosols and maximum flood surfaces may also be enriched in uranium. Controls on this enrichment are unclear, but the uranium is often associated with phosphates. Diagenesis, particularly processes of dolomitisation, may also lead to uranium enrichment in carbonates.

3. SPONTANEOUS POTENTIAL

The Spontaneous Potential (SP) log measures the natural, or spontaneous, potential difference between a movable electrode in a borehole and a fixed surface electrode. The spontaneous potential is measured in millivolts (mV). Measurement of the SP log requires electrical continuity between the tool electrode and the formation; consequently the SP log cannot be recorded in boreholes filled with nonconductive muds. Equally, if the resistivity of the formation fluids and mud filtrates are the same then the SP log will appear featureless.

The existence of an SP current requires (1) A conductive borehole fluid, (2) a difference in salinity between the formation and borehole fluids, and (3) a porous and permeable bed or formation, surrounded by low porosity and impermeable formations (Figure 3.1). When two fluids of different salinities are in contact, the potential difference results in the movement of ions by electromotive forces (electrochemical and electrokinetic components), the movement of ions between the formation and borehole establishes an electric current which can be measured.

Electrochemical components of the SP (E_c)

Figure 3.1 provides a simple example where a permeable formation is overlain by a thick shale. Two fluids are present, mud filtrate and formation (interstitial) fluid – both of which only contain sodium chloride (NaCl). Both fluids are conductive, but the formation fluid has a higher salinity than the borehole fluid (and mud filtrate). The basis of the electrochemical component (E_c) of the SP is the diffusion of ions on a high to low concentration gradient, typically from the uninvaded zone to the borehole.

The clay structure and charges on individual layers means that shales are permeable to Na^+ cations, allowing them to move from the porous formation into the shale, but are impervious to Cl^- anions. The movement of cations (positively charged), from the high saline formation fluid to lower salinity borehole fluids, causes an electric current and the force causing the ions to move constitutes a potential across the shale-permeable formation interface. This is called the *membrane potential* (Figure 3.1). The red arrows in Figure 3.1 show the direction of the current reflecting movement of the cations through the shale.

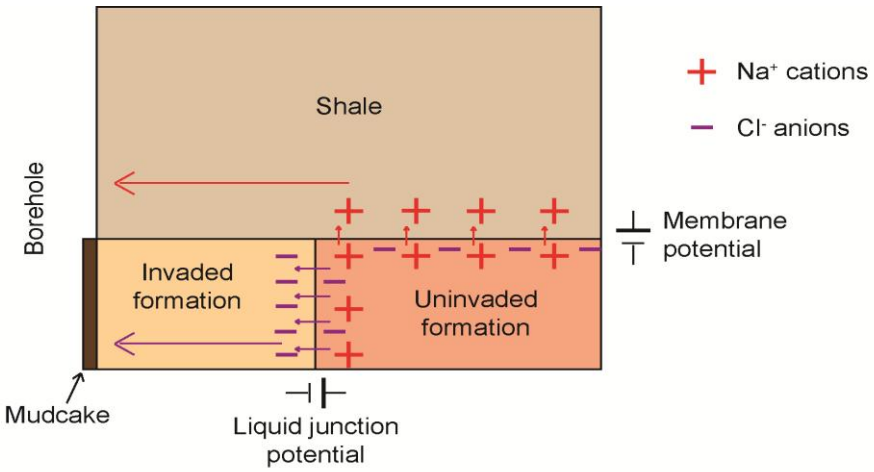

Figure 3.1. Sketch illustrating the principles of principles that establish a spontaneous potential.

A second component of the electrochemical potential occurs at the interface between the invaded and uninvaded zones, where the mud filtrate and formation water are in direct contact. At the interface between the two fluids Na^+ and Cl^- ions are able to move (diffuse) between the two solutions. Cl^- anions have greater mobility than the Na^+ cations, therefore a net flow of anions occurs from the high to low salinity fluids (the purple arrows in Figure 3.1). Again, the force causing the anions to move is a potential across the liquid interface, called the *liquid junction potential*. The movement of negative ions in one direction results in a conventional electrical current in the opposite direction. Combining the electrical currents of the membrane and liquid junction potentials can be considered to result in a current moving from the borehole, into the permeable formation, then to the shale and back to the borehole (Figure 3.2). Effectively the shale appears to have a positive spontaneous potential, while the permeable formation appears negative.

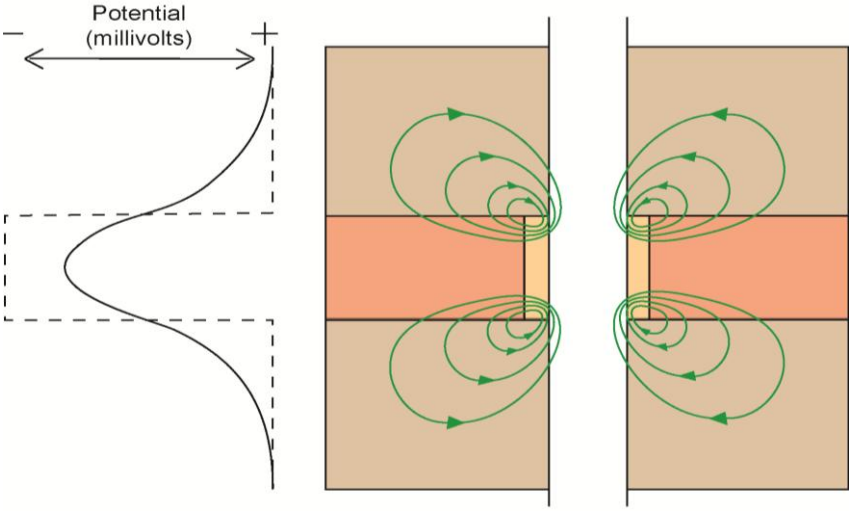

Figure 3.2. Diagrammatic representation of the spontaneous potential in a permeable formation surrounded by impermeable formations (modified from Schlumberger, 1991).

Electrokinetic components of the SP (E_k)

The *electrokinetic potential*, also known as the streaming or electrofiltration potential, is produced as an electrolyte (saline fluid) flows through a permeable, nonmetalic, and porous material. In the case of SP measured in the borehole, the electrokinetic potential results from the movement of mud filtrate through the mudcake. The magnitude of the electrokinetic potential is determined by a number of factors, primarily the differential pressure producing flow through the mudcake, and the resistivity of the electrolyte. During the initial stages of mudcake formation mud filtrate flow through is substantial, resulting in a significant E_k. As the mudcake thickens its permeability decreases rapidly, isolating the borehole from the porous formation. Subsequently, flow rates into the formation decrease and the E_k stops being produced. The electrokenetic potential is negligible in most reservoir boreholes. In wireline log analysis the spontaneous potential is assumed to be solely from the electrochemical potentials described above.

PRESENTATION OF THE SPONTANEOUS POTENTIAL LOG

The SP log is typically presented on a linear scale, in track one of a log plot (with caliper and GR measurements). Scale of the SP log will vary depending on the potentials encountered, it normally various from negative values on the left to positive values on the right (e.g., Figure 3.3). If the SP log is seen to *drift* from positive to negative values in an individual bed, or formation, this is an indication of poor data quality.

USES OF THE SPONTANEOUS POTENTIAL LOG

The SP log can be used to

- Detect permeable and impermeable beds
- Detect boundaries between permeable and permeable beds
- Estimate the volume of shale (V_{sh}) in a permeable bed
- Determine the formation water resistivity in the uninvaded zone (R_w)

QUALITATIVE INTERPRETATION OF THE SPONTANEOUS POTENTIAL LOG

As there are no absolute values for the SP log, measurements are relative to over- and underlying sediment types, both qualitative and quantitative interpretation of the SP logs focuses on deflections from a baseline (i.e. how the curve moves to the left or right). A zero SP measurement is usually calibrated for any thick shales present in the succession, this is referred to as the *shale baseline* (e.g. Figure 3.3). Permeable beds will deviate from the shale baseline, causing deflections (or excursions). The maximum deflection from the shale baseline is used to define a *sand line* (Figure 3.3).

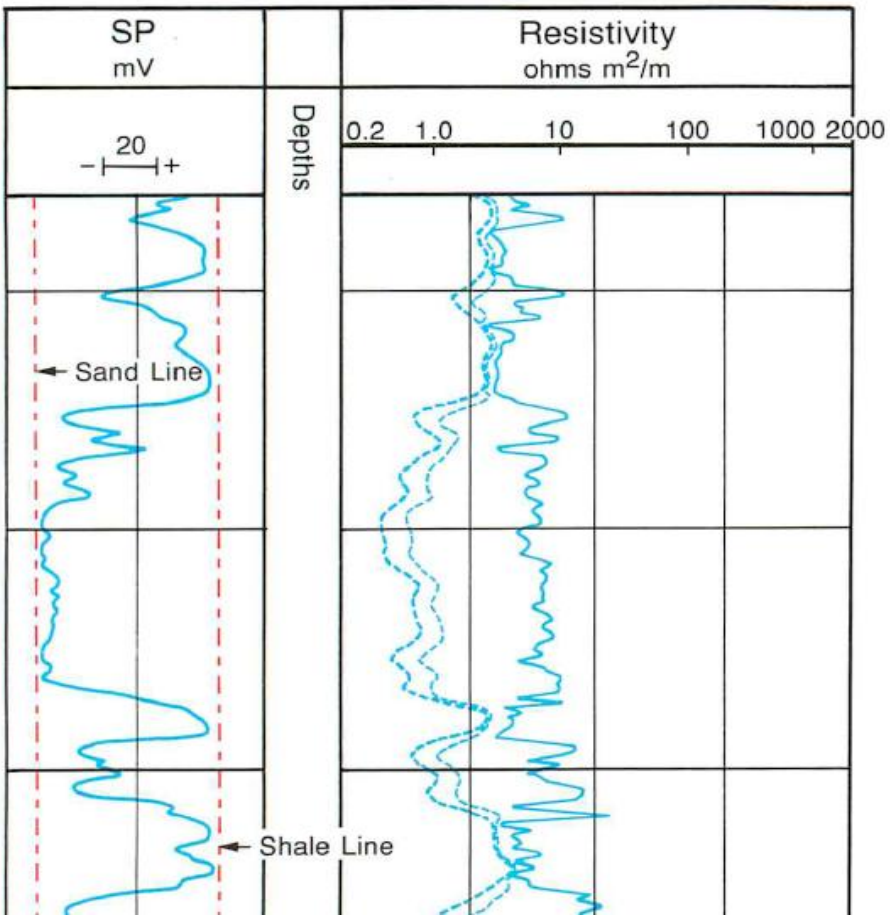

Figure 3.3. Example of an SP log (in track one) for a succession of sand and shale beds (Schlumberger, 1991).

Deflections to the left, toward negative values, are regarded as *negative* or *normal* deflections – this occurs in formations where the formation water has a greater salinity than the borehole / mud filtrate ($R_w < R_{mf}$). This is the case illustrated by the current directions in Figure 3.2. *Positive deflections* (or reverse deflections) occur when the mud filtrate salinity is greater than the formation water salinity ($R_w > R_{mf}$). Positive deflections are less common, but can be observed in formations with brackish or fresh formation water. If the salinity of mud filtrate and formation fluids are the same then deflections will be small and the curve will appear featureless ($R_w = R_{mf}$). As a result, deflection of the SP log can be used use to give a qualitative estimate of the composition of formation waters, relative to the mud filtrate (Figure 3.4, left).

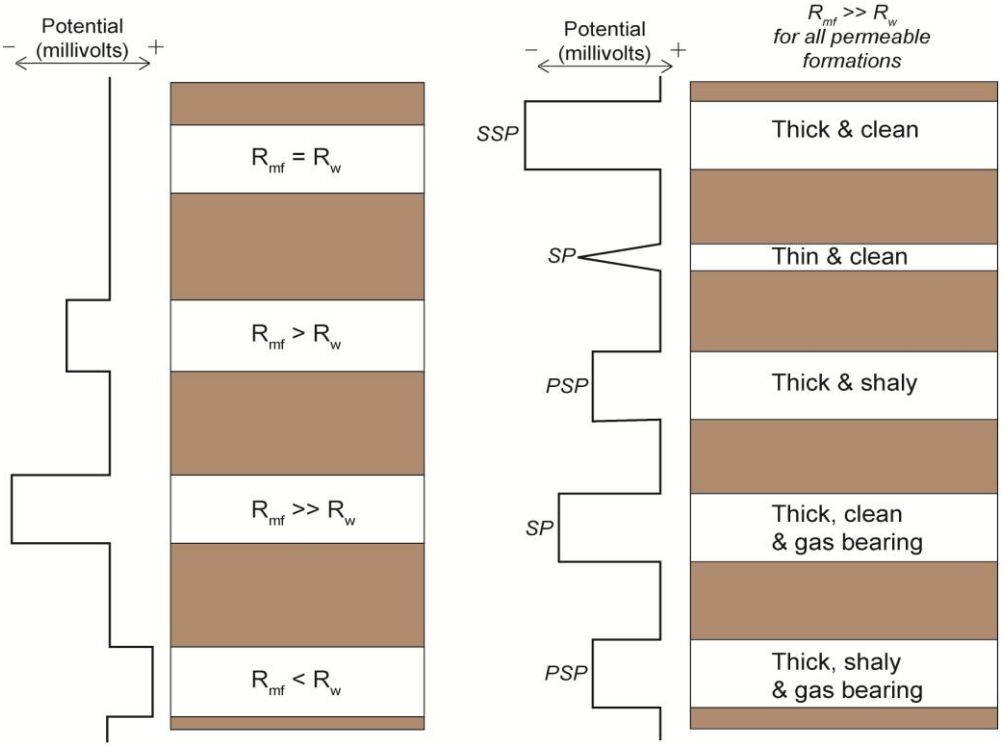

Figure 3.4. Schematic illustration of the factors influencing the amplitude and shape of SP deflections. R_w – formation water resistivity in the uninvaded zone, R_{mf} – resistivity of the mud filtrate (modified from Asquith & Krygowski, 2004).

The *static spontaneous potential* (SSP) represents the maximum SP deflection from the shale baseline, observed in a thick, shale-free, porous and permeable bed or formation, in which salinity of borehole and formation fluids are different. The magnitude of the SSP can calculated using Equation 3.1.

$$SSP = -K \log\left(\frac{c_w}{c_{mf}}\right) \qquad \text{(Equation 3.1)}$$

Where c_w and c_{mf} – conductivity of the formation water and mud filtrate, respectively, and K is a constant dependant on reservoir temperature (K = 61 + (0.133 x temp in ^oF) or K = 65 + (0.24 x temp in ^oC)).

The minimum bed thickness required to develop an SSP is around 6 m (20 ft). In beds thinner than 6m a correction must be applied to the SP log measurement to obtain an SSP. Each service company will provide their own chart to calculate and apply this correction, an example of which is shown in Figure 3.5.

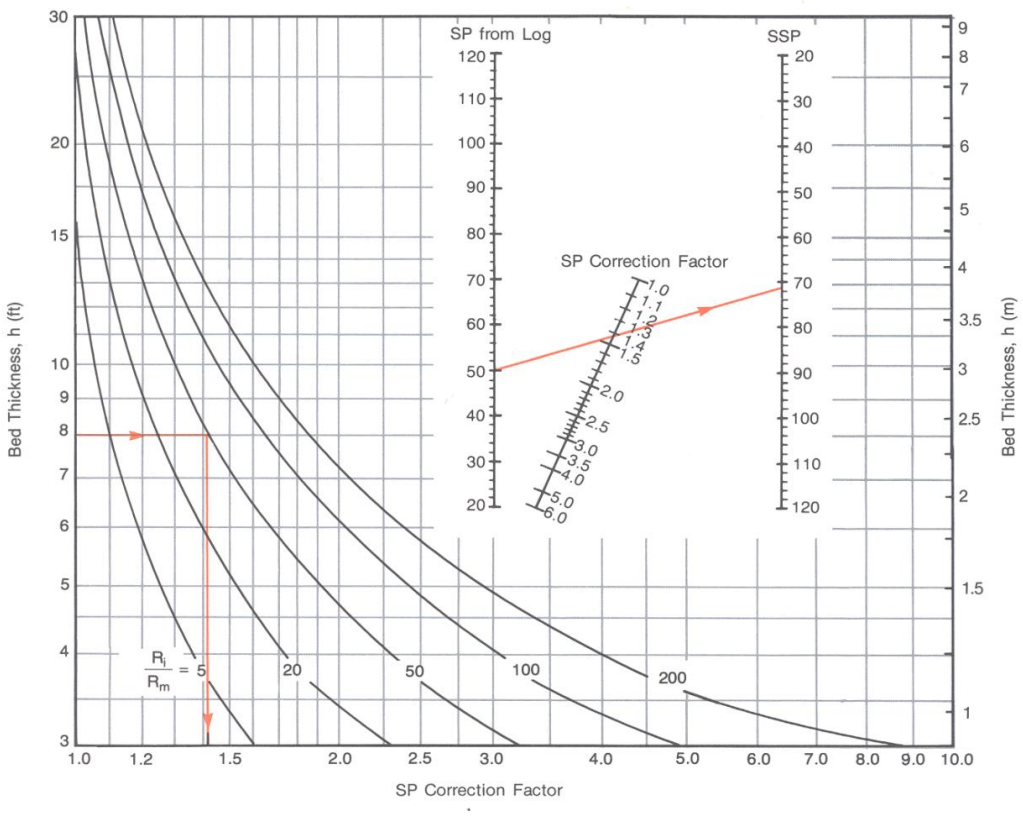

Figure 3.6. SP bed-thickness correction to determine SSP from SP (Western Atlas, 1995). Ri = Rw, Rm = resistivity of the mud (must be converted from surface temperature to reservoir temperature).

Factors influencing the shape and amplitude of SP deflections (Figure 3.5, right)

Bed thickness – from the discussion of SSP above, we can see that the measured SP deflection can be highly influenced by bed thickness. The thinner the porous and permeable bed, the more narrow, rounded and lower amplitude of the SP deflection. Only clean beds, thicker than 6 m (20 ft) will display a well developed, flat topped SSP.

Bed resistivity – high resistivity formation will produced reduced SP deflections. For example if high hydrocarbon saturations are present in the porous formation.

Shale content – the presence of shale in a porous and permeable formation will reduce the SP deflection. In water-bearing formations the amount of reduction in the SP deflection is related to the proportion of shale present, we will come back to this regarding SP as a method for estimating Vsh below. Thick shaly sandstone SP deflections are referred to as the pseudostatic spontaneous potential (PSP).

Contact between mud filtrate and formation water resistivity (R_{mf} and R_w, respectively) – as discussed above, with reference to Figure 3.5 (left).

It should be noted that the diameters of the borehole and/or invasion have a very small effect on the SP deflection, and are in general ignored.

To summarise, qualitative interpretation of the SP log can be used to identify permeable beds and to an understanding of the salinity of formation waters *relative* to the drilling mud. It should be emphasised that there is **not** a direct relationship between the amplitude of an SP deflection and the permeability of a formation.

QUANTITATIVE INTERPRETATION OF THE SPONTANEOUS POTENTIAL LOG

The SP log can be used in quantitative interpretations of (1) shale volume in a shaly sand and (2) formation water resistivity, R_w.

Shale volume (V_{sh}) from the SP log

The volume of shale in a permeable zone can be calculated using either Equation 3.2 or 3.3.

$$V_{sh} = 1 - \left(\frac{PSP}{SSP}\right) \qquad \text{(Equation 3.2)}$$

$$V_{sh} = \frac{PSP - SSP}{SP_{sh} - SSP} \qquad \text{(Equation 3.2)}$$

Where: V_{sh} – fractional shale volume, PSP – pseudostatic spontaneous potential (max SP in shaly formation), SSP – static spontaneous potential (max SP in nearby clean and thick sandstone), and SP_{sh} – value of SP in nearby shale (shale baseline, usually around zero).

Formation water resistivity in the uninvaded zone (R_w) from the SP log

The resistivity of formation water in the uninvaded zone (R_w) can be estimated from the SP log using a variety of equations or charts, each service company will have their own versions of the charts but the same answer should be obtained regardless. In this example we will use standard Schlumberger chart to illustrate the method.

It must be emphasised that R_w can only be sensibly estimated in the water bearing zone of a reservoir formation. *This should NOT be attempted in a shale or a hydrocarbon bearing zone*.

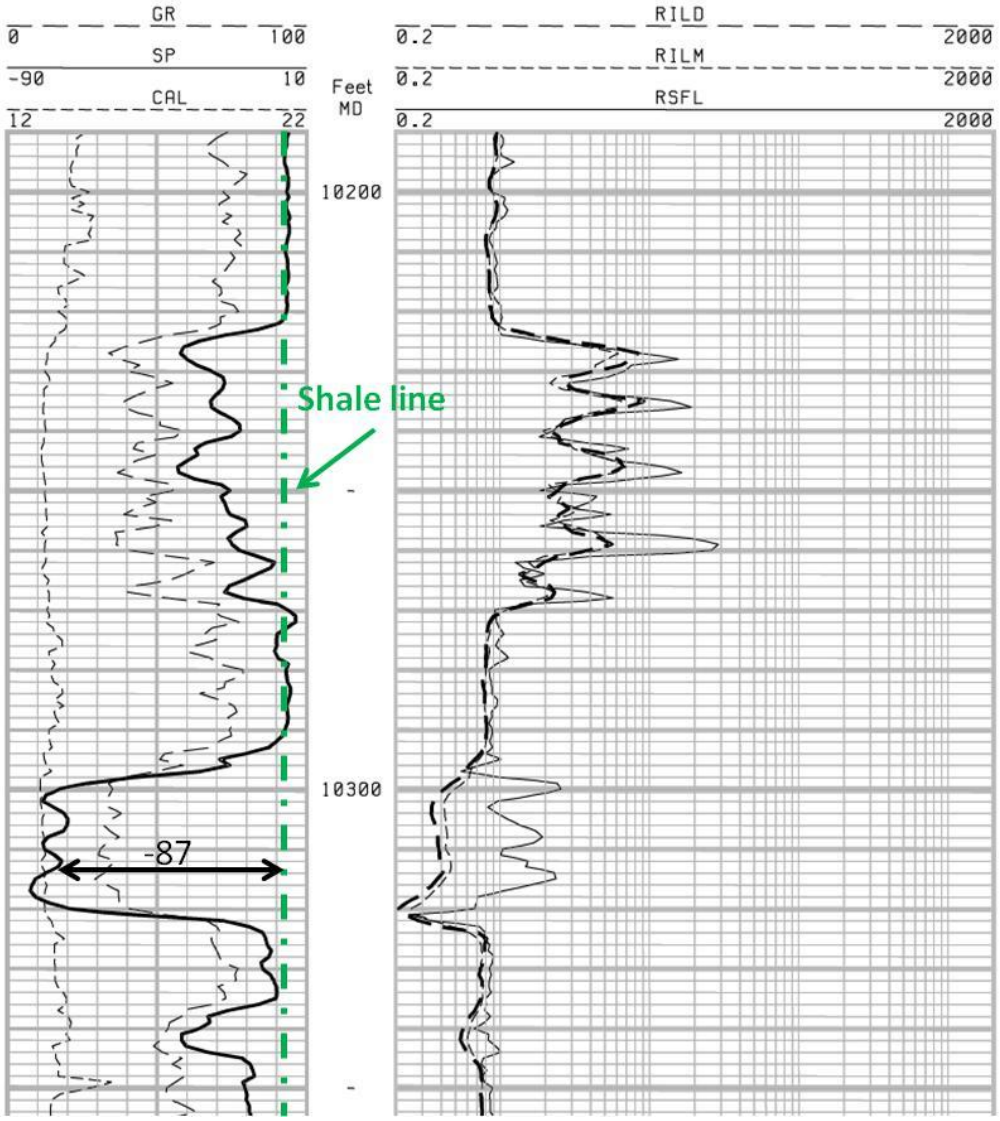

Figure 3.7. Electrical log suite for a succession of sandstone and shale beds (modified from Asquith & Krygowski, 2004).

The log suite for this example is presented in Figure 3.7. The bottom hole temperature (BHT) is measured as 175 ^{o}F at 11,192 ft, and the resistivity of the mud filtrates was measured to be 0.58 ohm.m at 75 ^{o}F (surface conditions).

1) Select a thick, clean permeable formation or bed that is water bearing and read of the difference between shale and sand lines (the SP deflection). This should be thicker than 6 m (20 ft), with low GR, low resistivity, and with a large SP deflection.

   We choose 10,315 ft. SP shale +5, SP sand -82 = SP -87 mV

2) Estimate the temperature at the reservoir depth chosen, using Schlumberger Chart Gen-2 (Figure 3.8). If this is within 150 m (500 ft) of the bottom of the hole, then the estimated formation temperature (EFT) will be the same as the bottom hole temperature (BHT) for all practical purposes.

   Our reservoir depth is more than 150 m above the bottom of the hole so we convery BHT to EFT using Figure 3.8. We find that a BHT of 175 ^{o}F at 11,192 ft corresponds to an EFT of 168 ^{o}F at 10,315 ft.

3) Convert the resistivity of the mud filtrate (R_{mf}) from surface temperature to EFT at reservoir depth, using Schlumberger Chart Gen-6 (Figure 3.9)
   R_{mf} measured as 0.58 ohm.m at 70 ^{o}F (surface temperature), therefore this can be converted using Figure 3.9. R_{mf} at reservoir temperature of 168 ^{o}F is 0.26 ohm.m.
4) Convert R_{mf} to R_{mfe} (equivalent mud filtrate resistivity) using the guidelines on Figure 3.10. Then use Schlumberger Chart SP-1 (Figure 3.10) to calculate R_{we} using the SP deflection and R_{mfe}.
   R_{mf} at 75 ^{o}F is greater than 0.1 ohm.m, therefore R_{mfe} = 0.85 x 0.26 = 0.22 ohm.m
   Plotting an SP of -87 at 168 ^{o}F on Figure 3.10 gives an R_{we} of 0.017 ohm.m.
5) Convert R_{we} to R_{w} using Schlumberger Chart SP-2 (Figure 3.11)

   An R_{we} of 0.017 ohm.m at 168 oF corresponds to an <u>Rw of 0.026 ohm.m</u>

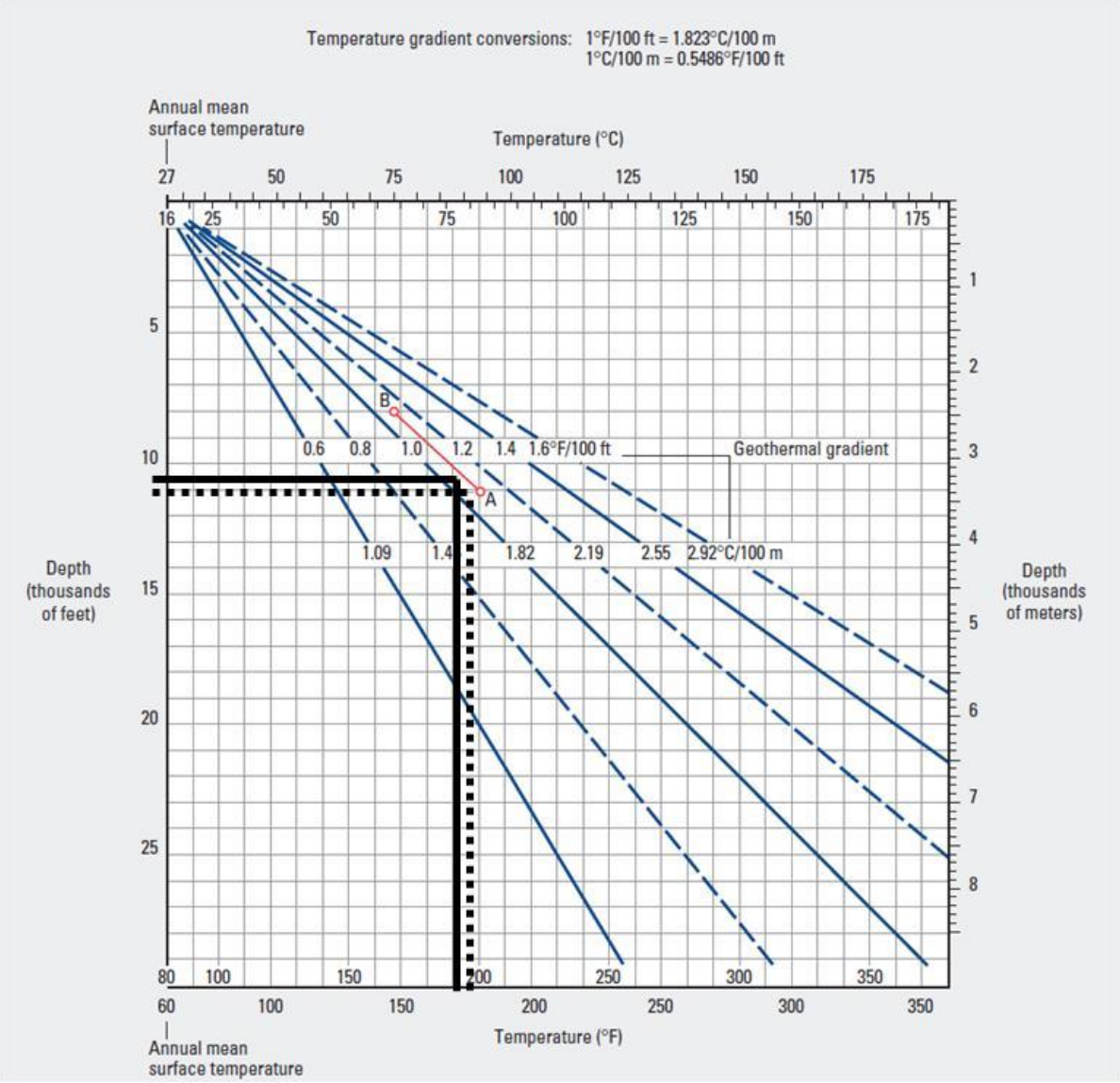

Figure 3.8. Schlumberger Chart Gen-2. Estimation of EFT from BHT, assuming a linear geothermal gradient (Schlumberger, 2009).

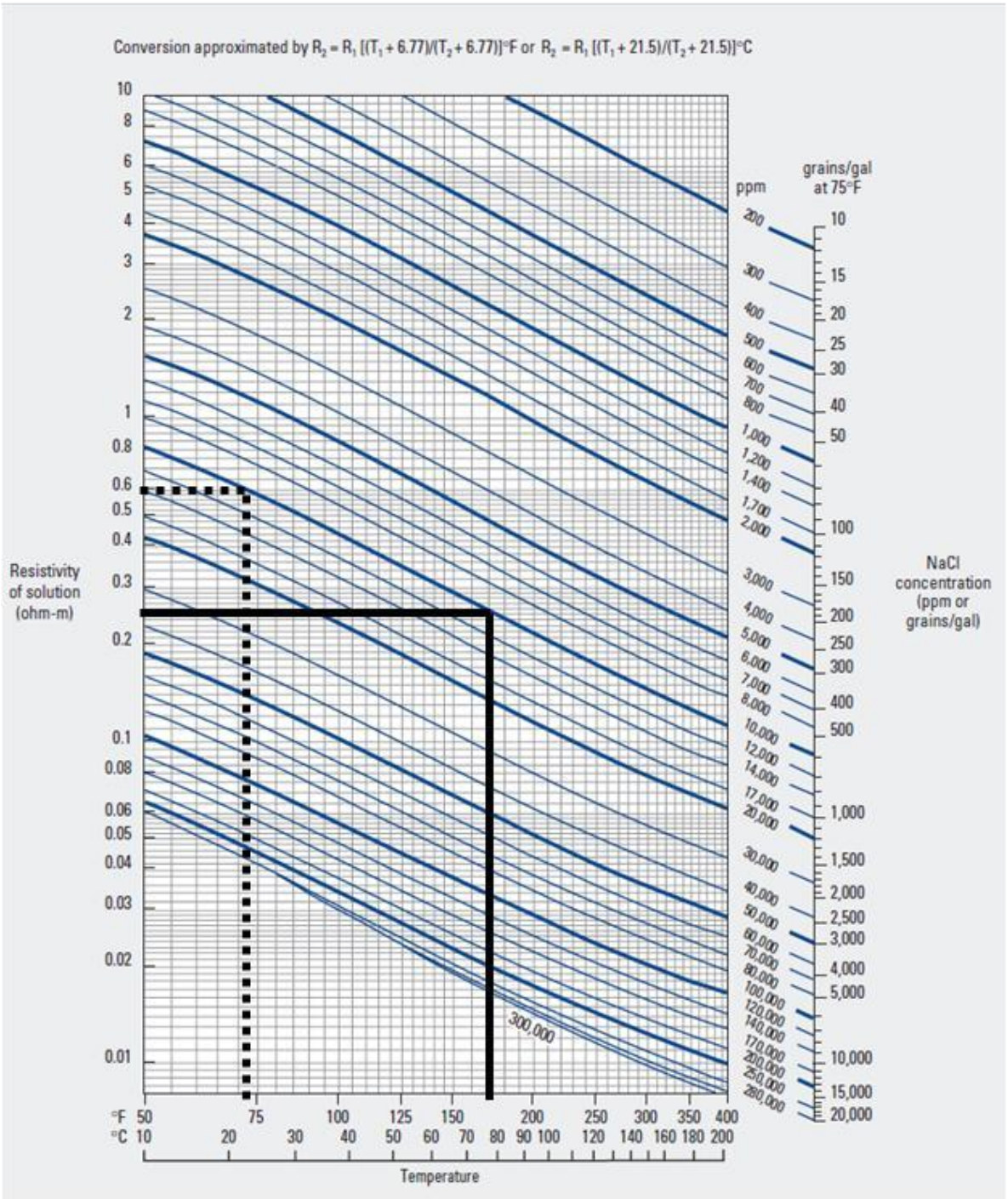

Figure 3.9. Schlumberger Chart Gen-6. Resistivity conversion chart for different temperatures (Schlumberger, 2009).

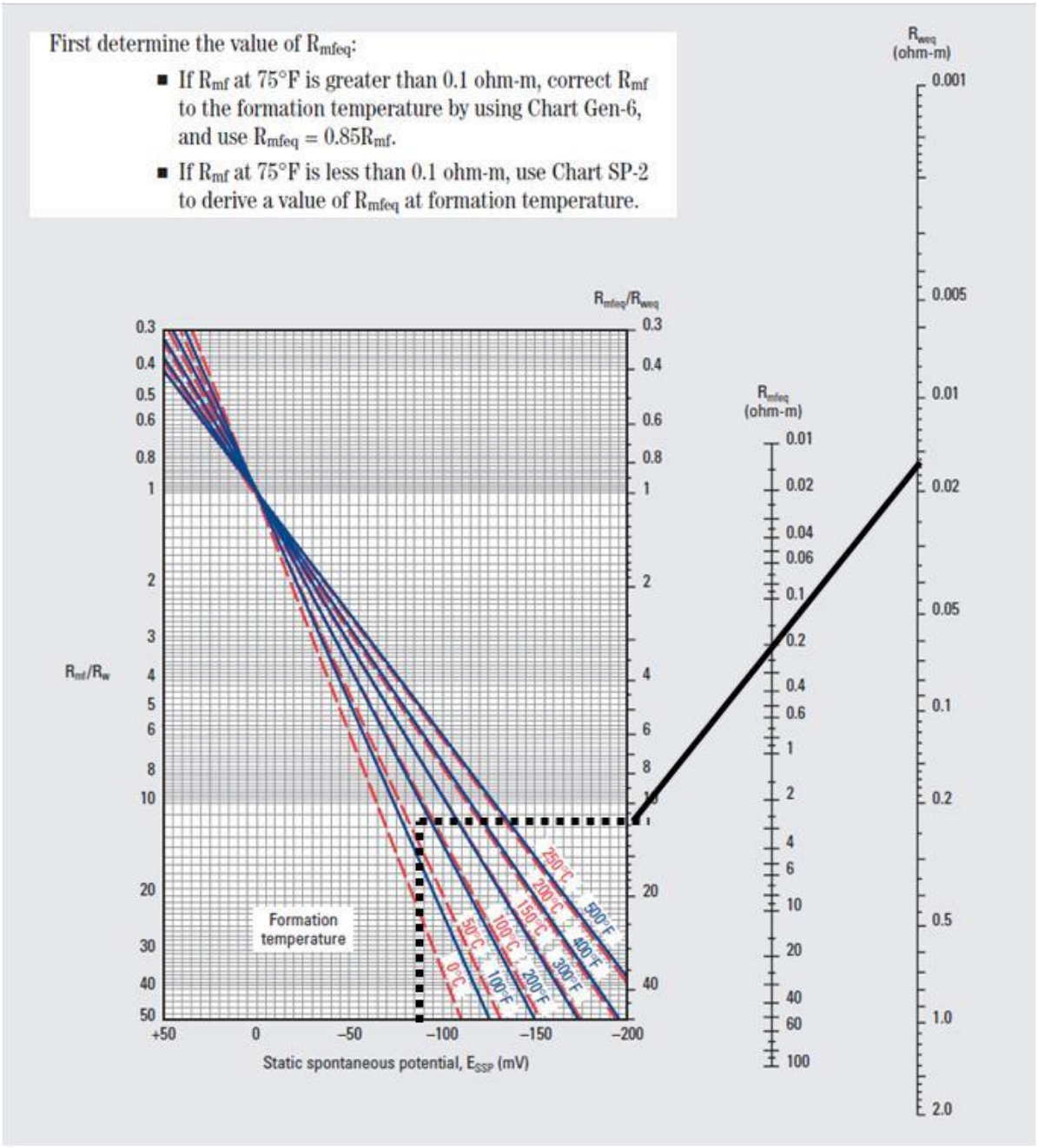

Figure 3.10. Schlumberger Chart SP-1. R_{we} determination by the SP method (Schlumberger, 2009).

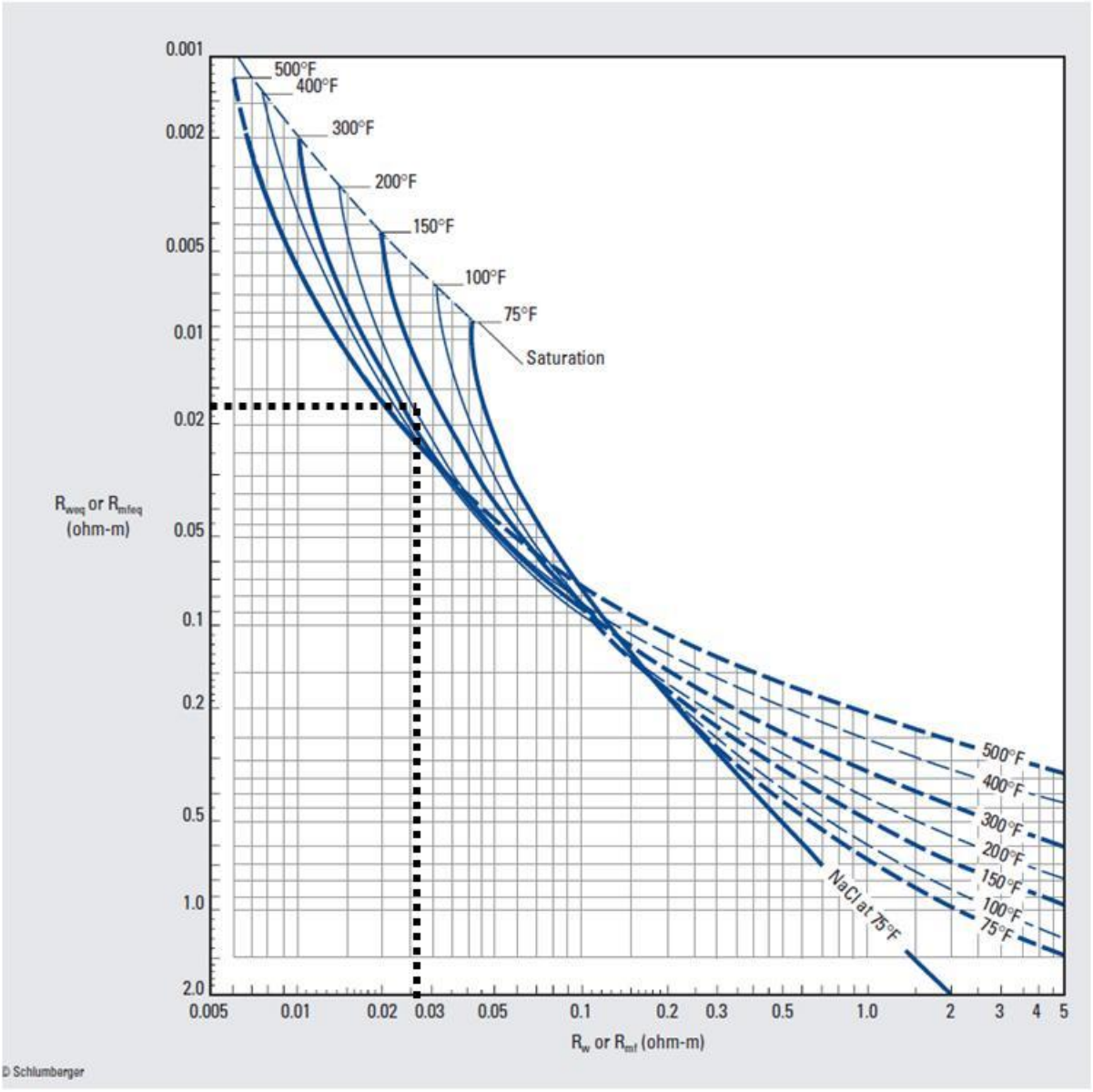

Figure 3.11. Schlumberger Chart SP-2. Converting Rwe to Rw based on formation temperature relationships (Schlumberger, 2009).

4. BULK DENSITY LOGS

The density log provides a continuous measurement of the formation's bulk density. Bulk density is a result of the solid matrix (mineralogy), porosity and any fluids present. *Bulk density* may be referred to as ρ_b or RHOB, and is measured in grams per cubic centimetre (g/cm^3, $g.cm^{-3}$). If the effects of porosity and fluid are removed from the bulk density measurement, i.e. the formation is non-porous, then the measured density reflect only the solid framework of the rock. This is referred to as the *grain* or *matrix density* (ρ_{gr} or ρ_{ma}, Table 4.1). For example, a sandstone with no porosity will have a grain density of 2.65 g/cm^3 (the density of pure quartz). A quartz-rich sandstone with 10 % porosity, saturated with fresh water (fluid density of 1.0 g/cm^3) will have a bulk density of 2.49 g/cm^3.

Matrix	Density (g/cm^3)	Fluid	Density (g/cm^3)
Quartz (*sandstone*)	2.64	Fresh water	1.0
Calcite (*limestone*)	2.71	Salt water	1.15
Dolomite (*dolomite*)	2.85	Oil	0.85
Anhydrite (*evaporite*)	2.98	Gas	0.0008
Gypsum (*evaporite)*	2.32		
Halite (*evaporite*)	2.04		
Lignite (*coal*)	1.19		

Table 4.1. Typical matrix and fluid densities (Schlumberger. 1991, Rider & Kennedy, 2011).

The bulk density log provides an indication of formation lithology if no porosity is present. However, this can be misleading in the presence of porosity and different fluids (Figure 4.1). The primary use of the density to log is an indicator of porosity. It can also be used to identify evaporates, hydrocarbon gas, and in the evaluation of shaly sands and more complex lithologies, overburden pressures and rock mechanical properties.

PRINCIPLES OF MEASUREMENT FOR THE DENSITY LOG

There are two main types of density logging tools; the Formation Density Compensated (FDC) log, and the Litho-Density log (LDT). The density measuring device of both tools is comparable; in general Litho-Density logging tools have replaced the FDC since the 1980's.

The density tool needs to be in contact with the borehole wall, and so a caliper is used to push the tool against one side of the borehole. A radioactive source, such as caesium (^{137}Cs), is mounted on a pad on the side of the tool in a shielded sidewall skid and applied to the borehole wall (e.g. Figure 4.2). The radioactive source emits a continuous beam of medium-energy gamma rays (at *c.* 662 keV) into the formation. As described previously with regard to the gamma ray log, gamma rays can be thought of as high velocity photons. As the gamma rays collide with the electrons in the formation they lose energy to the electron, and continue moving in a different direction until the gamma ray is weak and

absorbed by an atom. This interaction is known as Compton-scattering, a denser the rock will lead to more collisions. Some of the scattered gamma rays will reach one of a pair of scintillation detectors (short spaced at 15 cm from the source, and long spaced at 30 – 45 cm from the source). The number of gamma rays detected reflects the electron density of the formation, i.e. the number of electrons per cubic centimetre.

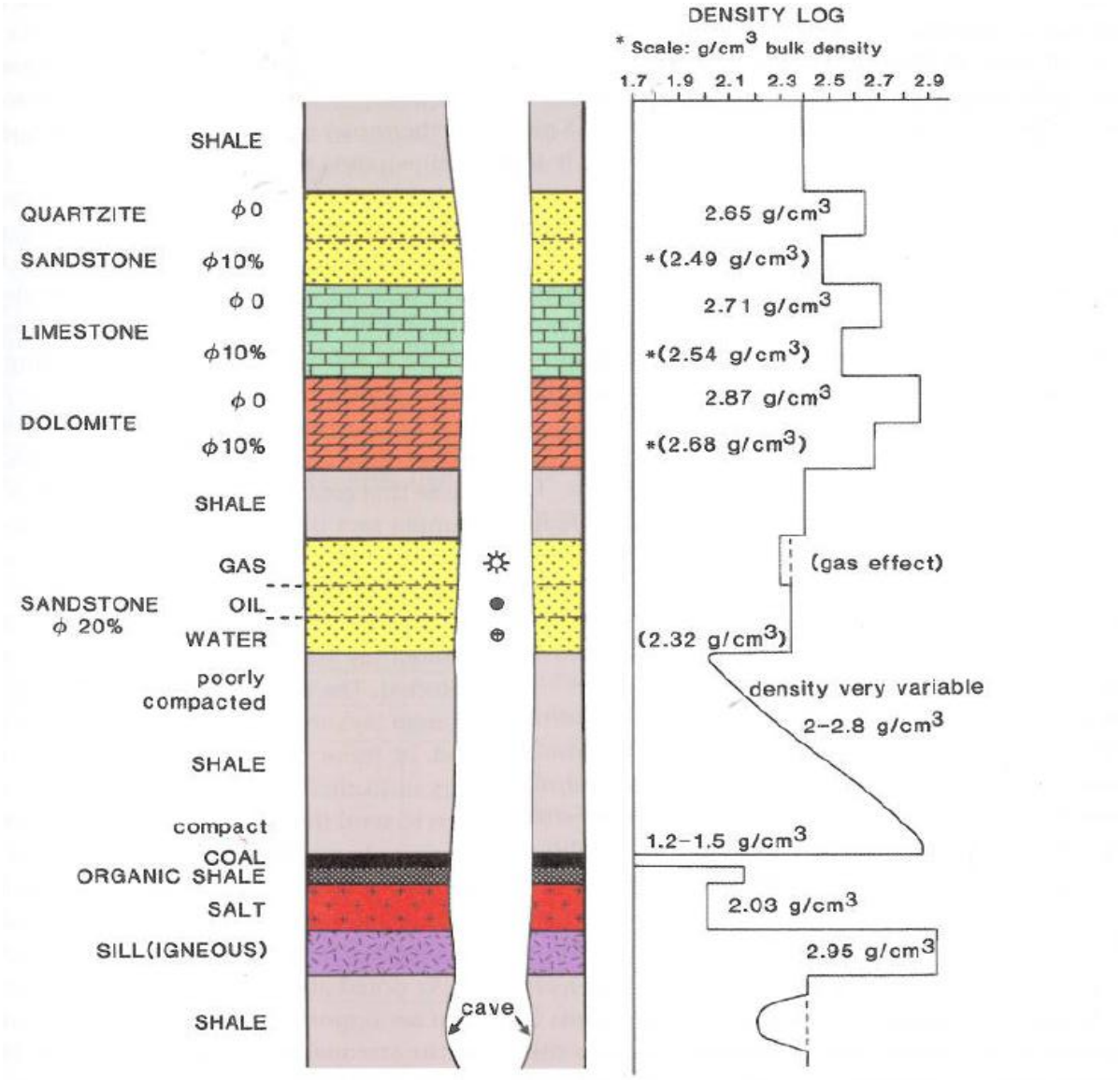

Figure 4.1. Illustration of some typical log responses for the bulk density log. Assumes porosity filled with a fresh water of density 1.0 g/cm^3 (Rider & Kennedy, 2011).

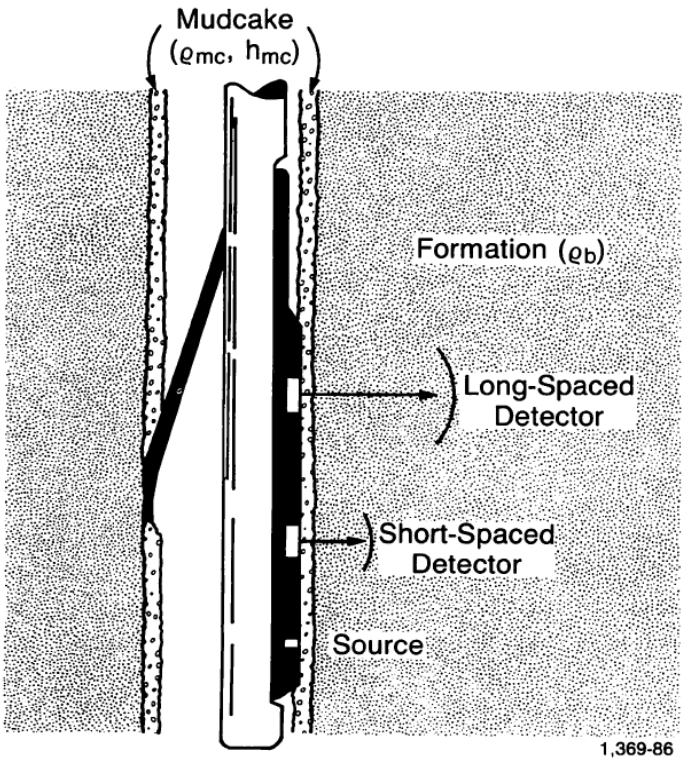

Figure 4.2. Schematic drawing of the dual spacing Formation Density Compensated (FDC) logging device (Schlumberger, 1991).

The depth of investigation for the density tools depends on the source to detector spacing, however this is typically very shallow into the formation. This is the main reason that the tool is pushed against the borehole wall. The short spaced detector is more sensitive to borehole effect (rugosity or mudcake build up), and the long spaced detector is influenced more strongly by the formation. A comparison of the two detectors is used to identify any borehole effects on the formation density measurements and correct for them. Two outputs are produced for wireline log display and interpretations; the corrected bulk density log (ρ_b or RHOB), and an indication of the correction applied ($\Delta\rho$ or DRHO). An example of the outputs from the density logging tool are provided in Figure 4.3. The $\Delta\rho$ curve is often used alongside the caliper log to provide an indication of borehole and data quality – a large correction of greater than 0.15 g/cm^3 is considered to indicate an unreliable bulk density log.

Bulk density log may be scaled from 2.0 to 3.0 g/cm^3, or from 1.95 to 2.95 g/cm^3, where density increases to the right of the track. Bulk density is traditionally plotted in the same track as neutron porosity (section 5).

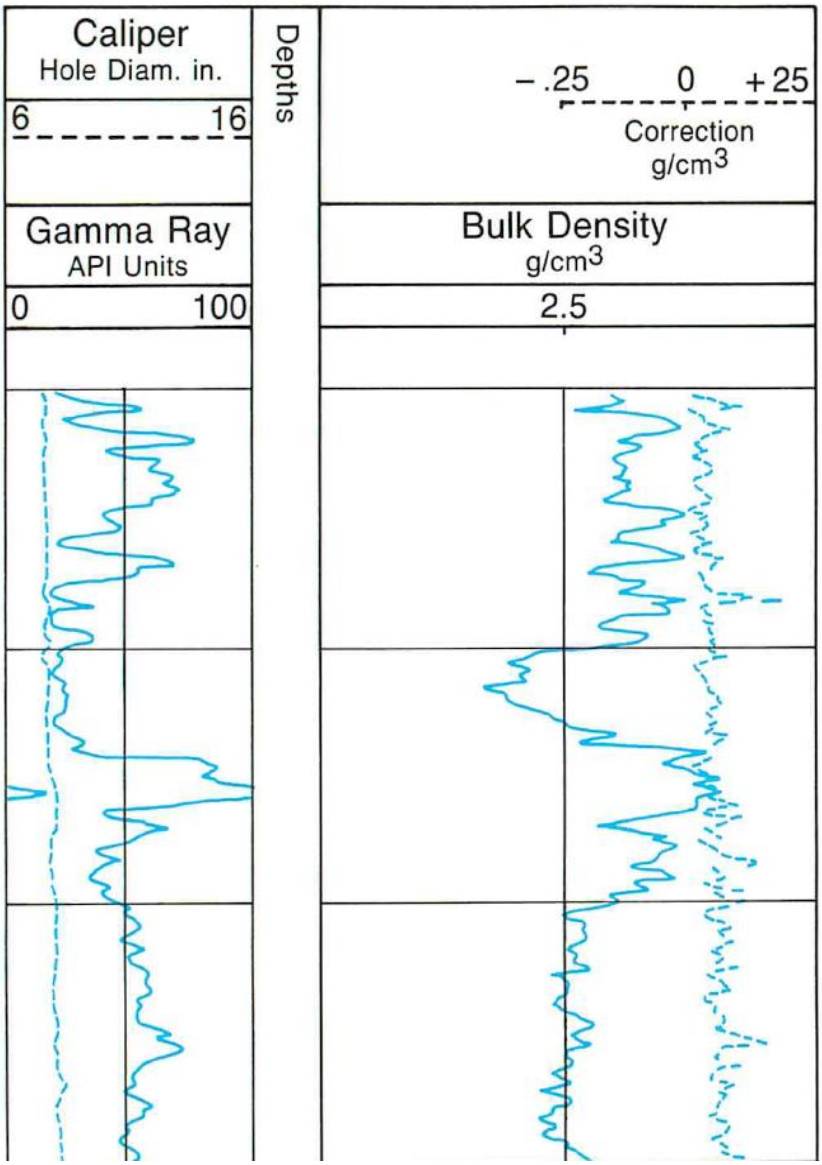

Figure 4.3. Bulk density log presentation, an example for the FDC tool (Schlumberger, 1991).

The Litho-Density Log

The measurement principles described above are applicable to both the Formation Density Compensated log, and the Litho-Density (LDT) Log. However, the LDT detectors have been designed to have greater count rates, resulting in lower statistical variability than the FDT tool. Detection of greater count rate allows the LDT to also provide a measurement of the photoelectric absorption index of the formation (P_e or PEF). Although both density and P_e logging make use of gamma ray detection

from a source, photoelectric absorption involves lower energy gamma rays than Compton scattering, typically below 100 keV (Figure 4.4).

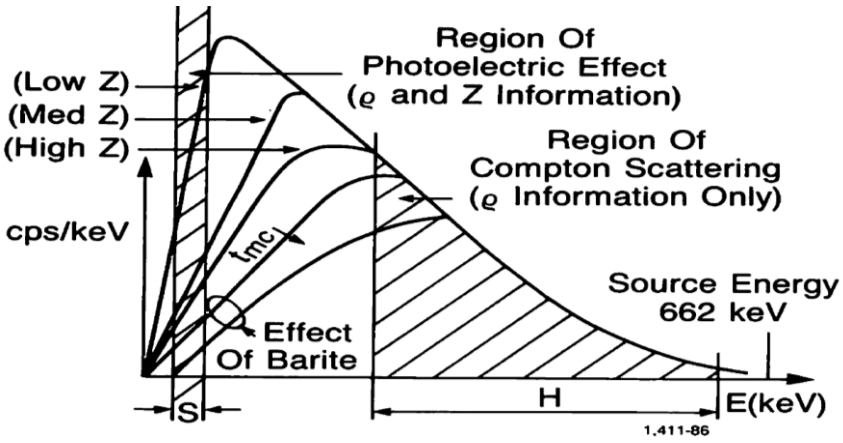

Figure 4.4. Variations in the energy spectrum for gamma rays detected in a formation, with constant density and three different atomic numbers (*Z*) (Schlumberger, 1991).

Low energy gamma rays can be absorbed by atoms, transferring the gamma ray energy to bound electrons. If electrons gain enough energy they leave the atomic orbit and are ejected from the atom, becoming a *photoelectron*. The degree of gamma ray absorption is dependent on the atomic number (*Z*) and the electron density of the atom, i.e. how many electrons are present. The photoelectric absorption index is calculated by comparing the gamma ray counts in the high (Compton scattering) and low energy regions. Figure 4.4 illustrates that three formations can have the same bulk density (Compton scattering region), but different magnitudes of absorption in the low energy region – the *volumetric absorption index* (U). Equation 4.1 shows that the count rate in the photoelectric absorption energy region (U) is dependent on the electron density (ρ_e) and the photoelectric absorption index (P_e).

$$U = P_e \times \rho_e \qquad \text{(Equation 4.1)}$$

Matrix	Formula	Density, ρ_e (g/cm^3)	P_e (barns/electron)	U ($barns/cm^3$)
Quartz (*sandstone*)	SiO_2	2.65	1.806	4.79
Calcite (*limestone*)	$CaCO_3$	2.71	5.084	13.77
Dolomite (*dolomite*)	$CaMg(CO_3)_2$	2.85	3.142	9.00
Anhydrite (*evaporite*)	$CaSO_4$	2.96	5.055	14.95
Gypsum (*evaporite)*	$CaSO_4 2H_2O$	2.32	3.420	8.11
Barite	$BaSO_4$	4.5	266.800	1070.00

Table 4.2. Typical mineral log measured bulk density, P_e, and U values (Schlumberger. 1991).

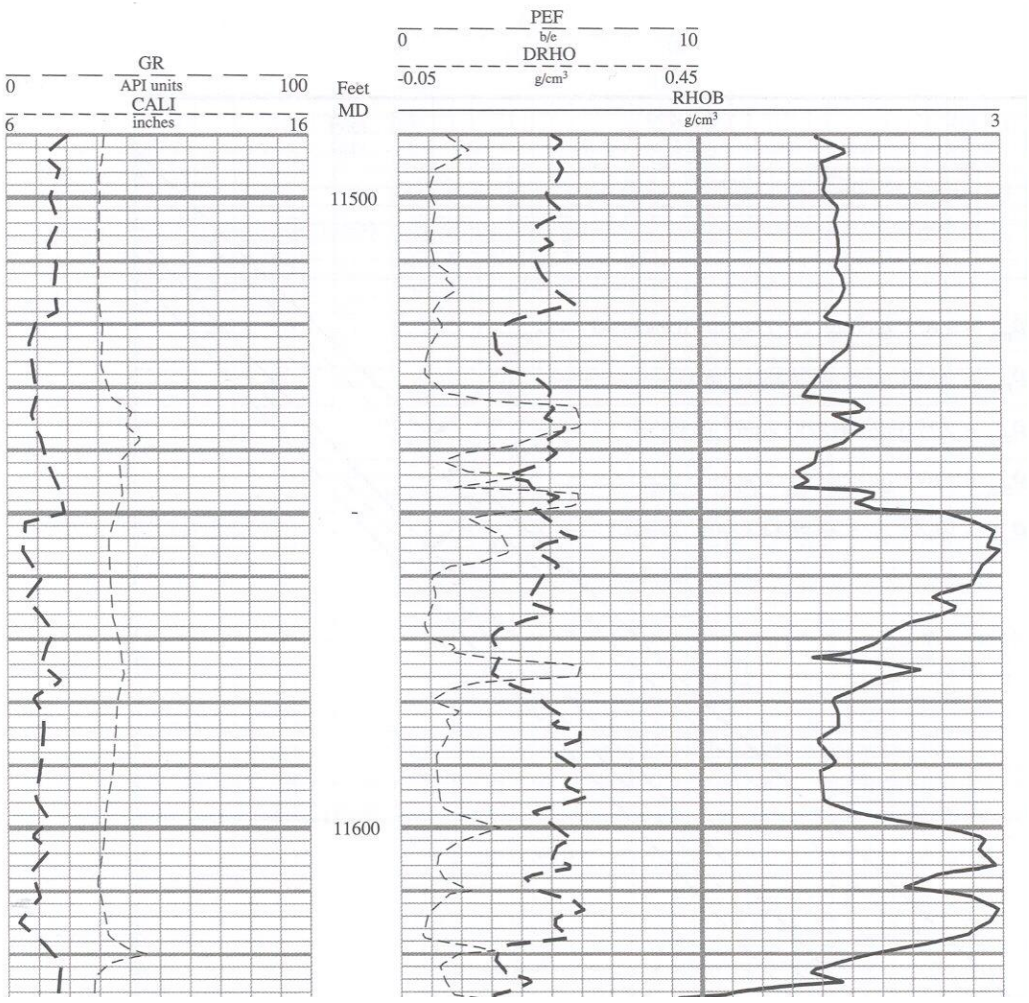

Figure 4.5. Illustration of the LDT bulk density and P_e log presentation (Asquith & Krygowsky, 2004).

Use of the Photoelectric Absorption Index Log

The primary use of the P_e log as an indicator of lithology, or rather mineralogy. As shown in table 4.2, quartz, calcite and dolomite can be clearly separated in the log response. The P_e log is independent of porosity, and so can be used in combination with bulk density in interpretation.

The sensitivity of the P_e log to heavy elements (e.g. Barite at 266.8 barns/electron) can be problematic when heavy, barite-rich drilling muds are used. Even the slightest concentration of barite in the mud can cause the photoelectric absorption index to be unusable.

QUANTITATIVE USE OF THE DENSITY LOG

The bulk density of a formation is a function of the matrix density, porosity and the density of fluid(s) occupying the pore space (Figure 4.6). The most common used application of the bulk density log is to determine porosity of the formation. The empirical relationship shown in Equation 4.2 can be re-arranged for this purpose (Equation 4.3), giving porosity as a fraction of the total volume (multiply by 100 if percentage is required).

$$\rho_b = \emptyset\, \rho_f + (1 - \emptyset)\, \rho_{ma} \qquad \text{(Equation 4.2)}$$

$$\emptyset = \frac{\rho_{ma} - \rho_b}{\rho_{ma} - \rho_f} \qquad \text{(Equation 4.2)}$$

Where: ρ_b – bulk density from the log, ρ_f – density of the fluid, ρ_{ma} – matrix or grain density, and Ø – porosity.

The bulk density tools have a shallow depth of investigation into the formation, around 15cm (6 in.). Consequently, the pore fluids in permeable formations are typically mud filtrate with densities ranging between 1.0 to >1.1 g/cm^3. Fluid density can be calculated based on the fluid composition, or its resistivity (and therefore salinity). Matrix density can be looked up from various tables (e.g. Table 4.1). Table 4.3 illustrates the effect of different matrix and fluid densities on porosity estimation from a constant bulk density log measurement. Note that we are not interested in estimating porosity in shales in conventional reservoir analysis.

$\emptyset = \frac{\rho_{ma} - \rho_b}{\rho_{ma} - \rho_f}$				
Lithology	Matrix Density (g/cm^3)	Fluid Density (g/cm^3)	Bulk Density Log (g/cm^3)	Porosity (fraction)
Sandstone		1.1	2.5	
Limestone		1.1	2.5	
Dolomite		1.1	2.5	
Sandstone 2		1.0	2.5	
Sandstone 3		0.8	2.5	

Table 4.3. Porosity estimation for a bulk density log measurement of 2.5 g/cm^3 using grain and fluid densities (*select the appropriate grain densities from Table 4.1, and calculated porosity*).

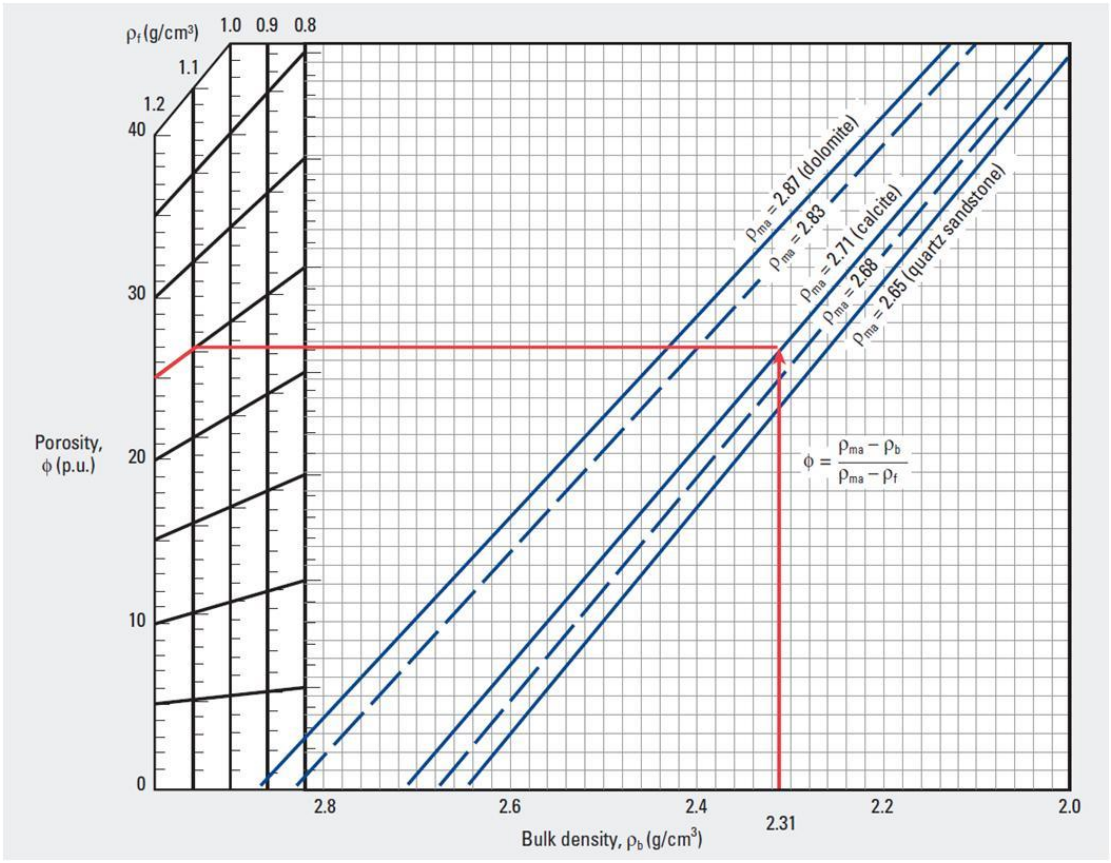

Figure 4.6. Schlumberger Chart Por-3. The empirical relationships between porosity and bulk density for different matrix and fluid densities. Example shown if for a bulk density of 2.31 g/cm^3 with limestone lithology (Schlumberger, 2009).

Matrix density has a much more significant effect on porosity estimation from the bulk density log than fluid density (e.g. Table 4.3). Clearly we need to ensure that the correct lithology is identified, and suitable matrix density is used in porosity calculation to avoid significant over- or underestimation of porosity. Lithology can be indicated by the P_e log, as described previously. Alternatively drilling cuttings and core sample may be used to determine lithology. Combinations of multiple wireline log measurements (spectral gamma ray, bulk density, neutron porosity, and sonic) may be used as qualitative lithology indicators – this will be covered further in section 7.

Oil does not normally have a noticeable effect on porosity estimation for the density log. However, gas will lead to a significant overestimation of porosity. Where gas is identified it can be corrected for using various charts and equations provided by service companies.

5. NEUTRON LOGS

The Neutron, or *Neutron Porosity*, Log is another radioactive logging tool. It is not, as the name suggests, a direct measure of porosity in the formation – the neutron log actually provides a measure of the amount of hydrogen in a formation, the *hydrogen index*. Its principle use is in the identification of porous formations and *estimation* of porosity using empirical relationships.

PRINCIPLES OF MEASUREMENT FOR THE NEUTRON LOG

A neutron is an electrically neutral particle, with mass almost identical to a hydrogen atom. A source emits a continuous stream of high-energy neutrons into the formation. The source is traditionally chemical, such as a combination of beryllium and a heavy radioactive element (e.g. Americium). Alpha particles from the radioactive element collide with beryllium nuclei and produce high energy protons (at 4.5 MeV). Neutrons are emitted at a rate of roughly 10^8 neutrons per second. Some modern tools use a *neutron generator*, rather than a chemical source. Neutron generators use a fusion reaction to generate a pulse of neutrons with energy levels *c.*14 MeV.

As the neutrons move through the formation they collide with other nuclei, this is thought of as elastic 'billiard-ball' collisions. At each collision the neutron loses some of its energy and so slows down. The amount of energy lost with each collision depends on the mass of the nuclei the neutron collides with. The greatest energy loss occurs when the neutron strikes a nuclei of similar mass, i.e. a hydrogen atom. Collisions with smaller and larger nuclei have little effect on the neutrons energy level. After the neutron has made enough collisions its energy drops to *c.*0.025 eV ('thermal velocities'). At this time the neutron simply diffuses randomly until it is captured by another nucleus. The nucleus that captures the neutron becomes intensely excited and emits a high energy gamma ray.

Two types of detector can be used in Neutron tools. Older tools from the 1950s used a gamma ray Scintillation detector that recorded a simple count rate, as described previously for the gamma ray and bulk density tools. More traditionally, the Neutron tool has two neutron detectors (e.g. Figure 5.1). Neutron detectors are similar to Geiger counters. In the centre of the detector is a vessel containing a low pressure gas, such as Helium-3 (He^3) or boron tri-fluoride, which strongly absorbs low energy neutrons to produce a positive ion. The positive ions produce small pulses of electrical current which are measured and recorded by the tool.

When hydrogen concentration of formation is large, most of the neutrons emitted by the tool are slowed and captured within a short distance of the tool, resulting in low count rates. If hydrogen content of the formation is small then the neutrons can travel further before being captured, increasing the count rates. Therefore, if we assume that hydrogen is only present in pore space, the neutron tool count rate is inversely proportional to porosity (in a clean, non-shaly, formation).

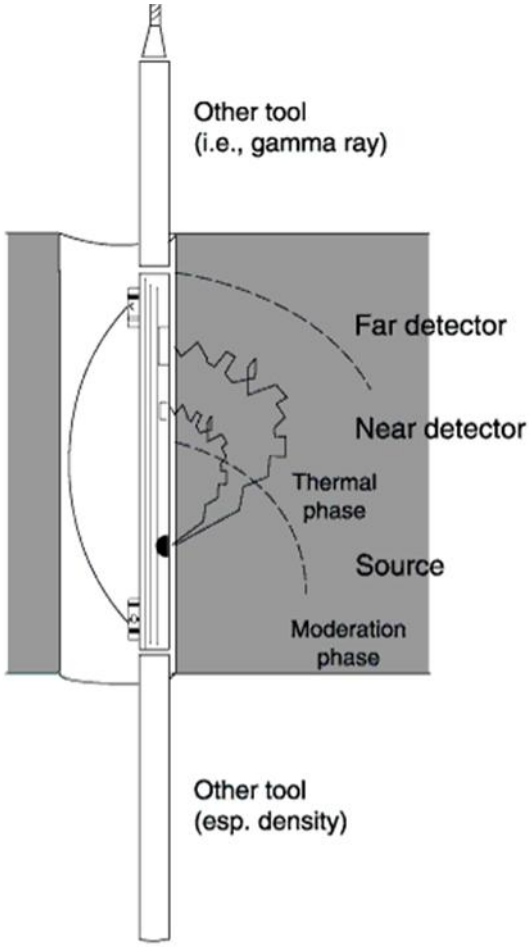

Figure 5.1. Schematic illustration of a typical Neutron tool (Rider & Kennedy, 2011).

Neutron detectors can be either *thermal* (low energy neutrons) or *epithermal* (higher energy neutrons) detectors. Tools that only measure electrons in the moderation phase (Figure 5.1) respond primarily to epithermal neutrons, e.g. the Sidewall Neutron Porosity tool (SNP). *Compensated neutron logs* (CNL) use two detectors, a near and far detector, to measure thermal neutrons, and some epithermal neutrons (Figure 5.1). The CNL is designed to account for environmental factors, such as borehole diameter and drilling mud weight, in a similar way to the density tools. The neutron porosity log is calculated from the ratio of near and far detector counts. Associated gamma ray detectors produce a Thermal Decay Time log.

The neutron porosity tool is traditionally calibrated to a sample of pure limestone, saturated with fresh water (by the American Petroleum Institute, API). Here a zero value for neutron porosity corresponds to a limestone with no porosity (density 2.7 g/cm^3). This results in porosity units that assume a limestone matrix. If the matrix is not pure limestone then true porosity will be different to that indicated by the neutron log. For example, the porosity of a sandstone will be *c.*4 porosity units (p.u.)

greater than shown by the limestone matrix. The effects of lithology on a clean, water-bearing, gas-free sample can be estimated using service company charts, such as Figure 5.2.

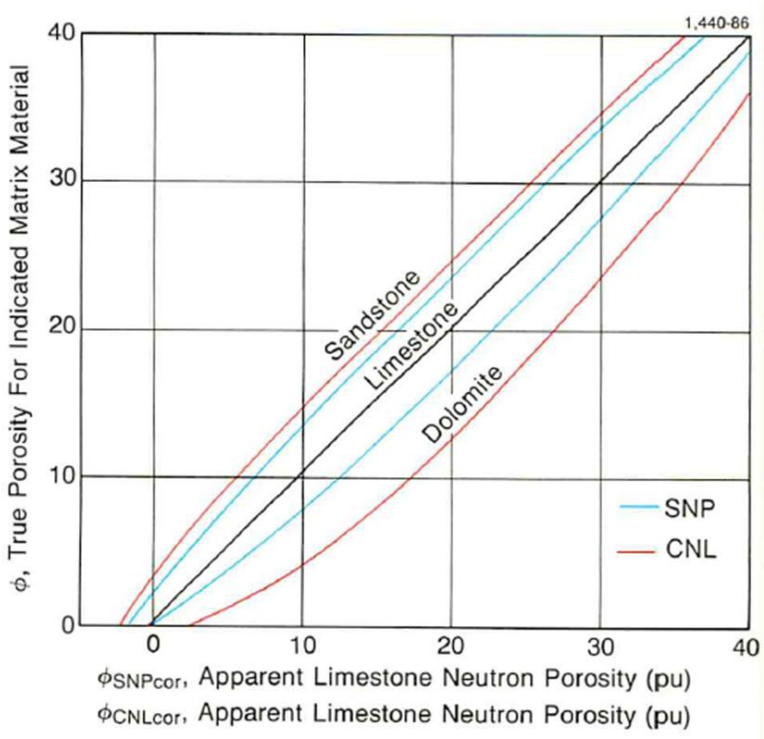

Figure 5.2. Schlumberger Chart Por-13a. Illustrating the effect of lithology on neutron porosity measurement (Schlumberger, 1991). Sandstone values are typically higher, and dolomite values are typically lower than the limestone matrix porosity units.

PRESENTATION OF THE NEUTRON LOG

The neutron porosity log is presented on a linear scale in track two of the log plot, with bulk density (the neutron log is usually either blue or dashed, while density log is a red or continuous line). Neutron porosity is normally displayed as a fraction (p.u.) rather than percentages (as shown in Figure 5.3). Porosity units (p.u.) decrease from left to right. If the tool is calibrated to limestone, then units will range from 0.45 (45 %) on the left to -0.15 (-15 %) on the right of the track (a limestone matrix scale). Note that scales are not set, different companies and individuals may choose to display data on different scale which may influence your interpretation – be certain to check scales when you begin your analysis.

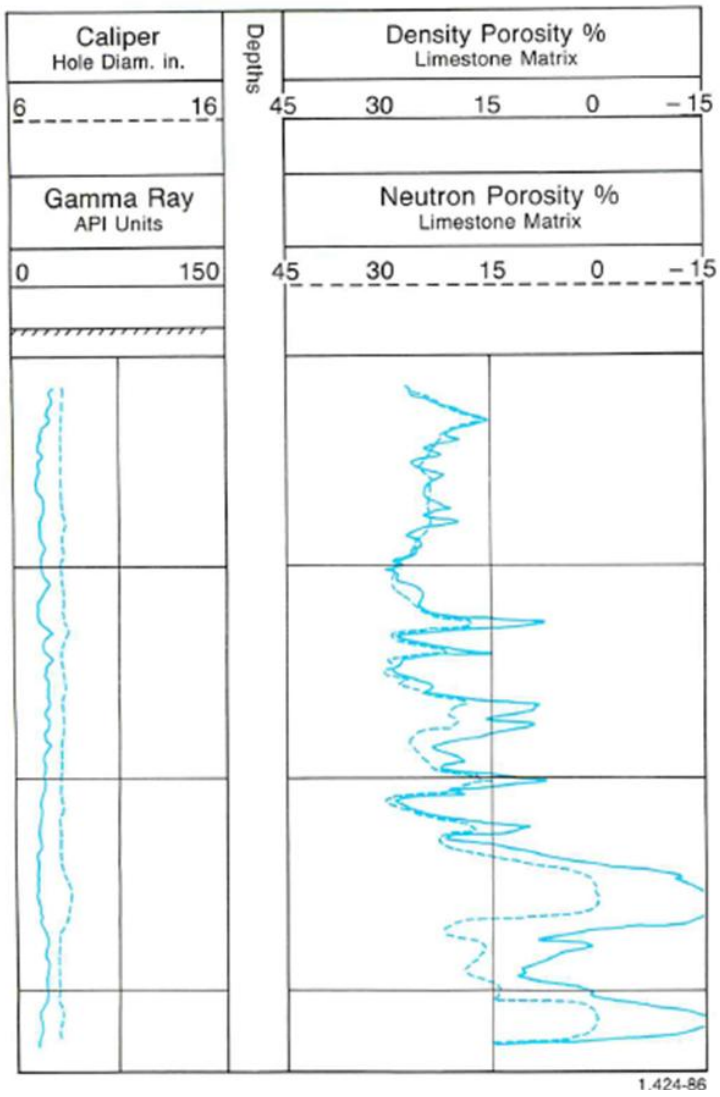

Figure 5.3. Presentation of the Compensated Neutron Log (CNL) in track two of a typical log-depth plot (Schlumberger, 1991). Note porosity derived from density are displayed for comparison. Neutron porosity is typically presented as a fraction, rather than the percentage shown here.

APPLICATION OF THE NEUTRON LOG

Porosity from the neutron log

In a clean, water-bearing formation the only hydrogen present is in formation water, filling pore space. The neutron porosity log (e.g. CNL) measures total porosity, it does not differentiate between free and bound fluids. Hence, in the case of Figure 5.3, neutron porosity is typically greater than the

porosity derived from a bulk density log (which measures effective porosity). In samples other than clean, pure limestone, the true porosity can be derived from the neutron porosity log using a chart such as that shown in Figure 5.2.

Liquid hydrocarbons (oil) have similar hydrogen indexes (concentrations) to water. In oil bearing formations porosity can be derived from the neutron porosity log in the same way as for a water bearing formation. However, gas has a much lower hydrogen index that varies with temperature and pressure. If gas is present near the borehole then the neutron log will significantly under-estimate porosity (the *"gas effect"*). Corrections for gas can be made, and will be discussed in section 7. The best use of this phenomenon is in detecting gas bearing zones. Figure 5.4 illustrates that detection of gas zones is best done with a combination of the neutron log (under-estimating porosity, it shifts to the right of the track) and bulk density (which over-estimates porosity, shifting to the left of the track).

Shales generally have a significant hydrogen index (e.g. index of 0.09 – 0.37, corresponding to neutron porosity values of 25 – 75 %). In the case of shale the neutron porosity value is clearly much greater than the actual effective porosity of the rock. Along with bound water, the neutron tool will also measure water of crystallisation. For example, gypsum is typically not porous but will return a large apparent porosity because of the significant hydrogen content within its chemical structure ($CaSO_4\ 2H_2O$).

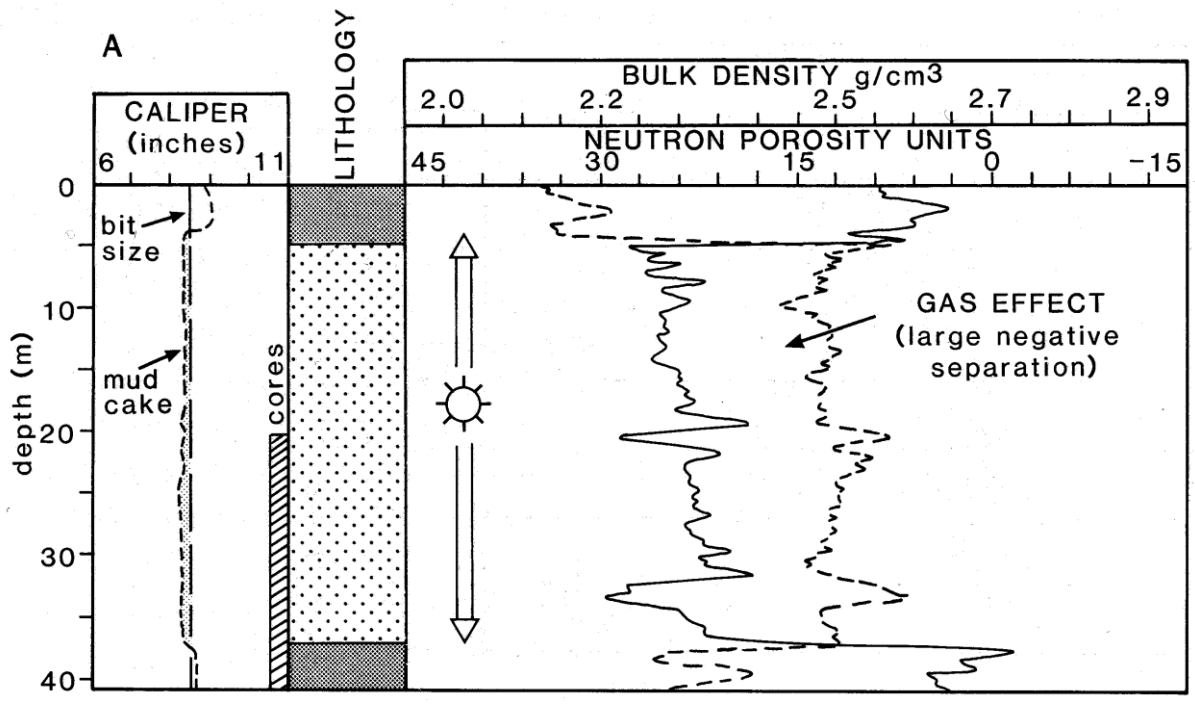

Figure 5.4. Log plot showing the effect of gas on neutron and density logs (Rider & Kennedy, 2011).

6. SONIC LOGS

The Sonic, or *acoustic* log is a measure of the time taken for a sound wave to travel through 1 foot of the formation. The travel time of the sound wave (*Δt* or DT, normally measured in micro-seconds per foot, μs/ft) depends on the lithology, porosity and saturating fluids of the formation. Interval travel, or *transit time* is the reciprocal of the velocity of a sound wave. Therefore if lithology and fluid type are known then the sonic log can be used as another estimate of porosity. There are a number of other applications of the sonic log, detailed later.

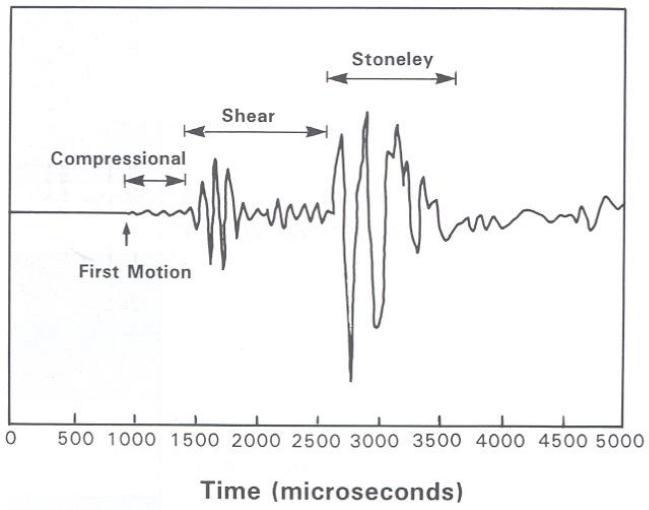

Figure 6.1. The full acoustic waveform that can be recorded in a borehole (Rider & Kennedy, 2011).

PRINCIPLES OF MEASUREMENT FOR THE SONIC LOG

In the simplest sense, the sonic tool consists of a transmitter that emits a sound wave pulse and one or more receivers at a set distance apart that pick up the wave as it moves pass the receiver (e.g. Figure 6.2).

Sources used in sonic tools are ultrasonic transmitters, which produce short pulses of sound waves at regular intervals. The sound waves used are typically in the frequency of 500 Hz to 30 kHz. Three main types of sonic wave can be detected by borehole tools – the compressional *or P wave*, the shear or *S* wave, and the Stoneley (*St*) wave. Older tools only measure the compressional wave arrival time. Modern tools can measure the complete wave train, providing compressional, shear and Stoneley waves (e.g. Figure 6.1 & 6.3). These notes will focus on application of the *P*-wave transit time log.

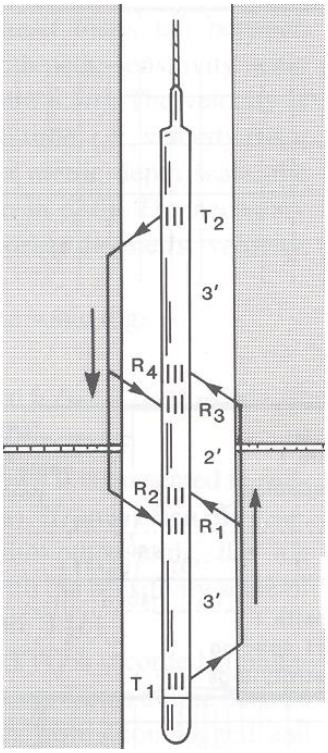

Figure 6.2. Schematic representation of the borehole compensated (BHC) sonic tool, with two transmitter-receiver sets, one of which is inverted (Rider & Kennedy, 2011).

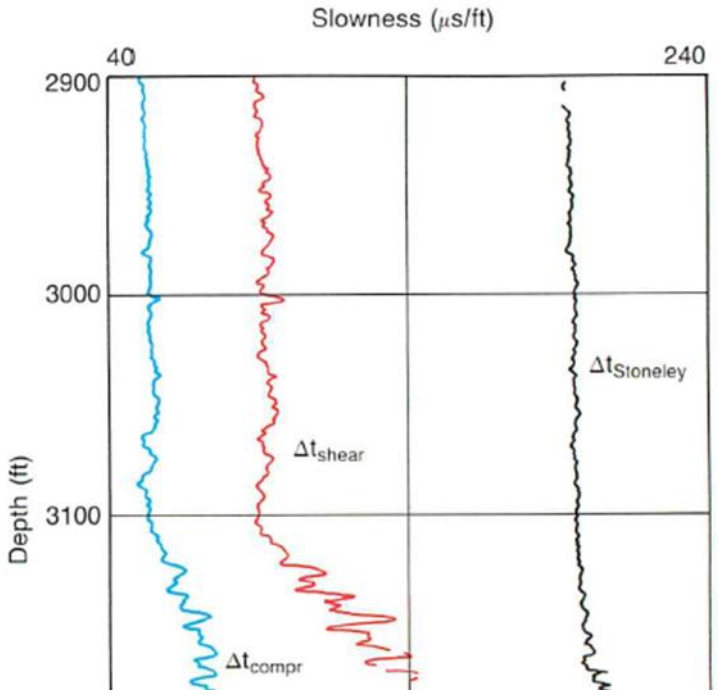

Figure 6.3. Example of compressional, shear and Stoneley wave travel time logs (Schlumberger, 1991).

In a dense, well cemented and consolidate rock with low porosity *P*-waves will move quickly through the formation, i.e. sound wave velocities (V_p) will be high. As transit time and velocity are inversely proportional, *P*-wave transit times will be low. Typically high porosity formations correspond to high transit times, and low porosity formations correspond to low transit times. Table 6.1 provides examples of *P*-wave transit time and velocity in a selection of reservoir rocks types.

Rock type (*no porosity*)	**Velocity (ft / sec)**	**Transit time (µsec / ft)**
Sandstone	18,000-19,500	56 – 51
Limestone	21,000-23,000	48 – 44
Dolomite	23,000	44
Anhydrite	15,000	50
Salt	17,500	66
Shale	5,880-16,660	170 – 60

Table 6.1. *P*-wave sonic velocities and transit times for typical reservoir rocks (Schlumberger, 1991).

The transmitter emits sound waves in all directions. The wave which has travelled from the transmitter directly through the mud column in the borehole is known as the *mud wave*. The mud wave will travel at low velocities through the low density drilling mud. Other *P*-waves will move through the drilling mud and into the formation. At the interface between the borehole and the formation waves intersecting the borehole wall at a critical angle will be refracted into the formation (Figure 6.4). As the *P*-wave moves through the formation its energy is dissipated and velocity is reduced. When the wave is slowed to a critical velocity the wave is refracted back into the borehole mud and towards the tool receiver (Figure 6.4). The time elapsed between detection of the first *P*-wave at the first and second receiver is measured. The average value measured by the two transmitters is calculated and presented as the *P*-wave transit time, compensating for any borehole effect (e.g. rugosity). The transmitter(s) used by most wireline tools are typically magnetostrictive or piezoelectric transducers that translate an electrical signal into an ultrasonic transducer. Borehole tools usually use piezoelectric transducers to convert sound waves (pressure pulses) into electromagnetic signals.

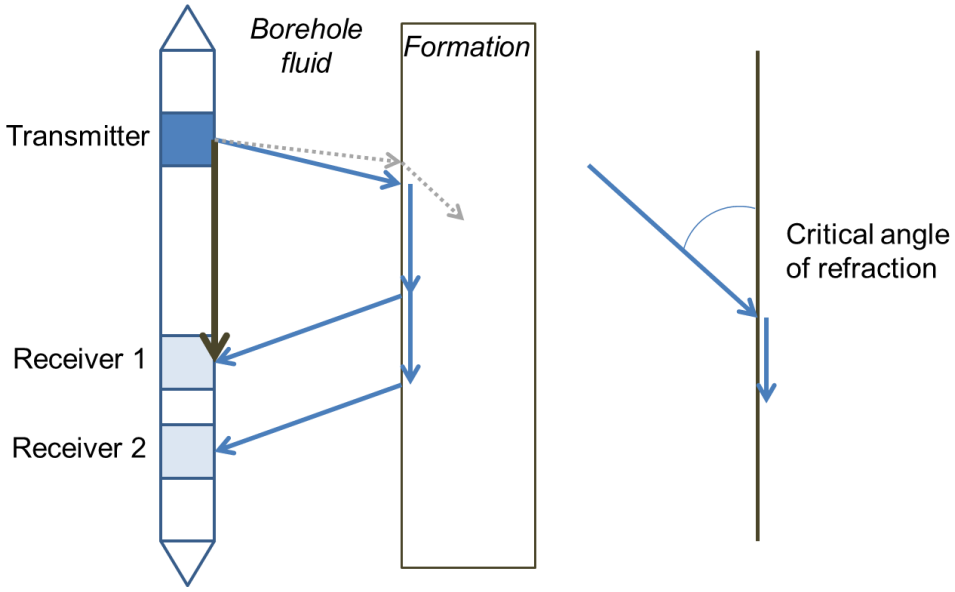

Figure 6.4. Schematic illustration of the travel paths of *P*-waves from through a reservoir formation.

There are three main sonic tools, the Borehole Compensated (BHC), Long-Spaced (LSS) and Array- (AST) sonic tools.

Borehole Compensated sonic tools

The Borehole Compensated sonic tool typically measures only the *P*-wave transit time. The BHC receivers are triggered by the arrival of the first arrival of compressional energy – *first motion detection*. The BHC uses one transmitter above and one transmitter below two sets of receivers (Figure 6.2). This set up it able to reduce the effects of borehole rugosity and errors associated with tool being tilted in the borehole. The transmitter and near receiver are typically 91 cm (3 ft) apart, and the near and far receivers are separated by *c*.60 cm (2 ft). The tool is optimized to be run in the centre of the borehole. If the tool is off-centred significant degradation in the signal to noise ratio should be corrected for. In large-diameter boreholes the first arrival detected may be the mud wave, rather than the *P*-wave refracted through the formation.

Long-Spaced sonic tools

Long-spaced tools operate in a similar way to the BHC tools. The main difference is that transmitter to receiver spacing is 2.4 – 3 m (8 -10 ft) or 3 – 3.7 m (10 – 12 ft). The larger spacing results in the measurement of waves that have moved deeper into the formation, at a greater depth of penetration, and therefore obtaining a *P*-wave transit time measurement less effected by borehole rugosity and formation alteration / damage. Figure 6.5 provides a comparison of the BHC and LSS transit times

measured in an enlarged borehole, the LSS response is assumed to be more representative of the actual formation.

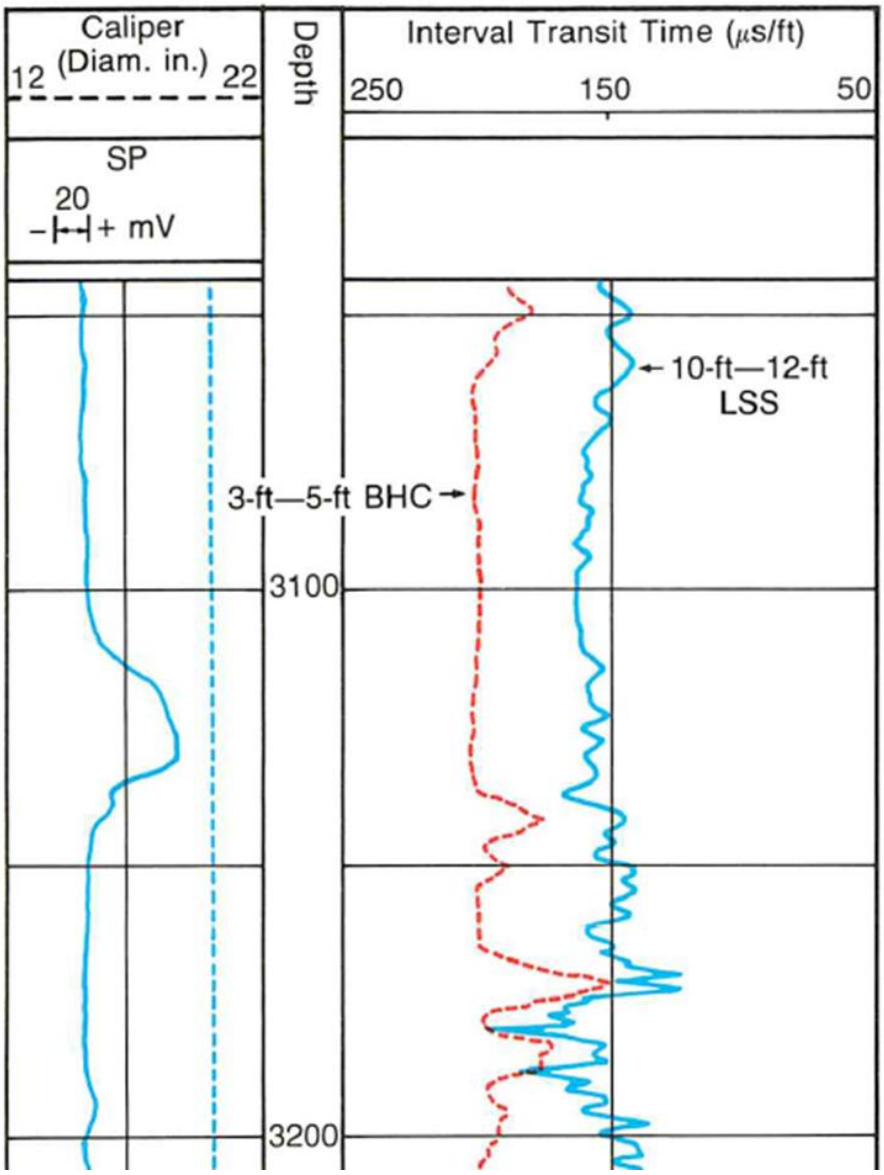

Figure 6.5. Comparison of the BHC and LSS sonic tools in an enlarged borehole (Schlumberger, 1991).

Array Sonic Tools

The Array Sonic Tool contains eight additional piezoelectric receivers, spaced 15 cm (6 in) apart, with the 2.4 m (8 ft) from the upper transmitter. Receivers 1 and 5 are used to make standard long-spaced borehole compensated P-wave transit time measurements. It is also possible to make a continuous measurement of the mud wave transit time. Waveforms measured by the eight receivers of the AST (Figure 6.5), can be used to analyse all waves propagating through the formations – the *P*-wave, *S*-

wave, and Stoneley wave transit times. The waveform processing technique is called *slowness-time coherence (STC)*.

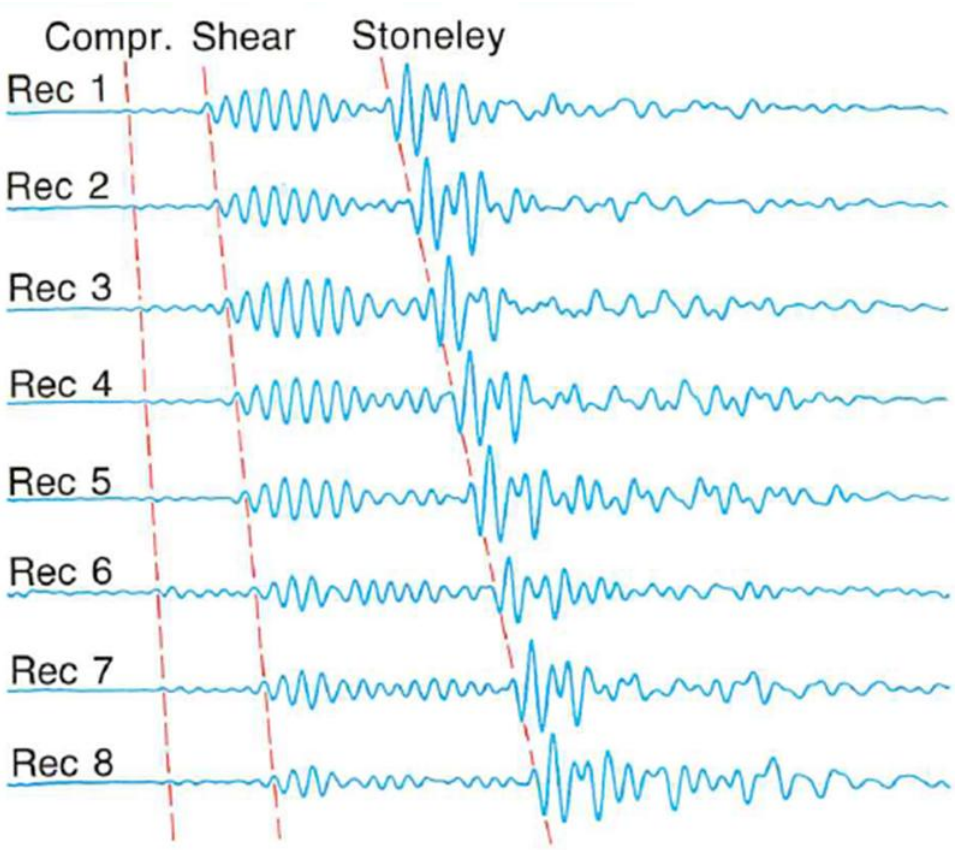

Figure 6.5. Example waveforms recorded by the eight receivers of the Array Sonic Tool (Schlumberger, 1991).

PRESENTATION OF THE SONIC LOG

P-wave transit times are measured over a range of *c*.44 μsec/ft for nonporous dolomite to 190 μsec/ft for water. Interval transit time is presented on a linear scale in Track 3 of a depth plot, with values increasing from 40 – 140 μsec/ft. Lower values are to the right of the plot and higher to the right (e.g. Figure 6.6). This scale means that, for a specific lithology, porosity increases to the left of the depth plot (as with the bulk density and neutron logs).

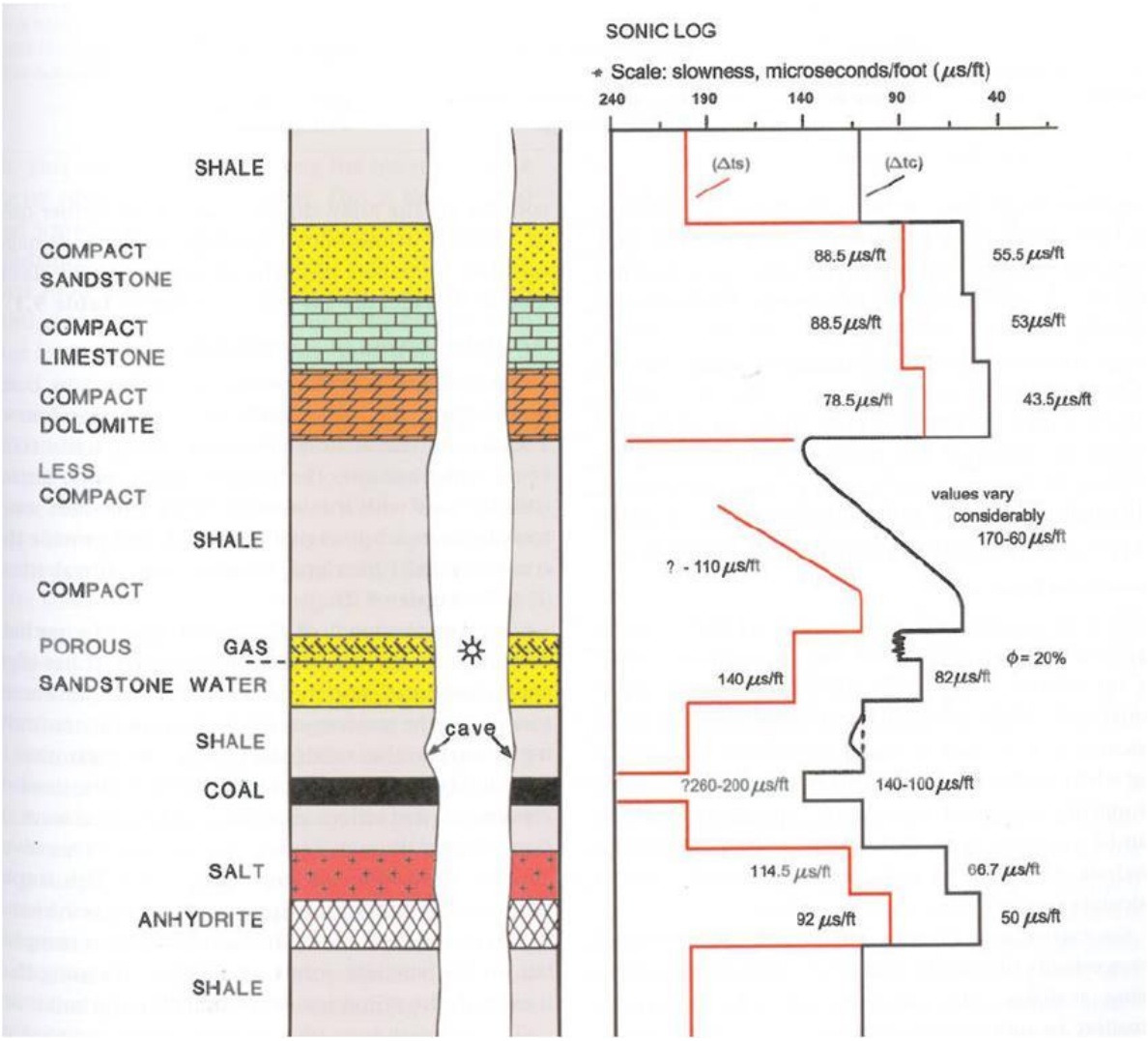

Figure 6.6. Illustration of some typical log responses for the Sonic log (Rider & Kennedy, 2011).

CYCLE SKIPPING

A sonic tool receiver is activated (triggered) by the first compressional wave that reaches it. Normally this is the *P*-wave that has refracted through the formation. However, sometime the first *P*-wave arrival is strong enough to trigger the near receiver, but is too weak to trigger the far receiver. Instead it is a second, later wave arrival that triggers the far receiver. The travel time measured is therefore too large and will influence the sonic transit time. This is normally recorded as a very abrupt and large increase in P-wave transit time – referred to as *cycle skipping* (e.g., Figure 6.7). Cycle skipping is most likely to occur in enlarged boreholes, unconsolidated or fractured formations, and high gas saturations where the acoustic signal is strongly attenuated.

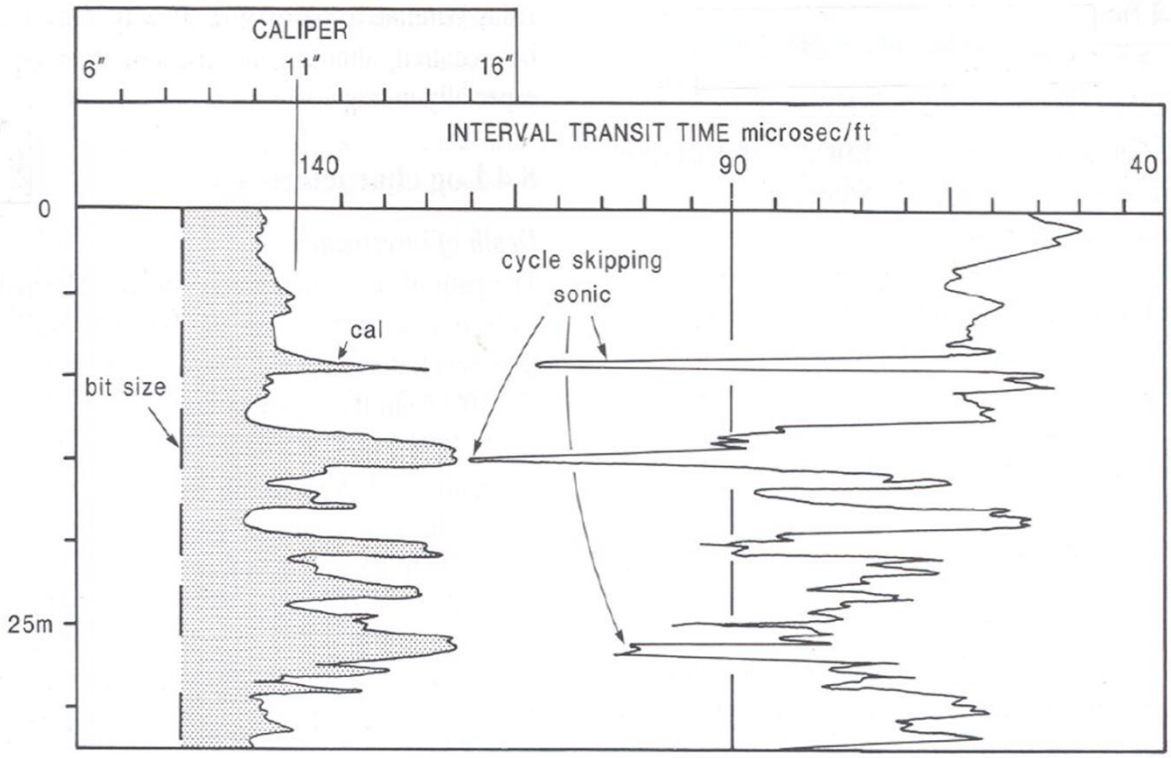

Figure 6.7. Example of cycle skipping in transit time measurements form the Borehole Compensated sonic tool (Rider, 1996).

APPLICATION OF THE SONIC LOG

Qualitative use of the Sonic Log is visual identification of lithology and porous formations (Figure 6.6). The travel time of the sound wave (Δt or DT, μsec/ft) depends on the rock matrix, porosity and saturating fluids of the formation. Typical range of sonic *P*-wave velocity and transit times for nonporous reservoir rock types are provided in Table 6.1. Porosity will increase transit times. Although shales and mudstones typically have low porosities. However, in shales transit travel times are usually higher (60 – 170 μs/ft). This is because shales and mudstones are less consolidated ('softer') than sandstone and carbonate formations. Therefore, as the *P*-wave moves through the shale its energy is dissipated, reducing velocity. Transit times will be decreased in more compacted shales, or those which contain calcareous cements.

POROSITY DETERMINATION FROM THE SONIC LOG ($Ø_E$)

Wyllie Time-Average Equation

Wyllie et al. (1956; 1958) developed a relationship between porosity and *P*-wave transit time for clean unconsolidated formations with uniformly distributed small pores, referred to as the *Wyllie*

Time-Average Equation (Equation 6.1). This equation can be re-arranged to estimate porosity from transit time as a function of matrix and fluid properties (Equation 6.2, also represented as Figure 6.8). Therefore for a known rock matrix and fluid type the formation porosity can be estimated from the sonic log. The fluid transit time 189 μsec/ft for a typical freshwater mud, and 185 μsec/ft for a salt water mud (assuming that the sonic log is responding to *P*-waves travelling through the invaded zone of a formation).

$$\Delta t_{log} = \emptyset_e \times \Delta t_f + (1 - \emptyset_e) \times \Delta t_{ma} \qquad \text{(Equation 6.1)}$$

$$\emptyset_e = \frac{\Delta t_{log} - \Delta t_{ma}}{\Delta t_f - \Delta t_{ma}} \qquad \text{(Equation 6.2)}$$

Where: $\emptyset_e$ – effective porosity, Δt_{log} – log measured P-wave transit time, Δt_{ma} – matrix P-wave transit time, and Δt_f – fluid P-wave transit time.

In typical reservoir sandstones with porosity of 0.15 – 0.25 p.u. (15 – 25 %) the sonic log appears to be relatively independent of disseminated shale and the actual fluid saturating the pores. In some high porosity sandstones, with low water saturation and a very shallow invasion (i.e. pores are filled with hydrocarbon, particularly gas, not mud filtrate) measured transit times will be large, leading to an over estimation of porosity using the Wyllie Time-Average equation. Shaly sands will also increase transit time, and estimated porosity values.

The Wyllie Time-Average equation can be applied to carbonate formations with intergranular porosity. However, when carbonates have undergone diagenesis or tectonic *secondary* processes they may contain pores (vugs and / or fractures) that are larger than the depositional, *primary*, porosity. *P*-waves seem to preferentially exploit the primary, intergranular pore space over the larger secondary pores. As a result, the sonic-derived estimates of porosity in carbonate formations will be lower than that measured by bulk density or the neutron log (the total porosity). If we subtract sonic porosity from density- or neutron-derived porosity the ***secondary porosity*** can be estimated.

In unconsolidated and / or insufficiently compacted sandstones porosity estimated form the sonic log using the Wyllie Time-Average equation are too high. An empirical correction factor can be included to account for unconsolidated formations (C_p, see equation 6.3). C_p varies from 1 to 1.8, and can be calculated, approximately, by dividing the sonic transit time value in over- or underlying shale beds by 100. C_p will vary with depth.

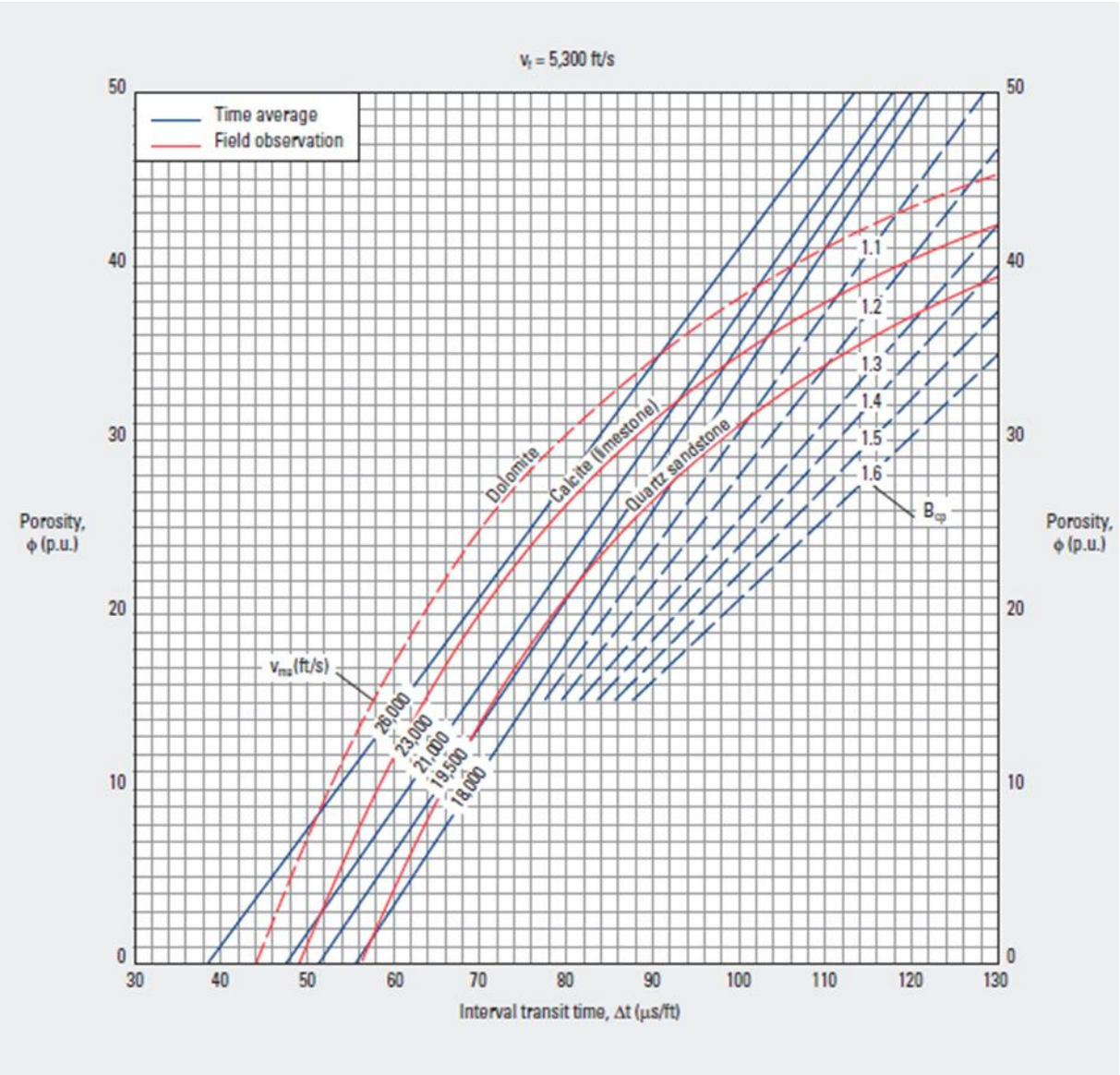

Figure 6.8. Schlumberger Chart Por-1, porosity evaluations from the sonic log (Schlumberger, 2009).

$$\emptyset_e = \frac{\Delta t_{log} - \Delta t_{ma}}{\Delta t_f - \Delta t_{ma}} \times \frac{1}{C_p} \qquad \text{(Equation 6.2)}$$

Raymer-Hunt-Gardner Equation

An alternate to the Wyllie Time-Average equation was presented by Raymer, Hunt and Gardner (1980). The Raymer-Hunt-Gardner equation (Equation 6.5) is completely empirical, based on a comparison of *P*-wave transit times with porosities measured on core and derived from other well logs (Figure 6.9). The constant (C) of 0.63 is commonly used. However, C can vary from 0.6 to 0.7

$$\emptyset_e = 0.63 \times \left(1 - \frac{\Delta t_{ma}}{\Delta t_{log}}\right) \quad \text{(Equation 6.5)}$$

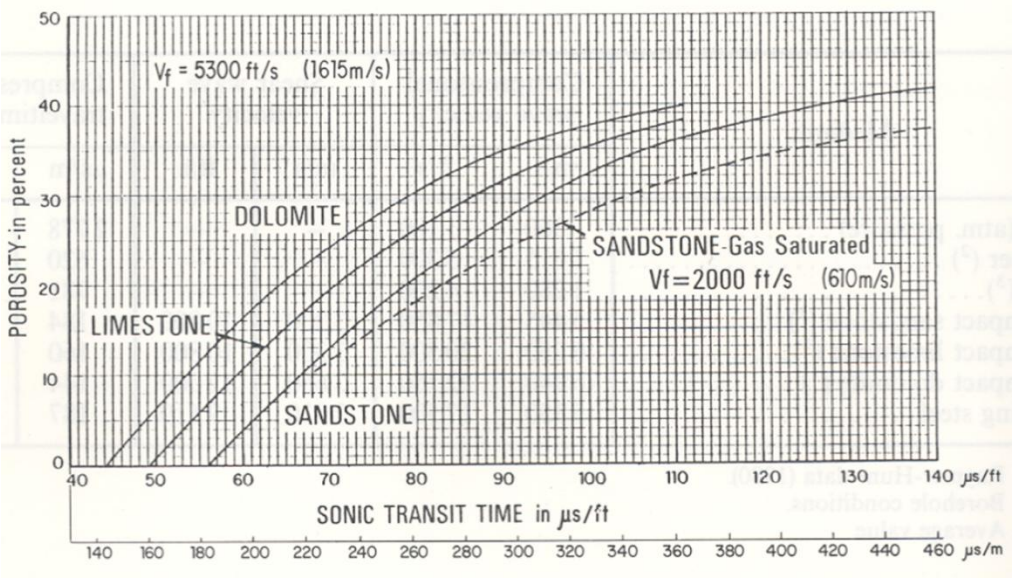

Figure 6.9. The Raymer-Hunt-Gardner graphical relationship between porosity and sonic transit time (Raymer et al., 1980)

Wyllie Time-Average: $\emptyset_e = \frac{\Delta t_{log} - \Delta t_{ma}}{\Delta t_f - \Delta t_{ma}}$				
Lithology	Matrix Δt (μsec/ft)	Fluid Δt (μsec/ft)	Δt log (μsec/ft)	Porosity (fraction)
Sandstone	57	189	80	
Limestone	52	189	80	
Raymer-Hunt-Gardner: $\emptyset_e = 0.63 \times \left(1 - \frac{\Delta t_{ma}}{\Delta t_{log}}\right)$				
Lithology	Matrix Δt (μsec/ft)	Fluid Δt (μsec/ft)	Δt log (μsec/ft)	Porosity (fraction)
Sandstone	57	189	80	
Limestone	52	189	80	

Table 6.2. Porosity estimation for a sonic *P*-wave log measurement of 80 μsec/ft, using different matrix types and the Wyllie Time-Average or Raymer-Hunt-Gardner equations. These are consolidated formations saturated with freshwater.

DETECTION OF ABNORMAL FORMATION PRESSURES

In a 'normal' succession, density will increase and sonic transit time will decrease with depth as the sediment becomes more compacted with burial (e.g. upper section of Figure 6.10). This is referred to as the *normal compaction trend*, and is commonly seen in shale formations – displayed by the shale transit times (Δt_{sh}).

For a set lithology and pore fluid as pore pressure increases the sonic transit time of a *P*-wave will increase (i.e. velocity of the *P*-wave is decreased). The shales that overlay formations with abnormally high fluid pressures will typically have an excess volume of pore water and appear *overpressured*. Overpressured shales can be easily detected in the sonic log depth plot as departures from the normal compaction trend toward high transit time values (e.g. around 2300 ft in Figure 6.10).

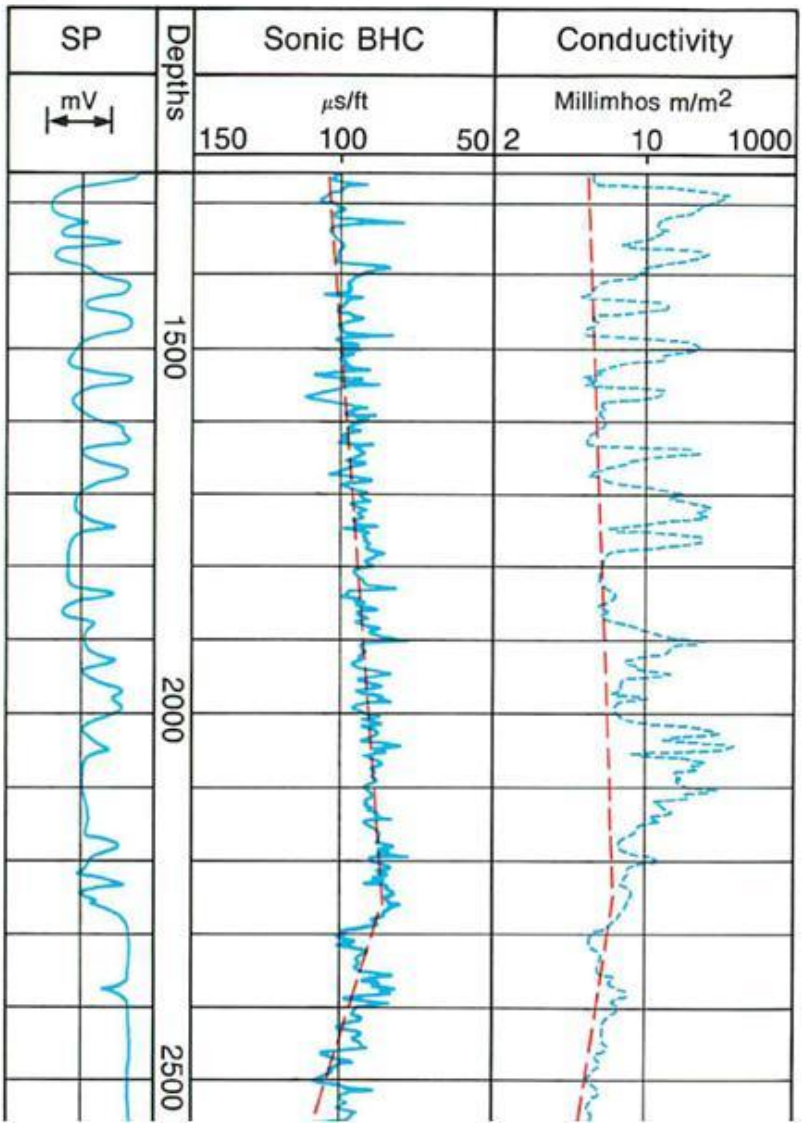

Figure 6.10. Detection of an overpressure shale zone using the Borehole Compensated sonic tool (Schlumberger, 1991).

IMPACT OF BOREHOLE DAMAGE ON SONIC LOG

As the first arrival *P*-wave generally moves at shallow depths through the formation, measured transit times can be affected by mechanical to the borehole wall (as outlined previously regarding hole size and rugosity). The borehole wall can also be damaged by chemical reactions with the drilling mud. An extreme example is shown in Figure 6.11, where progress chemical reaction between shales and drilling mud resulted in the swelling of clays. Over time the clays swell into the borehole and transit time increases. Normally wells are cased (closed) before this can happen, and sonic logs are recorded as soon as possible within a freshly drilled borehole.

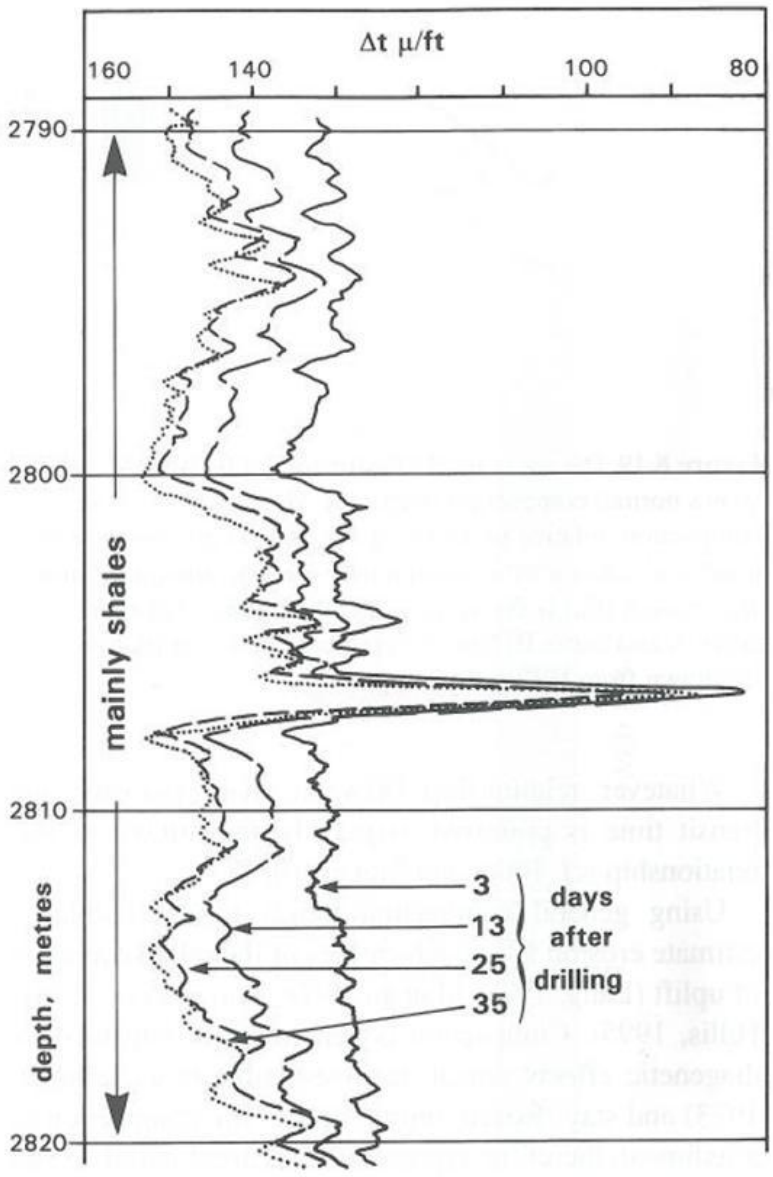

Figure 6.11. Shale alteration over 35 days post drilling, for an offshore well in Columbia (Rider, 1996).

7. LITHOLOGY & POROSITY FROM COMBINED LOG INTERPRETATION

Sections 4 – 6 have described the bulk density, neutron and sonic logs. Each of these can be used independently to estimate porosity in a reservoir formation. These log responses also depend on lithology (matrix, shale content) and fluid types. If a single lithology is know, from drilling cutting or core samples, the appropriate matrix values (ρ_{ma}, $\emptyset N_{ma}$, and Δt_{ma}, or the shale parameters; Table 7.1) can be used to derive the correct porosity values from the wireline logs. Use of single porosity indicator becomes more difficult when two lithologies are present, for example in shaly sandstones. Fortunately, density, neutron and sonic logs respond differently to key matrix minerals and fluid types. Combinations of these, and other, logs can be used to estimate lithology and provide a more accurate value for porosity.

Lithology	GR	Density	Neutron	Sonic	Resistivity	PE
	(API)	*(g/cm^3)*	*(p.u.)*	*(µsec/ft)*	*(ohm.m)*	*($barns/e^-$)*
Sandstone (0% Ø)	Low	2.65	-0.04	53	High	1.81
Limestone (0% Ø)	Low	2.71	0.0	47.5	High	5.08
Shale (0% Ø)	High	2.2 - 2.7 *(water content)*	High *(water content)*	50 – 150 *(water content)*	Low *(water content)*	1 – 5
Dolomite (0% Ø)	Low	2.87	+0.04	43	High	3.14
Anhydrite	Very low	2.98	-0.01	50	Very high	5.06
Salt	Low	2.03	-0.03	67	Very high	4.65
Water	n/a	1.0 – 1.1 *(salt & temp)*	1.0	180 – 190	0 – infinite *(salt & temp)*	0.36 *(+ salt)*
Oil	n/a	0.6 – 1.0 *(api)*	0.7 – 1.0 *(H2 index)*	210 – 240 *(api)*	Very high	Low
Gas	n/a	0.2 - 0.5 *(pressure)*	0.1 – 0.5 *(H2 index)*	~1000	Very high	Low

Table 7.1. Typical log values for common reservoir lithologies and fluids (modified from Baker Hughes)

QUALITATIVE ESTIMATION OF LITHOLOGY AND POROSITY

A qualitative guide to reservoir lithology and porosity can be gained by examining a suite of logs presented on a depth plot (e.g. Figure 7.1). Remember that bulk density, neutron and sonic logs are presented so that porosity increases to the left of the track. Bulk density and the neutron log are traditionally plotted in the same track on a limestone scale (track 2, Figure 7.1). This means that when the two curves overlay lithology may be a tight (non porous) limestone is present. Deflections of the bulk density and neutron logs can be used a qualitative lithology indicator, outlined below.

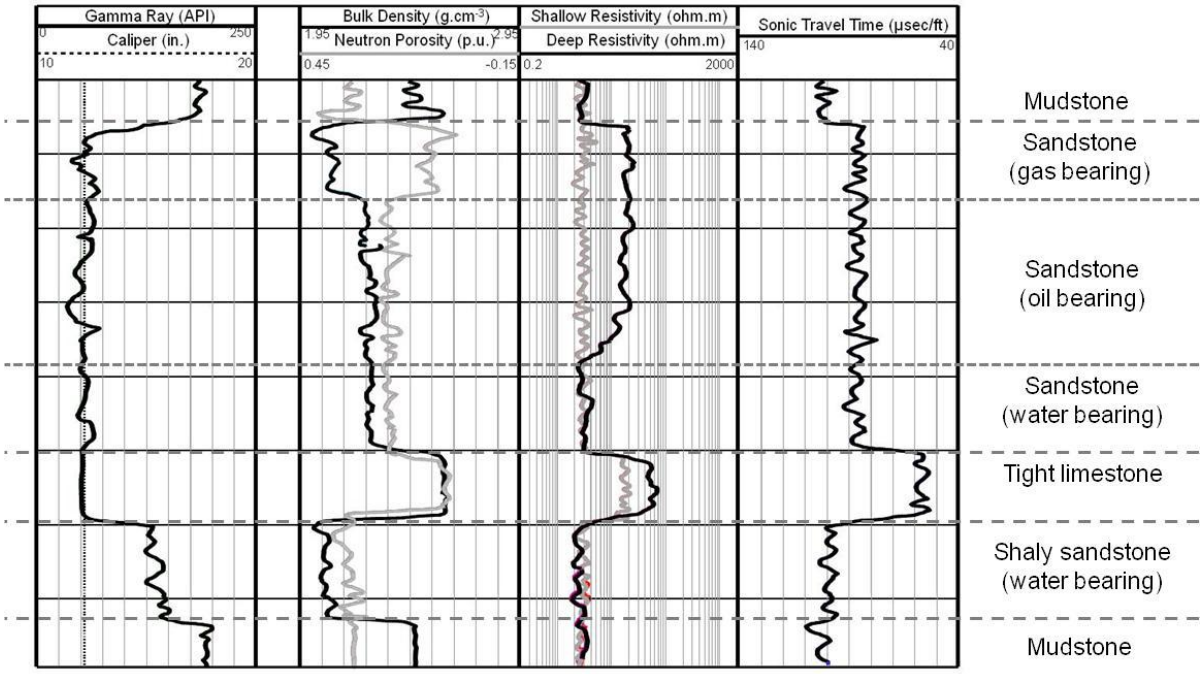

Figure 7.1. Schematic illustration of a typical wireline log suite through a reservoir formation (modified from Shell, 1994).

Sandstone – low gamma ray (non radioactive sands), bulk density deflected to the left and neutron log to the right, moderate transit times (depending on porosity). In water-bearing sandstones deep and shallow resistivity will be similar; the deep resistivity measurement will increase in hydrocarbon zones.

Shale – high gamma ray, bulk density deflected to the right and neutron log to the left. *Generally*, high sonic transit times and low resistivity values.

Shaly sandstone – moderate to high gamma ray. Bulk density deflected to the left and neutron log to the right (separation depending on shale content, separation will decrease with higher shale volume). Both density and neutron will typically be shifted toward the left of the track (suggesting higher porosity. Typically, shaly sands have moderate to high sonic transit times, and low resistivity values in water-bearing formation. Deep resistivity will increase if hydrocarbons are present.

Limestone – Low gamma ray (non radioactive carbonates). Bulk density and neutron log will overlay each other; in a tight limestone neutron will read 0 p.u., both curves will move to the left of the track with increasing porosity. Sonic transit time is generally lower in limestone, but will increase with porosity. Resistivity depends on porosity and fluid types (as with sandstone above), a tight limestone will typically have high resistivity values.

Gas – hydrocarbon gas and oil will have similar high deep resistivity responses. The best visual identification of gas is a very low bulk density value (over estimating porosity), and a very low neutron value (under estimating porosity). This is seen as a large deflection of the density log to the left, and large deflection of the neutron log to the right – *the gas effect*. Gas may also be recorded in slightly higher sonic transit times, than in underlying oil or water-bearing zones. In shaly sandstones the effect of shale and gas on the density and neutron logs may cancel each other out, removing the gas effect. Gamma ray logs will, generally, help to resolve this situation.

Qualitative interpretation of a log suite for broad lithology and porosity cannot be achieved using a single wireline log – as many of the traditional wireline logs as possible should be used to ensure a more accurate prediction. A selection of log plot examples are provided in figures 7.2 – 7.5.

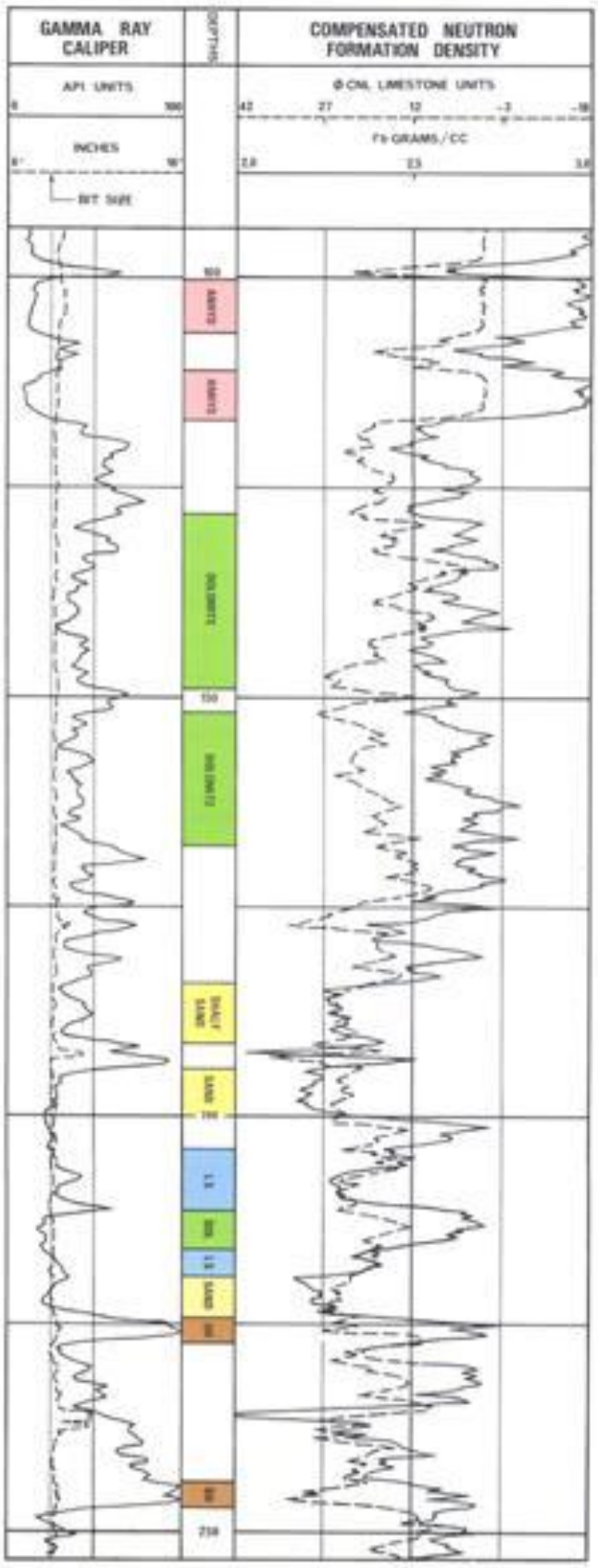

Figure 7.2. Example of Gamma Ray, Formation Density, and Compensated Neutron Logs (after Schlumberger).

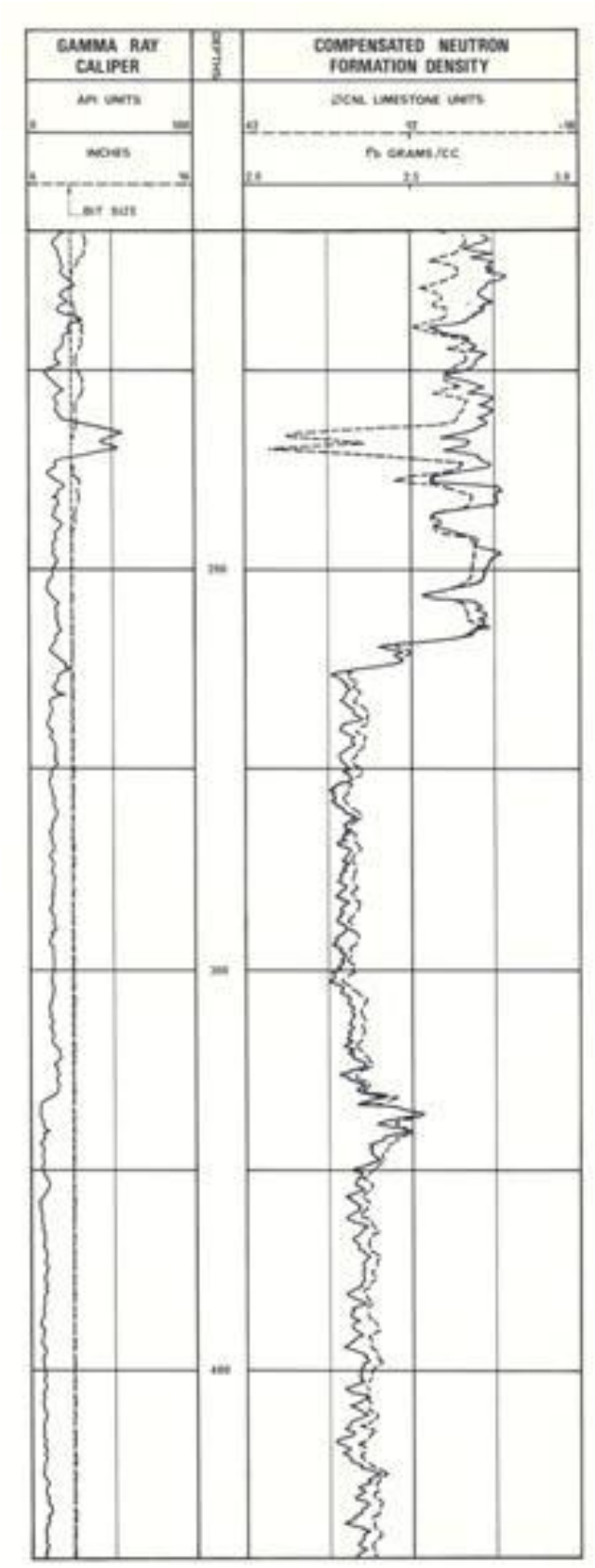

Figure 7.3. Example of Gamma Ray, Formation Density, and Compensated Neutron Logs in a limestone-dolomite succession (after Schlumberger).

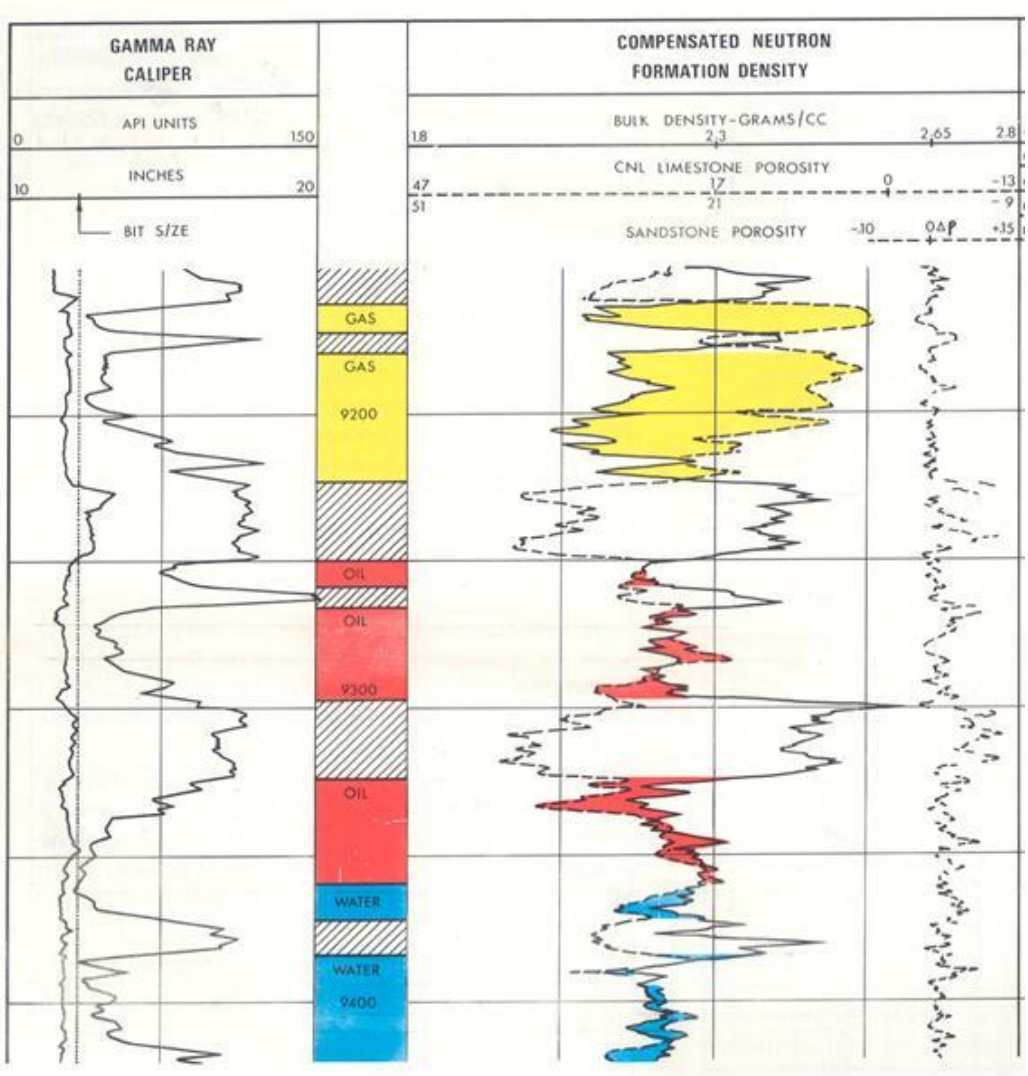

Figure 7.4. Example of Gamma Ray, Formation Density, and Compensated Neutron Logs in a sandstone succession containing water, oil and gas (after Schlumberger).

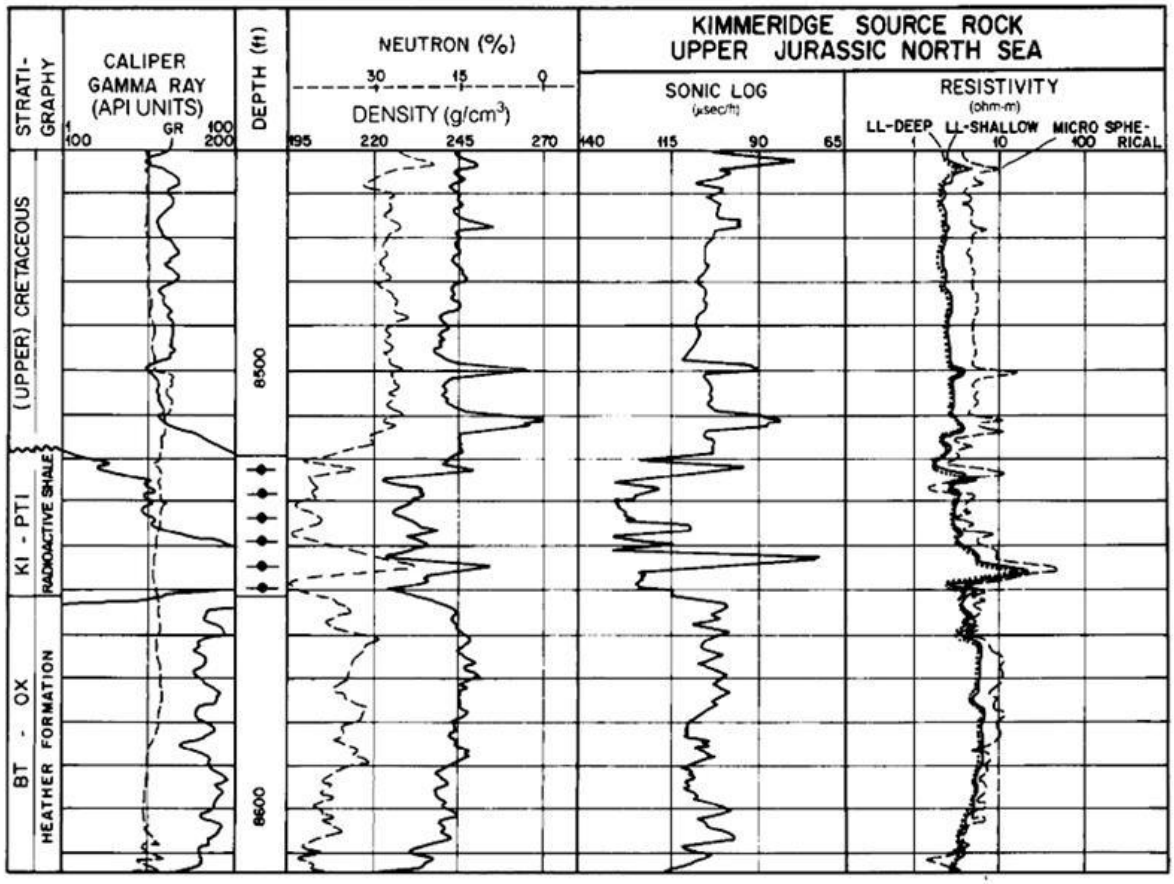

Figure 7.5. Log suite measured for the Upper Jurassic Kimmeridge shale of the North Sea (Meyer & Nederlof, 1984).

QUANTITATIVE ESTIMATION OF LITHOLOGY AND POROSITY BY CROSSPLOTTING

As illustrated above, the individual log responses are difficult to use for gross lithology identification. *Crossplots* provide a simple way to estimate lithology and porosity in a reservoir formation. The crossplots work best when a single lithology is present, but are also of use in binary, dual lithology formations (e.g. sandstone-limestone, limestone-dolomite, sandstone-shale). The four main types of crossplot are:

- Neutron – Density
- Sonic – Neutron
- Sonic – Density
- PE – Density

NEUTRON – DENSITY CROSSPLOTS

The Neutron – Density crossplot is the most commonly used and effective technique for determining gross lithology and estimating porosity. The neutron values are recorded on the x-axis (increasing from left to right), and bulk density on the y-axis (increasing from top to bottom). *Lithology lines* are presented on the plot, showing increasing neutron porosity with decreasing density. The lithology lines were constructed for clean, water-bearing, monomineralic formations. Two examples are shown in Figure 7.6; different charts are provided by the various service companies for use with specific wireline tools. The separation of the lithology lines on this plot indicate a good resolution for differentiating lithology using the Neutron – Density crossplot.

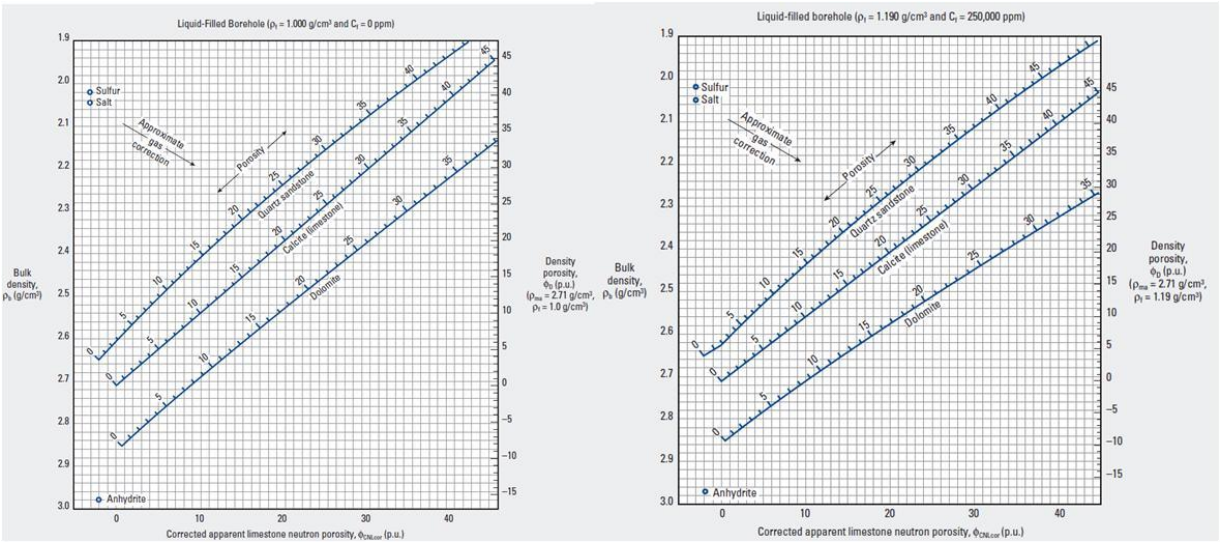

Figure 7.6. Two examples of Density – Neutron crossplots. Left) Schlumberger Chart Por-11, freshwater invaded zone, right) Schlumberger Chart Por-12, salt water invaded zone (Schlumberger, 2009).

Porosity estimation from the Neutron – Density crossplot

In a monomineralic formation the bulk density and neutron log value will plot (intersect) on a single lithology line (Figure 7.7, A). The location along the lithology line provides a porosity value. In a dual mineral system the bulk density and neutron values will intersect between two lithology lines, the relative distance of the point between the lines provides an estimate of the proportion of each mineral in the formation. For dual mineral systems porosity is estimated by taking a line perpendicular to the closest lithology line and reading off the porosity value (e.g. Figure 7.7, B).

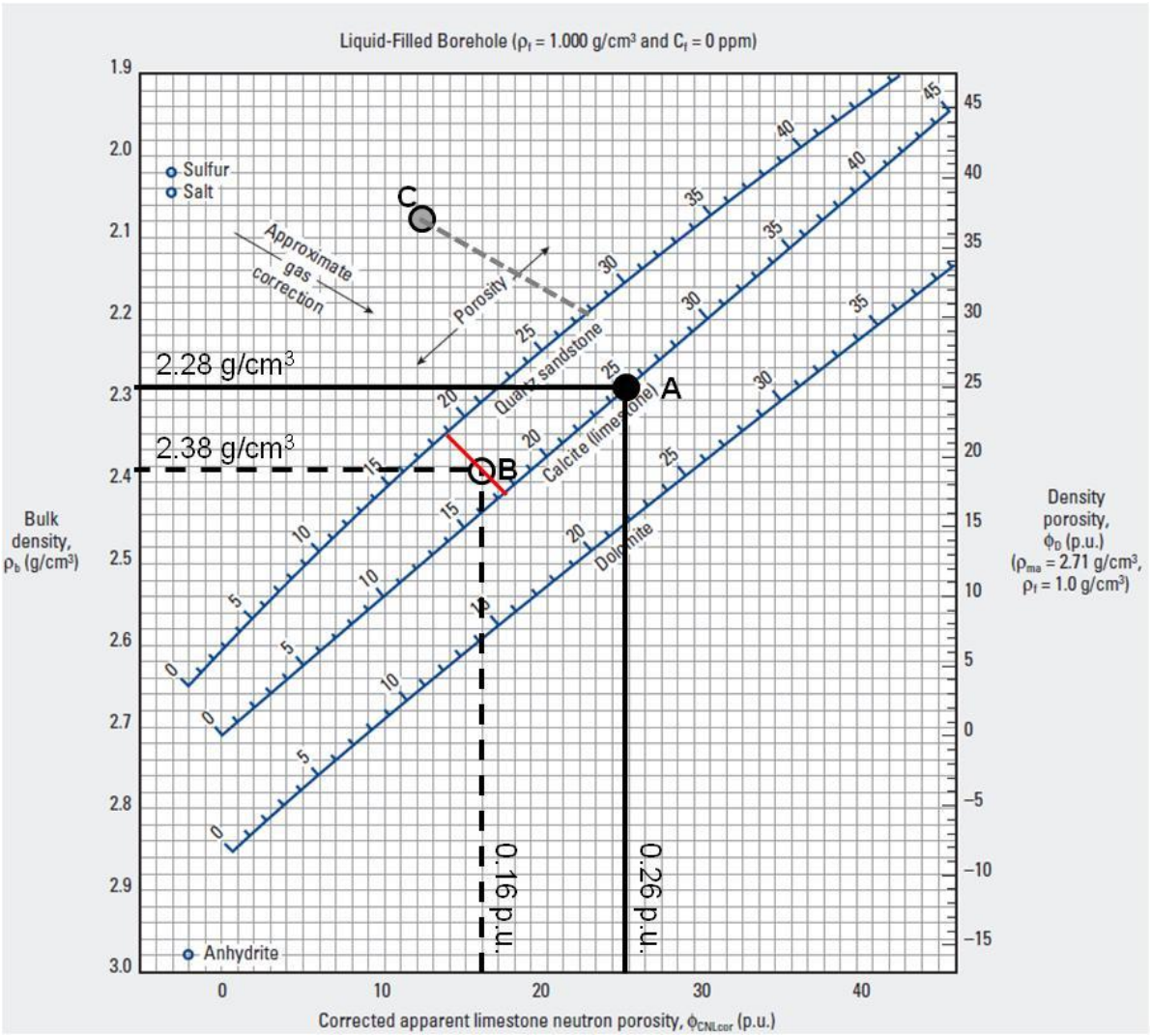

Figure 7.7. Examples lithology and porosity identification using the Neutron - Density crossplots (Schlumberger Chart Por-11). (A) log measurements of 2.28 g/cm^3 bulk density and 0.26 p.u. neutron. (B) log measurements of 2.38 g/cm^3 bulk density and 0.16 p.u. neutron. The diagonal line connecting (B) with the sandstone and limestone lines can be used to estimate proportions of each mineral, *c.* 40 % quartz and 60 % calcite, and porosity is read from the limestone line as ~17.5 % (0.18 p.u.). (C) log measurements of 2.08 g/cm^3 bulk density and 0.12 p.u. neutron, a gas-bearing sandstone.

Error in choosing the lithology line pair in a dual mineral system does not result in a large error in porosity. For example, a bulk density reading of 2.55 g/cm^3 and neutron value of 0.21 (21) p.u. can have a porosity of 18 % on the limestone line, or 18.3 % on the dolomite line.

Along with sandstone, dolomite and limestone, other lithologies can be identified using the crossplot, e.g. anhydrite, rock salt and gypsum.

A gas correction is also provided on the chart. If gas is present in the formation bulk density and neutron values will be under estimated, they will plot away from the lithology lines in the upper left corner of the crossplot. To correct for this, a line can be projected from point toward the appropriate lithology line. The correction line should be parallel to the gas correction arrow (e.g., Figure 7.7, C).

Shale volume from the Neutron – Density crossplot

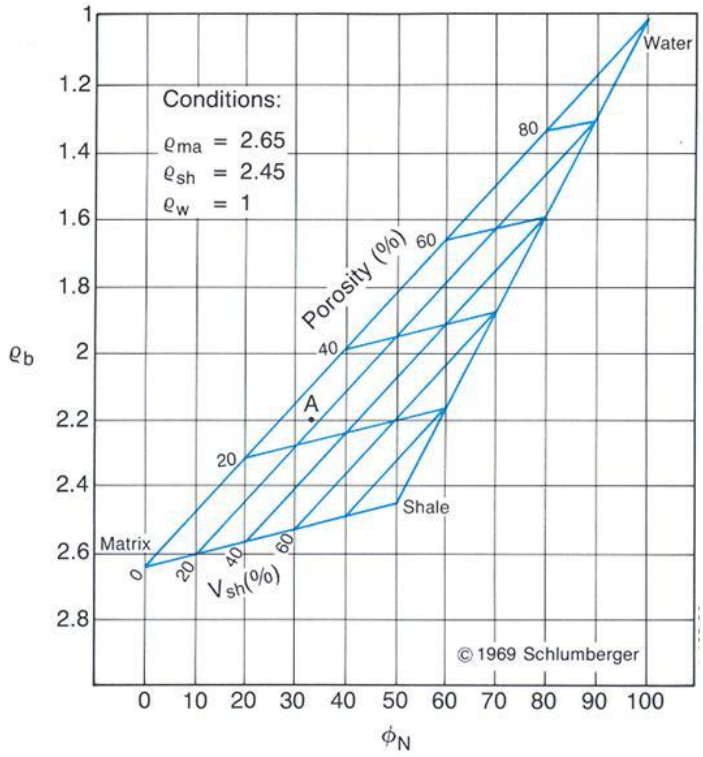

Figure 7.8. Illustration of the principles behind shale volume (Vsh) and porosity estimation using the Neutron – Density crossplot (Schlumberger, 1991).

If the lithology is identified as shaly sandstone (high gamma ray, with sandstone density-neutron separation, Figure 7.1), then the Neutron – Density crossplot can be used to determine the volume of shale or mudstone (Vsh) and correct measured porosity for any clays filling the pore space. The basic principles are illustrated in Figure 7.8.

The *matrix* point (M) is defined as a clean, nonporous material, e.g. quartz with density of 2.65 g/cm^3 and 0 neutron p.u. The fluid, or *water*, point (F) is defined as 100 % porosity that is fully saturated by water, e.g. density of 1.0 g/cm^3 and 1 (100) neutron p.u. The *shale* point (S) is defined as a shale or mudstone without any porosity, fluid or matrix, e.g. density of 2.45 g/cm^3 and 0.5 (50) neutron p.u.

Porosity increases on a line connecting M and F, the *porosity (or lithology) line*. Shale content increases on a line connecting M and S, the *shale line*. Between the end-points each line can be divided into fractions or percentages (Figure 7.8). When a measurement falls within the M-S-F triangle its porosity and shale volume can be calculated; for example in Figure 7.8, a line parallel to the shale line is used to connect point A to the porosity line (giving a porosity of *c*.25 %), and a line parallel to the porosity line can be used to connect point A to the shale line (giving a shale volume of *c*.18 %).

In reality formations with bulk density values less than 2.0 g/cm^3 and neutron values greater than 0.5 (50) p.u. are rare and so only the bottom left quadrant of the chart is used (e.g. Figure 7.7).

The standard procedure to determine porosity and shale volume in a shaly sandstone is outlined below, using Figures 7.9 and 7.10: Point D has density 2.42 g/cm^3, and neutron of 0.33 p.u., it falls below the sandstone line, and is identified as a shaly sand – no limestone or dolomite cuttings were observed, and the gamma ray is higher than in neighbouring clean sandstones.

1) Read the average bulk density and neutron values for a thick, neighbouring shale from the log suite, preferably below or above the reservoir formation. If the shale is a bed within the reservoir the maximum values should be used. Plot the shale point on the Neutron – Density crossplot (e.g. 2.38 g/cm^3 and neutron 0.18 p.u, Figure 7.9).

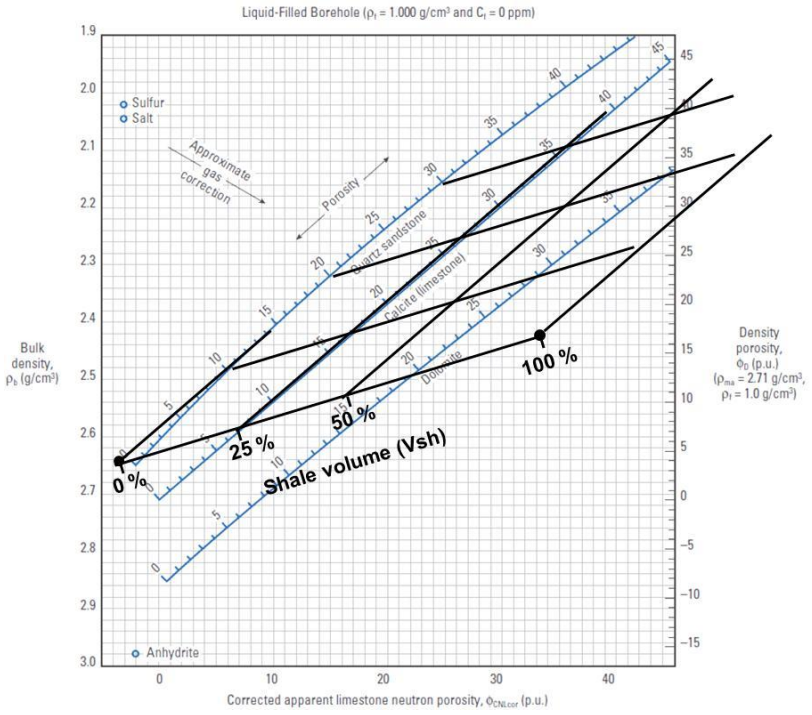

Figure 7.9. Illustration of establishing porosity and shale lines on a Neutron – Density crossplot (modified from Schlumberger Chart Por-11, 2009). The shale point was measured as density of 2.42 g/cm^3, and neutron of 0.33 (33) p.u.

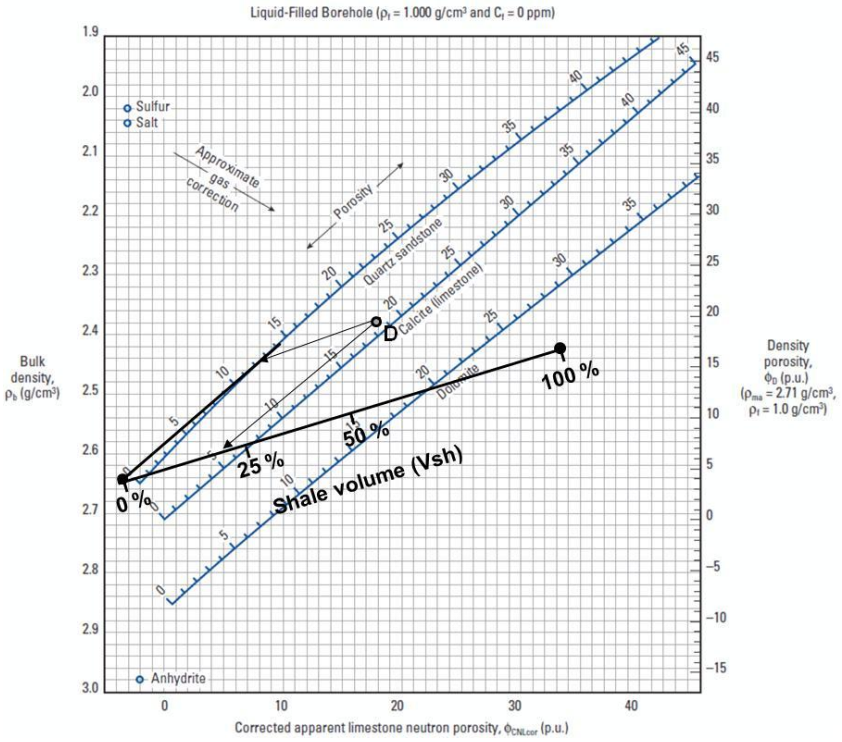

Figure 7.10. Illustration of how porosity and shale volume can be determined for a shaly sandstone formation with density 2.38 g/cm^3 and neutron 0.18 (18) p.u. (modified from Schlumberger Chart Por-11, 2009). The shale point was measured as density of 2.42 g/cm^3, and neutron of 0.33 (33) p.u., see Figure 7.9.

2) Straighten the curved, low porosity end of the sandstone line to represent a matrix point for quartz (density 2.65 g/cm^3 and neutron -0.04 p.u.).
3) Join the shale point to the matrix point to obtain a shale line.
4) Draw equiporosity lines parallel to the shale line.
5) Divide the shale line to represent 10 % increases in shale volume from the matrix point. Draw equi-shale lines parallel to the porosity line (Figure 7.9 only shows the 0, 25, 50 and 100% equi-shale lines for clarity).
6) From reservoir formation point D project a line parallel to the equi-shale lines to determine a corrected porosity value, from the porosity line (e.g. 12.5 %, Figure 7.10). Project a line parallel to the equiporosity lines to determine the shale volume, from the shale line (e.g. Vsh 20 %, Figure 7.10).

OTHER CROSSPLOTS

The Neutron – Density crossplot is but one of four traditional crossplotting methods. The principles of quantitative determination of porosity, and shale volume, and qualitative estimation of lithology are the same for all cross plots types.

Sonic – Neutron crossplot

The Sonic – Neutron crossplot displays neutron values on the x-axis (increasing from left to right), and sonic transit time on the y-axis (decreasing from top to bottom). Lithology lines are presented on the plot, showing increasing neutron porosity with increasing transit time. Two sets of lithology lines were constructed for clean, water-bearing, monomineralic formations; one using the Wyllie Time-Average and one using the Raymer-Hunt-Gardner (field observation) porosity equations for sonic transit time (Figure 7.11A). The large separations between lithology lines on the plot indicate good resolution of the main lithologies using this crossplot, and that porosity is largely independent of lithology. There is no correction provided for gas-bearing zones. An example is shown in Figure 7.11A; different charts are provided by the various service companies for use with specific wireline tools and fluid types.

Sonic – Density crossplot

The Sonic – Density crossplot displays sonic transit time values on the x-axis (increasing from left to right), and bulk density on the y-axis (increasing from top to bottom). Lithology lines are presented on the plot, showing increasing density decreasing with increasing transit time. Two sets of lithology lines were constructed for clean, water-bearing, monomineralic formations; one using the Wyllie Time-Average and one using the Raymer-Hunt-Gardner (field observation) porosity equations for sonic transit time (Figure 7.11B). There is little separation between the lithology lines and lithology resolution is poor. Porosity gradations do not fall on a straight line, therefore porosity is dependent on lithology for this crossplot. These is no correction for gas with this plot type. One example is shown in Figure 7.11B; different charts are provided by the various service companies for use with specific wireline tools and fluid types.

PE – Density crossplot

The PE – Density crossplot displays the photoelectric factor values on the x-axis (increasing from left to right), and bulk density on the y-axis (increasing from top to bottom). Lithology lines are presented on the plot, showing increasing density decreasing with increasing photoelectric factor. The lithology lines were constructed for clean, water-bearing, monomineralic formations. The large spacing between lithology lines indicated good lithology resolution using this plot. Like the Sonic – Density crossplot, equiporosity gradations do not fall on a straight line and so porosity determination is dependent on lithology – this can lead to large errors if matrix is not identified correctly. There is no gas correction for this crossplot. An example is shown in Figure 7.11C; different charts are provided by the various service companies for use with specific wireline tools and fluid types.

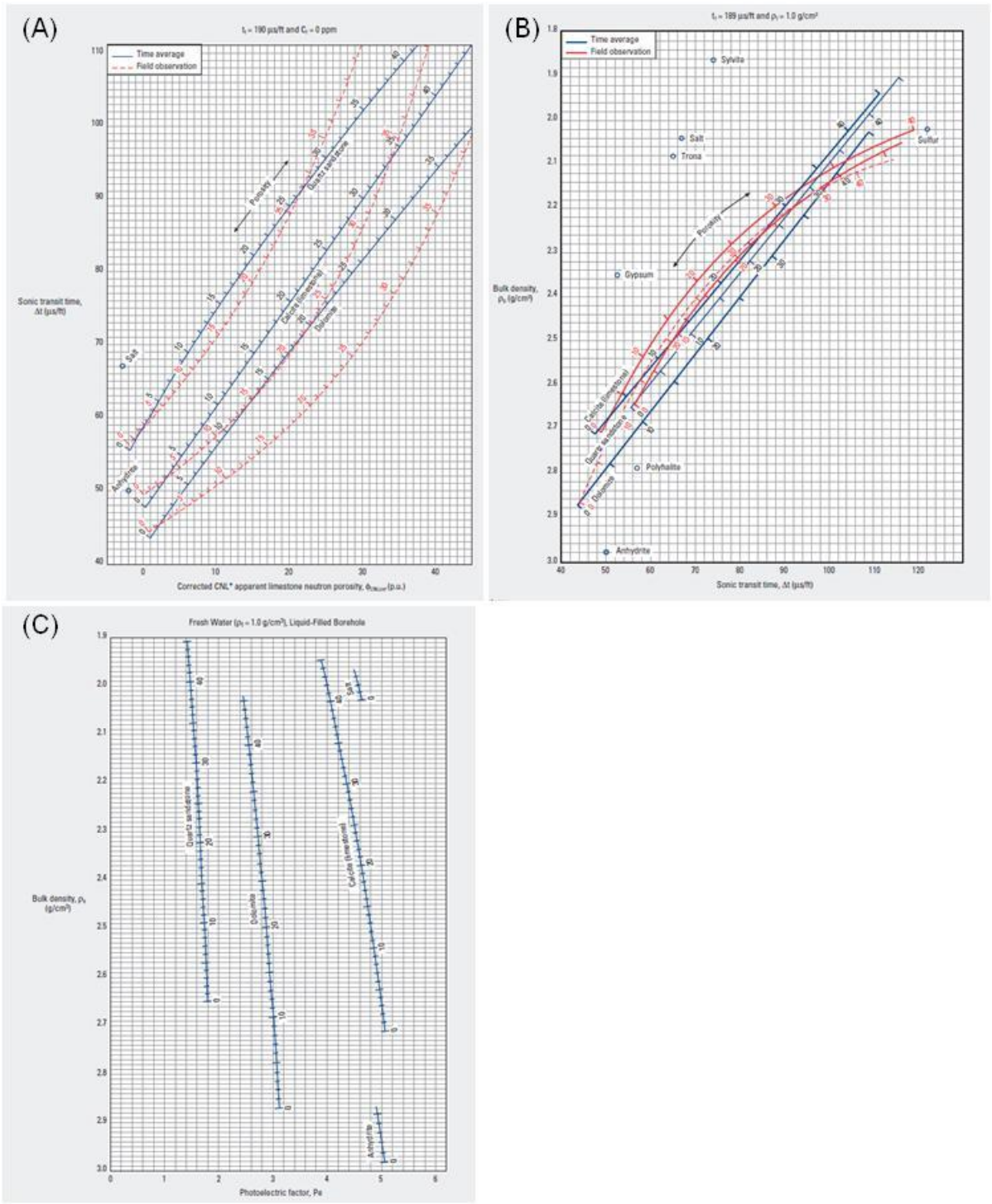

Figure 7.11. Examples (A) Sonic – Neutron crossplots, Schlumberger Chart Por-20, (B) Sonic – Density crossplots, Schumberger Chart Por-22, and (C) PE – Density crossplots, Schlumberger Chart Lith-3 (Schlumberger, 2009).

8. ELECTRICAL RESISTIVITY LOGS

Resistivity logs are the most commonly run wireline measurements. Electrical currents are generally not transported through rock matrix, moving instead through saline formation waters. Dry rock is a good electrical insulator, i.e. it does not conduct electrical currents. Rocks that contain *interstitial* water in their pore space or absorbed in their mineral structure (e.g. clay minerals) will be less resistive, or more conductive. The resistivity of water depends on the concentration of dissolved salts (e.g., NaCl) present; the more saline the water, the higher its conductivity. This resistivity can be measured using a variety of electrical wireline tools. Interpretation of the resistivity log is traditionally focused on understanding water and hydrocarbon saturation within the pore space of a reservoir rock. Resistivity measurements are used to determine saturations in the uninvaded zone (true resistivity, $\mathbf{R_t}$), and the flushed or invaded zone (R_{xo}).

RESISTIVITY THEORY

Resistivity is a fundamental property of any material. Electrical resistivity is the ability of a material to impede the flow of electrical current. Resistivity, or the *specific resistance*, of a material is the resistance measured across a unit cube (typically 1 m^3) at a specified temperature (Equation 8.1). Resistance refers to how a material opposes the flow of an electrical current. Resistivity is a measure of resistance with normalised dimensions, expressed in ohm-metres squared per metre (ohm m^2/m) or simply ohm-metres (ohm.m, Ω.m). Resistivity is the reciprocal of the conductivity (Equation 8.2). The conductivity, or rather the capacity to carry an electrical current, can be measured in the formation around the borehole.

$$R = r\,A/L \qquad \text{(Equation 8.1)}$$

$$R = \frac{1000}{C} \qquad \text{(Equation 8.2)}$$

Where: R – resistivity (ohm.m), r – resistance (ohm), A – cross-sectional area (m^2), L – length (m), and C – conductivity (millimhos/m, mmho/m).

Reservoir formation resistivities can range from 0.2 to >1000 ohm.m. Factors influencing resistivity in a clean, shale free, rock are (1) the resistivity of the formation water (R_w), (2) the temperature of the formation, (3) the presence of any hydrocarbons, and (4) the volume of pore space (Ø).

Where interstitial water contains dissolved salts (e.g. NaCl), the salt will dissociate into cations (positively charged ions, e.g Na^+) and anions (negatively charged ions, e.g. Cl^-). If an electric field is applied then the ions will carry an electrical current through the saline solution.

Formation resistivity factor (F)

The bulk resistivity of a water saturated formation (R_o) is proportional to the resistivity of the formation water (R_w). The constant of proportionality is called the *formation resistivity factor* (*F*). This relationship was observed by Archie in the 1920-1930s (Equation 8.3). *F* will equal one for a rock with 100 % porosity (i.e. 100 % fluid). As we add matrix to the rock, reducing porosity, bulk resistivity will increase (e.g. Figure 8.1). Formation factor can therefore be defined as a function of porosity (Equation 8.4); where '*a*' is the formation factor at 100 % porosity, and '*m*' is the gradient of slope between porosity and formation factor – the *cementation exponent*. Figure 8.1 illustrates that *m* is related to grain shape. Equation 8.4 is referred to as *Archie's First Law*. '*a*' will typically be 0.62 for unconsolidated sands, and 1.0 for compacted reservoir formations.

$$R_o = F \times R_w \qquad \text{(Equation 8.3)}$$

$$F = \frac{a}{\emptyset^m} \qquad \text{(Equation 8.4)}$$

Where: R_o – bulk resistivity, F – formation resistivity factor, R_w – resistivity of formation water, a – Archie tortuosity factor (1), Ø – porosity, and m – cementation exponent.

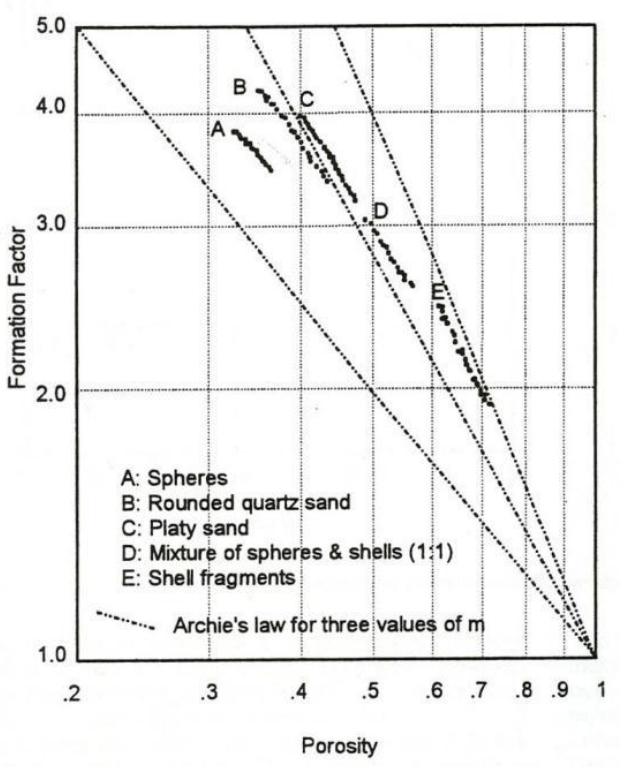

Figure 8.1. Formation factor plotted against porosity, showing the effect of particle shape on the *m* exponent (Jackson et al., 1995).

INVASION AND RESISTIVITY

The process of invasion has been described in section 1. Remember that invasion results in three zones in the formation surrounding a borehole, reflecting the migration of mud filtrate into porous and permeable rocks (Figure 8.2); the *flushed* or invaded zone, the *annulus* or transition zone, and the uninvaded zone. Each zone can contain different fluids and will therefore have different resistivities (Figure 8.1, Table 8.1).

	Borehole	**Flushed zone**	**Transition zone**	**Uninvaded zone**
Fluid resistivity	R_m *(Drilling mud)*	R_{mf} *(mud filtrate)*	R_{mf} & R_w	R_w *(formation water)*
Bulk resistivity		R_{xo}	R_{xo}:R_t	R_o *(water only)* R_t *(water & HC)*
Shoulder bed resistivity (R_s)				
Water saturation		S_{xo}	S_{xo}:S_w	S_w

Table 8.1. Fluid and bulk resistivities associated with invasion.

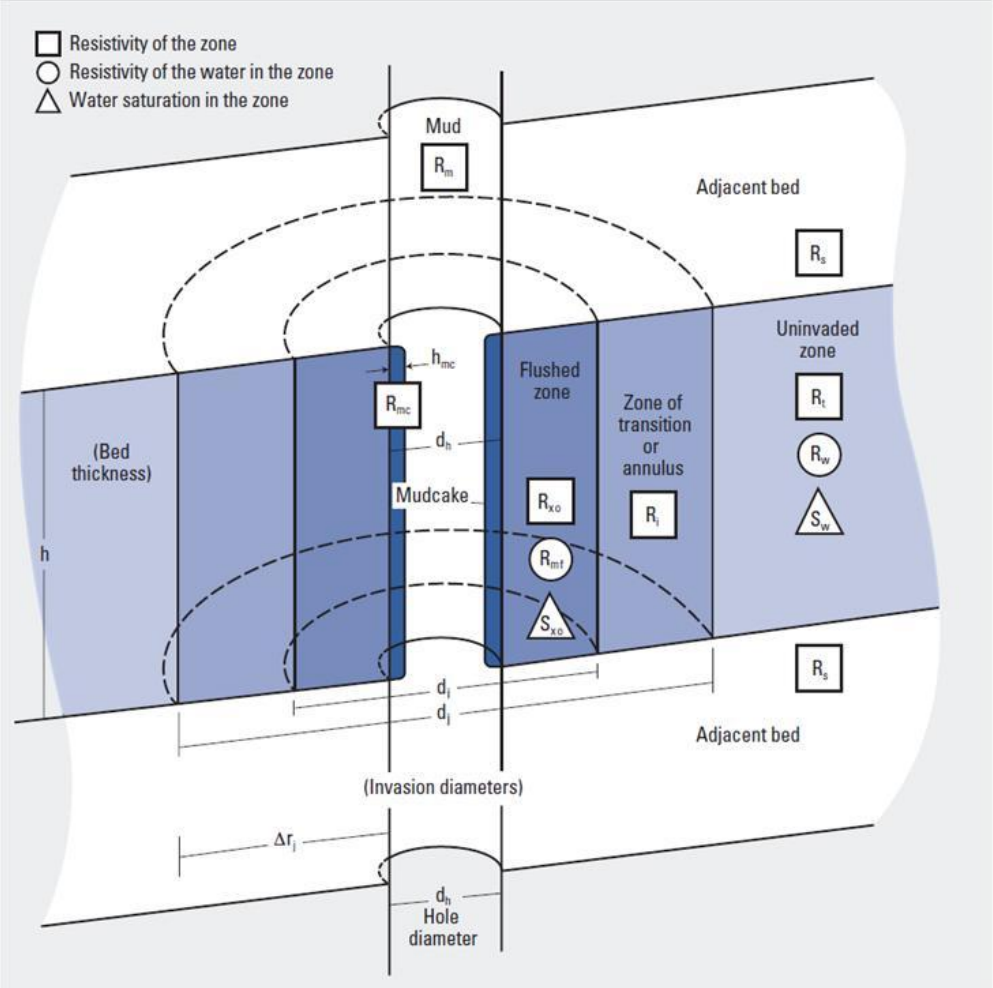

Figure 8.1. Illustration of the zones of invasion and their related resistivity and saturation types, *see Table 8.1*. R_s – resistivity of adjacent '*shoulder*' beds (Schlumberger, 2009).

For a given lithology and porosity, the distribution of different fluids in the zones surrounding a borehole will result in a *resistivity profile* (e.g. Figure 8.2). If the mud filtrate is of a similar salinity to the formation water then the profile will be flat. When the mud filtrate is of lower salinity than the formation water (a freshwater mud) resistivity will be high in the flushed zone, and will decrease toward the uninvaded zone (Figure 8.2). There are three commonly recognised resistivity profiles associated with invasion – a) step, b) transition, and c) annulus (Figure 8.3).

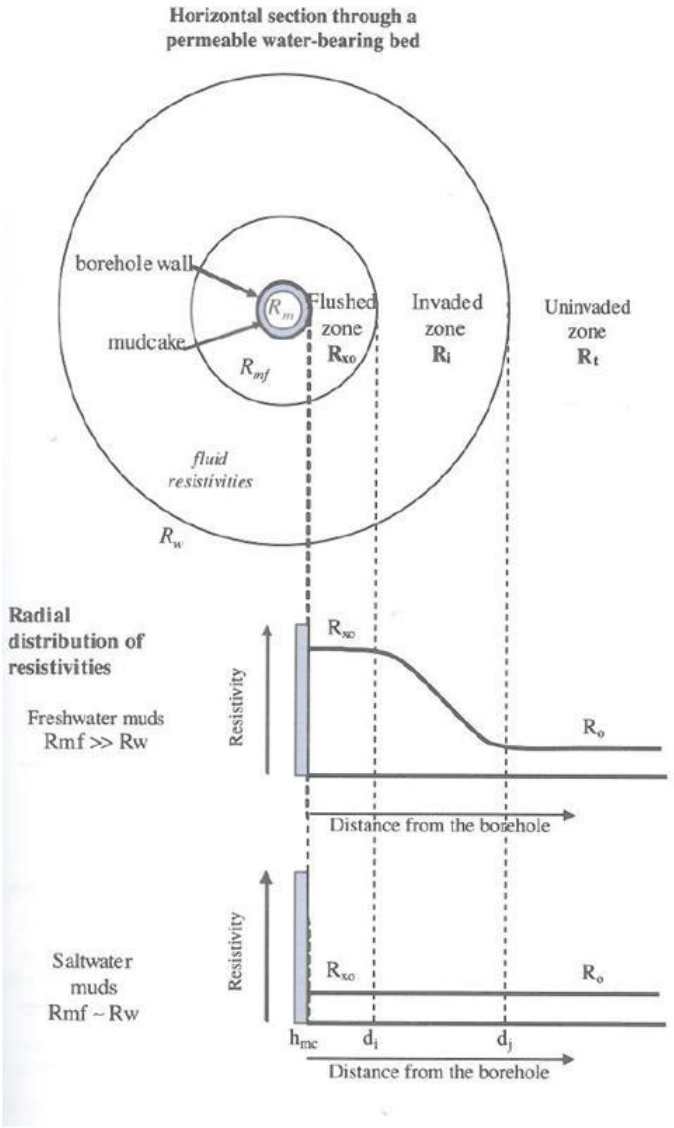

Figure 8.2. Resistivity profile for a transition zone style invasion of a water-bearing formation. Freshwater mud filtrate has greater resistivity than the formation water, saltwater mud filtrate has similar resistivity to the formation water (Asquith & Krygowski, 2004).

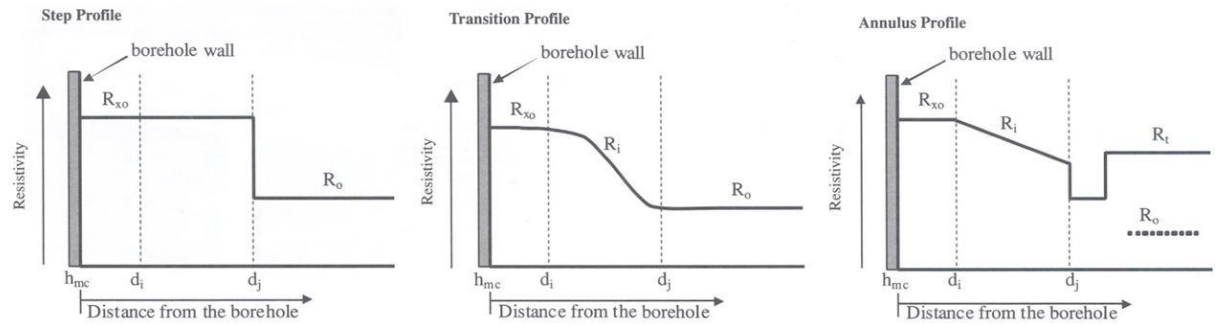

Figure 8.3. Resistivity profiles for three idealised versions of fluid distributions in the vicinity of the borehole (Asquith & Krygowski, 2004).

The *step profile* has a cylindrical geometry with an invasion diameter equal to d_j. There is no, or little, transition zone so that resistivity shows a sharp contrast between the flushed and uninvaded zones.

The *transition profile* also has a cylindrical geometry where the flushed zone diameter is equal to d_i, and a transition zone of diameter d_j-d_i. This is more realistic than the step profile.

The *annulus profile* also has a cylindrical geometry. The annulus profile only occurs in hydrocarbon-bearing formations. It is similar in theory to the transition profile for the flushed and transition zones. As the mud filtrate invades the formation hydrocarbons are displaced (moved out) first. Next, the formation water is pushed out in front of the mud filtrate forming an annular, or circular, ring around the invaded zone (Figure 8.3). The annulus effect is characterised by higher resistivity readings in the uninvaded zone (R_t).

Resistivity logging tools typically measure at shallow and deep depths into the formation (described below, '*principle of measurement*'). The shallow resistivity measurement responds to the flushed zone (R_{xo}), and the deeper measurement is assumed to measure the uninvaded zone (R_t).

PRINCIPLE OF MEASUREMENT OF THE RESISTIVITY LOG

CONVENTIONAL RESISTIVITY TOOLS (NON-FOCUSSED)

In the simplest terms, an electrical current is passed through the formation from current electrodes and the voltage is measured between measure electrodes. It is the measured voltages that provide the resistivity determination by a resistivity logging tool.

In the *normal device* (Figure 8.4, left), a constant current is passed through the formation between electrodes A and B. The resultant potential difference is measured between electrodes M and N. In

reality, electrodes A and M are located on the tool sonde, electrode B is located on the cable armor and electrode N is on an insulation-covered lower end of the wireline cable. The distance between A and M is the *spacing*; generally 40 cm (16 in.) for *short normal spacing*, and 160 cm (64 in.) for *long normal spacing*. The measurement point (O) is assigned at a depth half way between A and M.

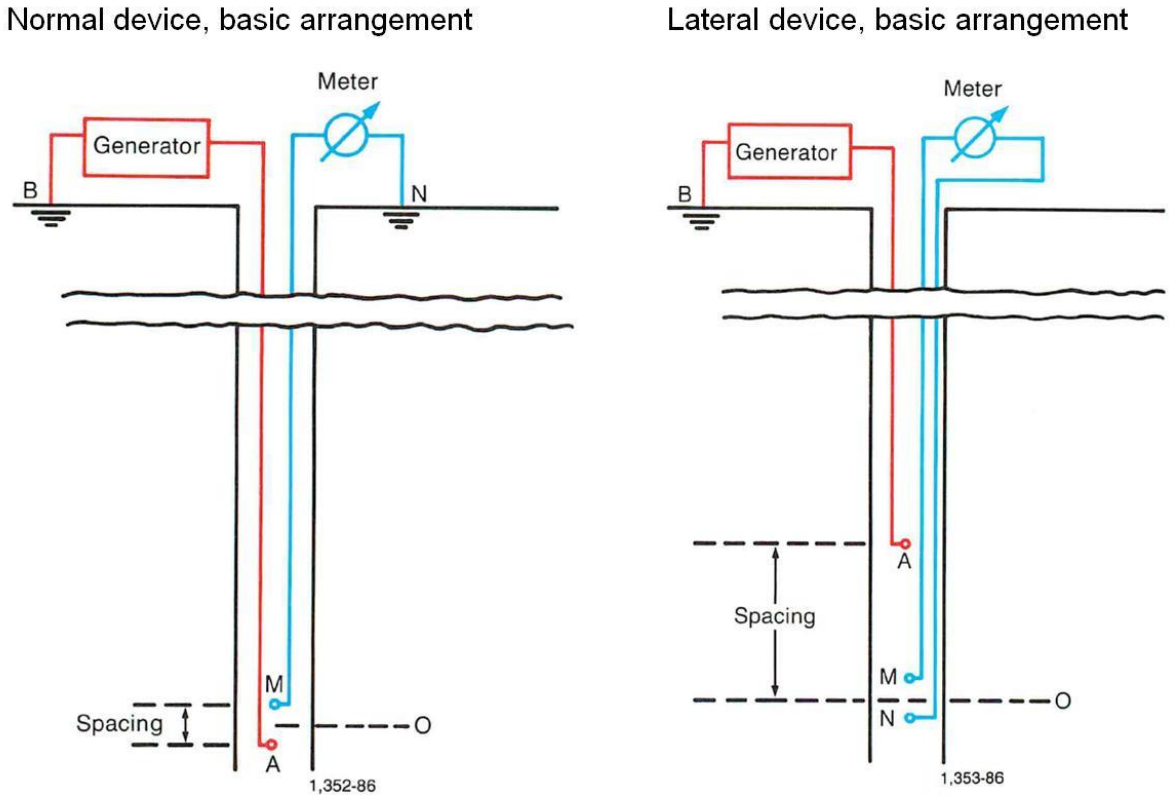

Figure 8.4. Schematic diagrams illustrating the principles of a 'normal' and 'lateral' resistivity logging tool (Schlumberger, 1991).

In the *lateral device* (Figure 8.4, right), a constant current is passed through the formation between electrodes A and B. The resultant potential difference is measured between electrodes M and N. Different to the normal device, electrodes M and N are located on to concentric spherical equipotential surfaces centred on A. Therefore, the voltage measured is proportional to the potential gradient between M and N. Again the measurement is assigned to depth O at the mid-point between M and N. For the lateral device, spacing is the distance between A and O (*c.* 570 cm, 18 ft 8 in.).

For the conventional logs the depth of investigation into the formation increases with the spacing between electrodes. The short normal log represents resistivity in the transition zone (R_i), and the long normal log represents resistivity in the uninvaded zone (R_t). A typical suite of conventional resistivity logs are shown in Figure 8.5.

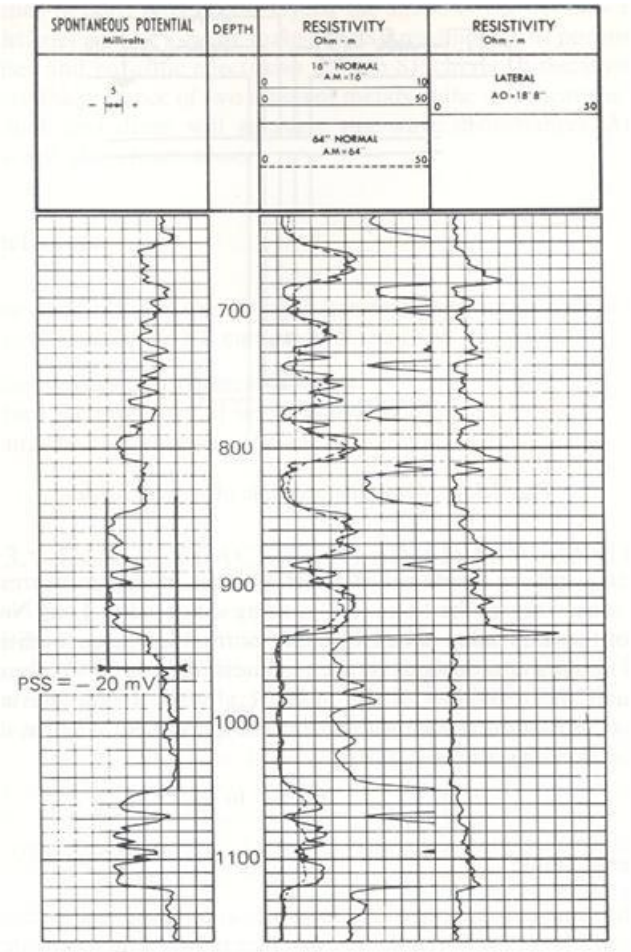

Figure 8.5. A suite of conventional resistivity logs, with the SP log in track 1 (Dresser Atlas, 1982).

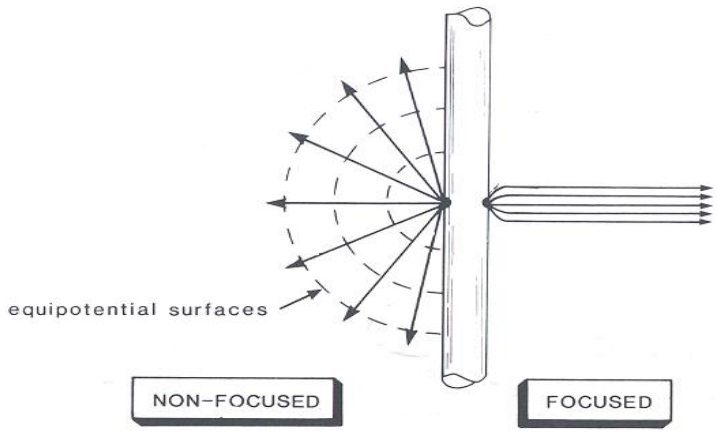

Figure 8.5. Schematic illustration of focussed and non-focussed electrical current distribution around a logging tool (Rider, 1996).

The conventional resistivity logs are not used in modern wireline tool strings, however you may come across them in old wells. The main problem with the conventional logs was that currents were not focused into the formation (Figure 8.5). This led to extensive charts being required for their interpretation, and corrections for borehole, bed thickness, and adjacent bed resistivity effects. Additionally, the conventional logs were relatively inaccurate for bed thicknesses less than 1.5 times the electrode spacing – they had poor vertical resolution.

FOCUSED RESISTIVITY TOOLS

Focused resistivity tools minimise the effects of the borehole and adjacent beds on resistivity measurements encountered for the conventional logging tools, and have excellent vertical resolutions. Focused resistivity tools were introduced in the 1950s and include the Laterologs. These tools measure resistivity in the invaded zone (R_{xo}), transition zone (R_i), and uninvaded zone (R_t); referred to as shallow, medium and deep resistivity logs, respectively. Boreholes need to contain conductive saltwater drilling muds for the focused resistivity tools to operate.

The standard setup of a focused resistivity tool is a central electrode (A_o), and three pairs of electrodes (M_1 & M_2, M_1' & M_2', A_1 and A_2). The electrodes of each pair are symmetrically located above and below A_o, the lower electrode of the pair is denoted as M_1' (e.g. Figure 8.6). A_0 emits a continuous current, referred to as the survey current. The *bucking electrodes*, A_1 and A_2, emit a current of the same polarity as the surveying electrode, forcing the current from A_0 laterally away from the tool and into the formation (Figure 8.6); preventing current from travelling along the tool string. The M electrodes are the measuring the potential difference between the A_o electrode and infinity. The potential difference and the current generated by the A_o electrode are used to calculate the formation resistivity.

To focus the survey current deep into the formation, both the A_1 and A_2 electrodes emit a bucking current (Figure 8.6, left). This provides the deep resistivity measurement (e.g. the Deep Laterolog, LLD). To obtain the medium resistivity measurement (e.g. Shallow Laterolog, LLS), only the A_1 electrode emits the bucking current, while the A_2 electrode sinks the current (Figure 8.6, right). Depth of investigation will depend on the distance between the two A electrodes.

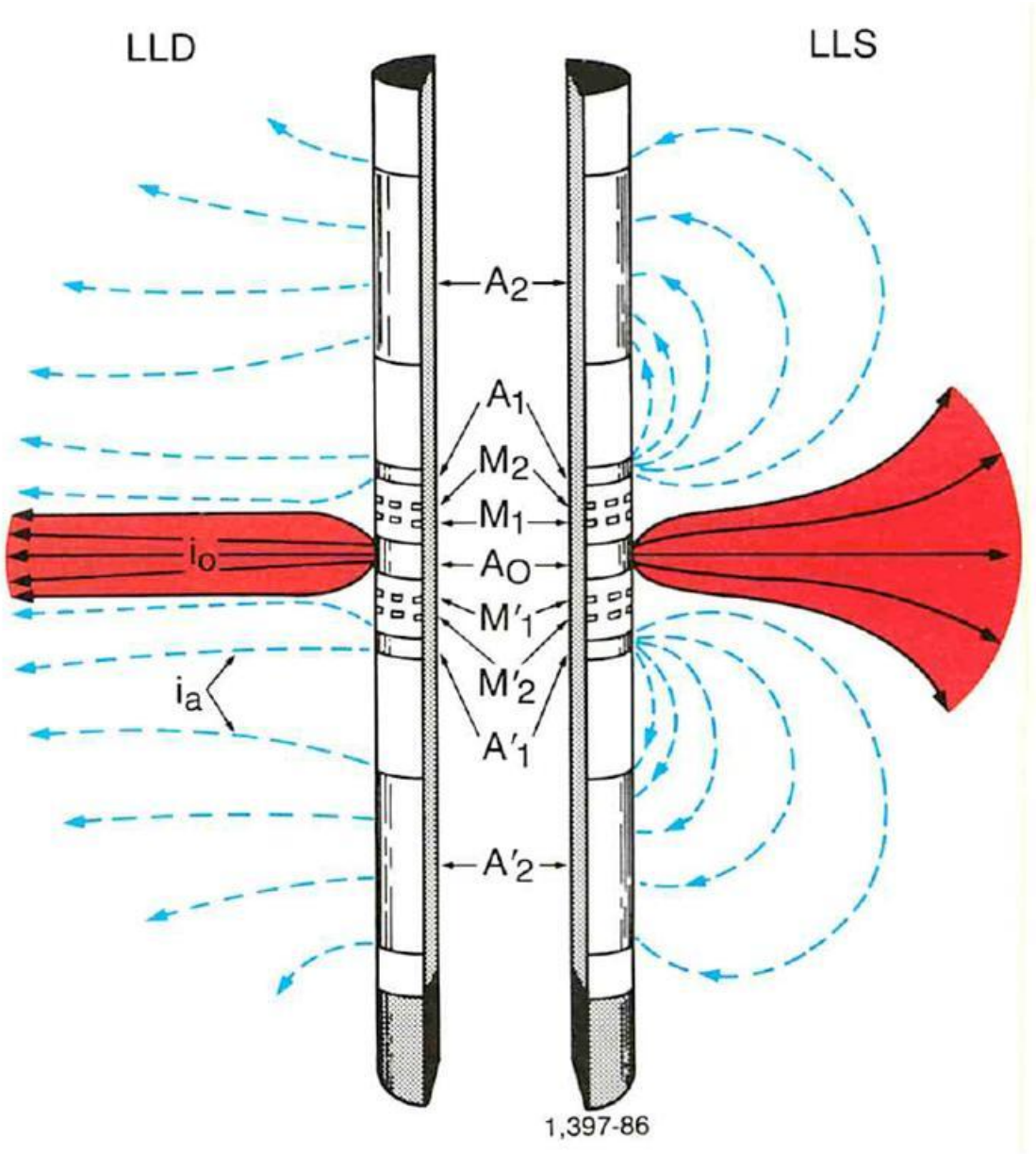

Figure 8.6. Schematic illustration of the Dual Laterolog (Schlumberger, 1991).

While the laterally focused devices focus the survey current into a planar disc, perpendicular to the tool / borehole, an alternate medium resistivity tool is the **Spherically Focused Log** (SFL). The SFL is configured with a single bucking electrode pair (A_1) nearest the surveying electron (Figure 8.7). Consequently, the SFL establishes essentially constant potential shells around the current electrode.

The micro-focused tools were designed specifically to measure formation resistivity in the flushed (invaded) zone (R_{xo}). The microlaterolog, for example, is a pad device comprising a similar electrode set up to the larger focused resistivity logs but at a much smaller spacing (e.g. Figure 8.8).

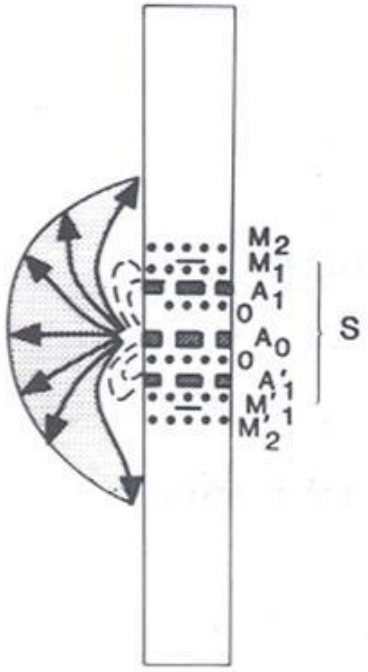

Figure 8.7. Schematic electrode configuration for the Spherically Focused Tool (Rider, 1996).

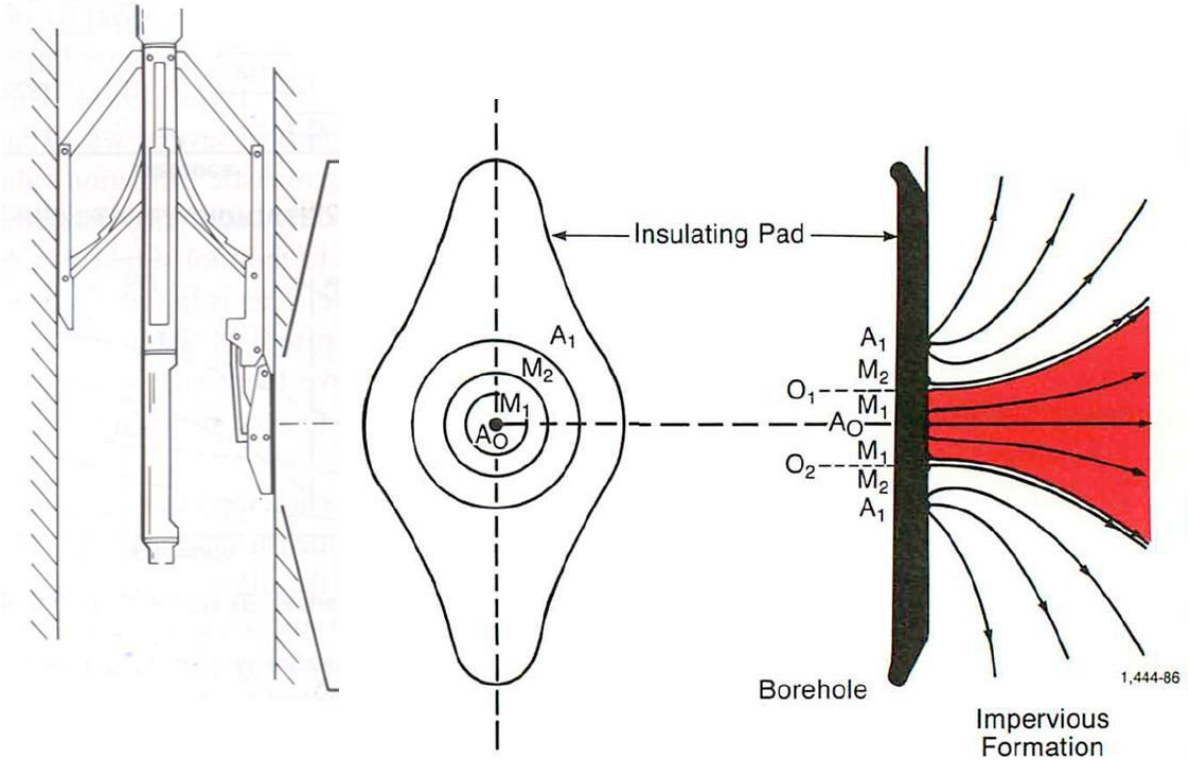

Figure 8.8. Schematic illustration of a micro-focused resistivity tool, e.g. the microlaterolog pad device (Modified from Rider, 1996 and Schlumberger, 1991).

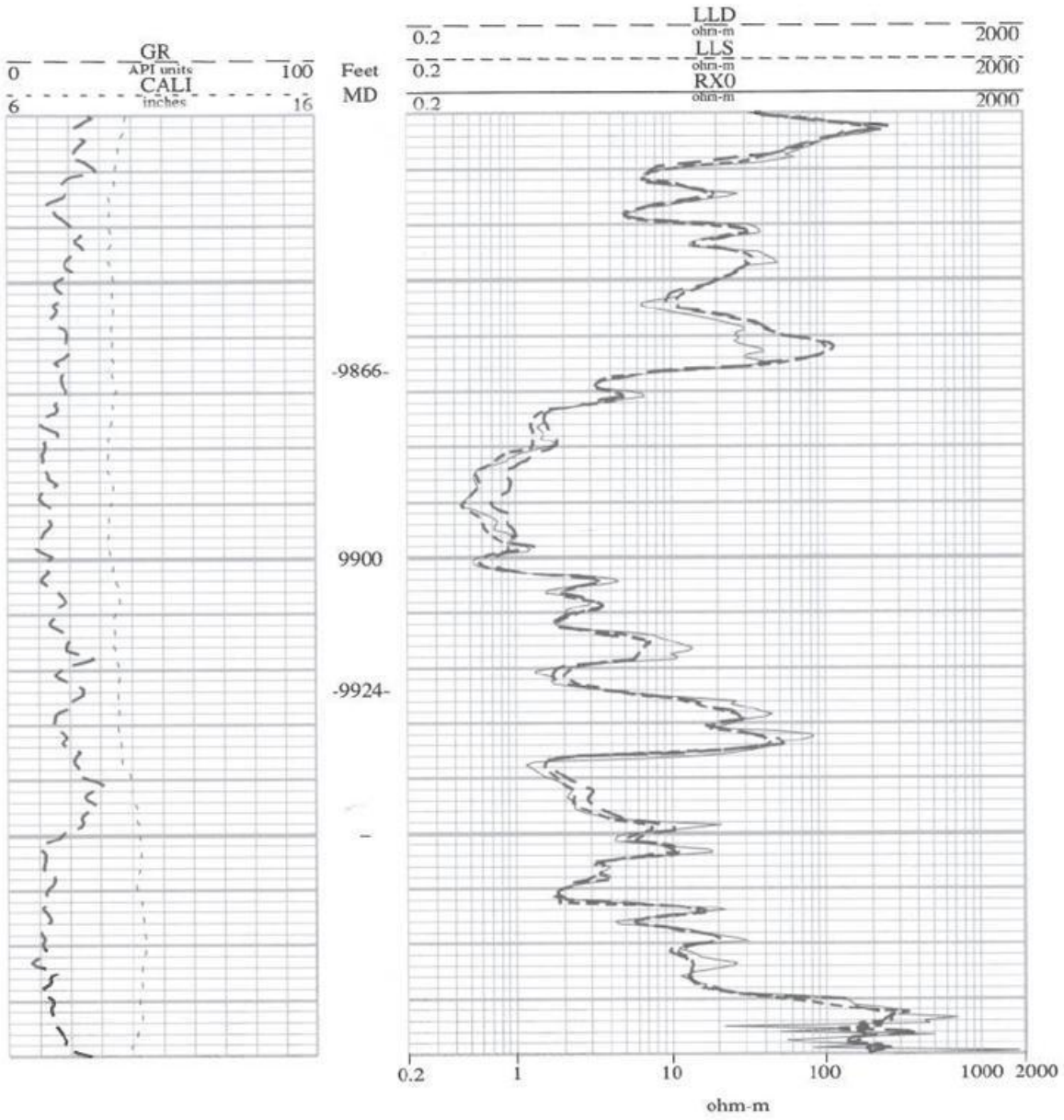

Figure 8.9. Example of laterally focused resistivity logs through a water-bearing formation. LLD – deep Laterolog, LLS – shallow Laterolog, and Rxo – microlaterolog (Asquith & Krygowski, 2004). ***Here, the mud filtrate is more conductive than the formation water – hence the microlaterlog measurement records lower resistivity than the shallow and deep measurements.***

INDUCTION TOOLS

Induction logging tools were originally developed to measure formation resistivity in boreholes containing oil-based, non-conductive drilling mud. Induction logs can also run in boreholes containing conductive drilling muds, alongside the focused resistivity tools – if the mud is not too saline, the formation is not too resistive, and the borehole is not too large.

A high frequency alternating current with constant intensity is sent through a transmitter coil. This creates a magnetic field around the tool, which induces eddy currents in the formation that flow in circulate ground loops coaxial with the transmitter coil. The eddy currents, in turn, create a magnetic field that induces a voltage at the receiver coil (Figure 8.10).

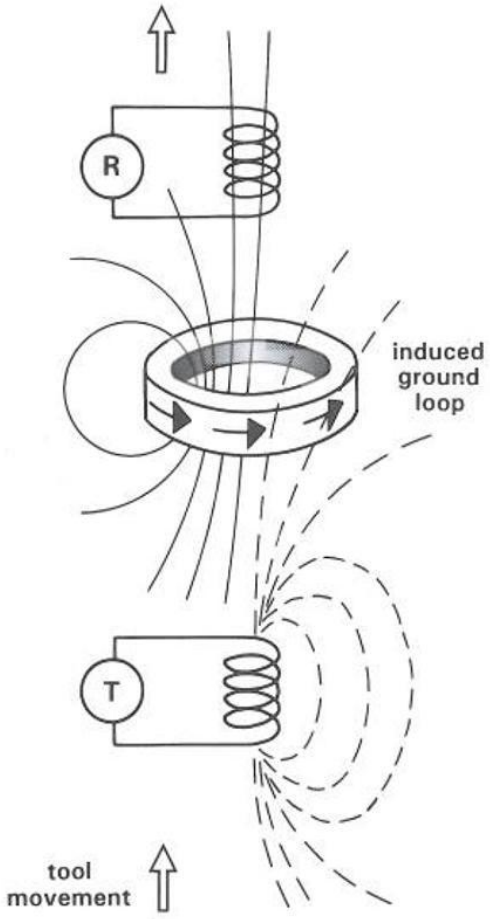

Figure 8.10. A sketch illustration of the principles of a simple induction tool. The vertical component of the magnetic field from the transmitting coil (T) induces a ground loop in the formation which in turn is detected by the receiver coil (R) (Rider, 1996).

As the alternating current in the transmitter coil is of constant frequency and amplitude, the ground loop currents are directly proportional to the ability of the formation to conduct the induced electrical current. Resistivity is derived from this potential voltage measure, conductivity.

In reality the induction tools contain many transmitter and receiver coils, and the response of the multi-coil device is derived from all possible combinations of two-coil transmitter-receiver pairs. These multi-coil devices act to focus their own currents, using bucking in a similar manner to that describe above.

Typical induction log tools include a deep reading device such as the ILD (Induction Log – Deep), and a shallow reading device such as ILM (Induction Log – Medium). Induction logs can be run in combination with the shallow focused or spherically focused resistivity devices for comparison (e.g. Figure 8.11). Note that because induction logs can be run in non-conductive muds we may observe the deep resistivity measurements recording lower values than the medium penetration devices.

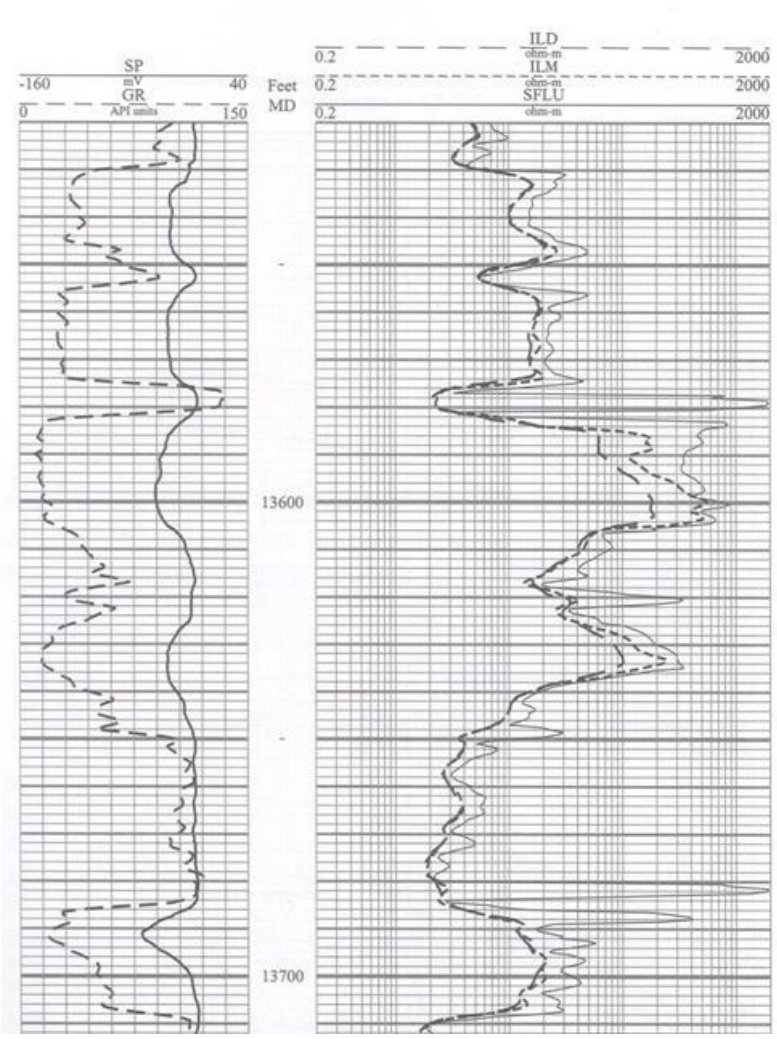

Figure 8.11. An example of the induction log suite (ILD and ILM), presented here with the Spherically Focused resistivity log for comparison (Asquith & Krygowski, 2004).

RECENT ADVANCES IN RESISTIVITY LOGGING

High Resolution Laterolog Array Tool (HRLA)

The High-Resolution Laterolog Array tool operates in six different 'modes'. It uses enhanced focussing to ensure all high resolution signals are recorded at the same time and tool position. The HRLA produces five depth- and resolution-matched measurements across a range of depths into the

formation (RLA1 < RLA2 < RLA3 < RLA4 < RLA5, e.g. Figure 8.12). The measurement RLA0 is also acquired, although seldom used, and provides a measure of resistivity in the borehole (i.e. R_m).

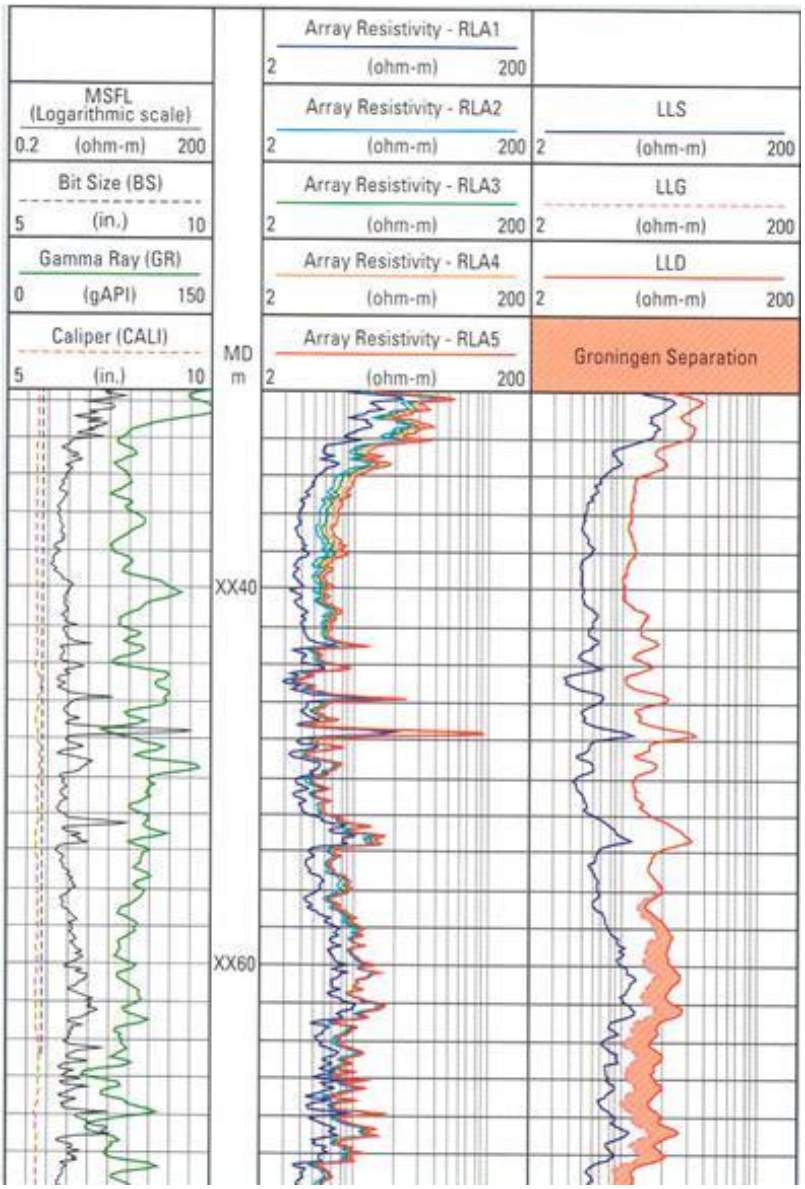

Figure 8.12. An example of the High-Resolution Laterolog Array curves in track 2 of this depth plot (after Schlumberger).

Array Induction Tool (AIT)

The Array Induction Tool operates in the same way as the standard induction tools, but it operates at multiple frequencies and used one emitter coil and four received coils. Signals are processed to generate resistivity curves at series of different depths of investigation at reduced vertical resolution

(e.g. Figure 8.13). Both the AIT and HRLA provide a more detailed understanding of the resistivity profile through invasion.

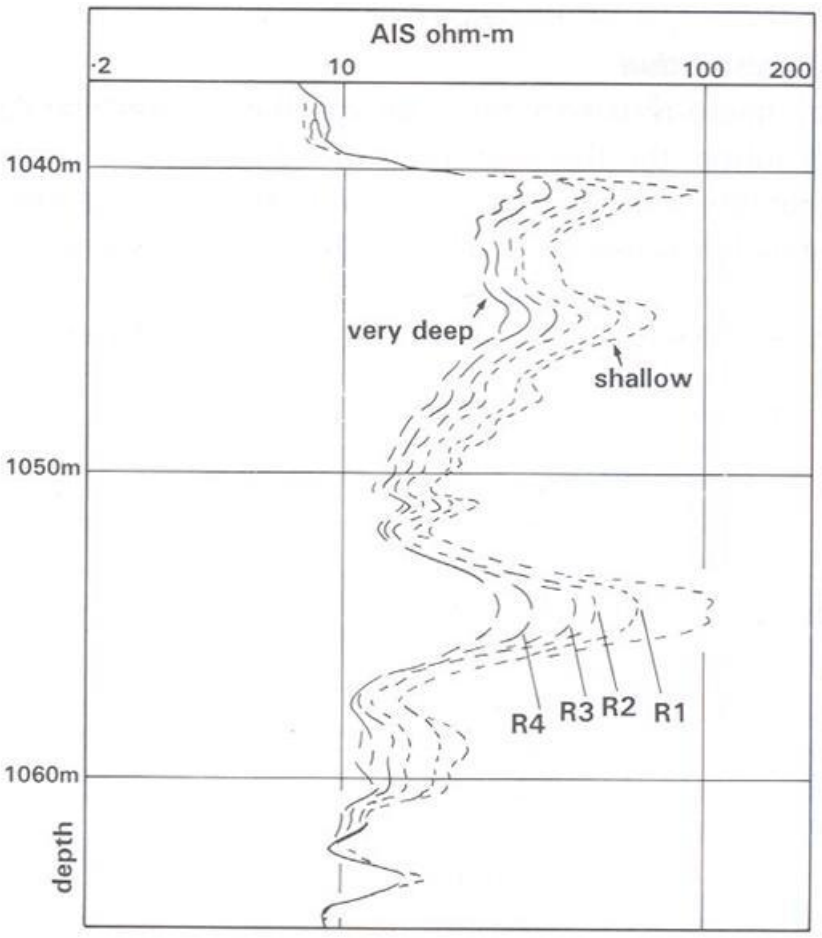

Figure 8.13. An example of the Array Induction Tool in a water-bearing limestone drilled with oil-based mud (Rider, 1996).

PRESENTATION OF THE RESISTIVITY LOG

Formation resistivity measurements can range <0.1 to >1000 ohm.m. Consequently, resistivity logs are traditionally presented on a logarithmic scale. The typical scale ranges from 0.2 to 2000 ohm.m, increasing from the left to right of the track. Scales may differ depending on the maximum resistivity of the formation and the level of detail required for interpretation. Deep, shallow, and micro-resistivity measurements will be displayed on the same track for comparison. See Figures 8.9 and 8.11-8.13 for examples.

QUALITATIVE INTERPRETATION OF THE RESISTIVITY LOGS

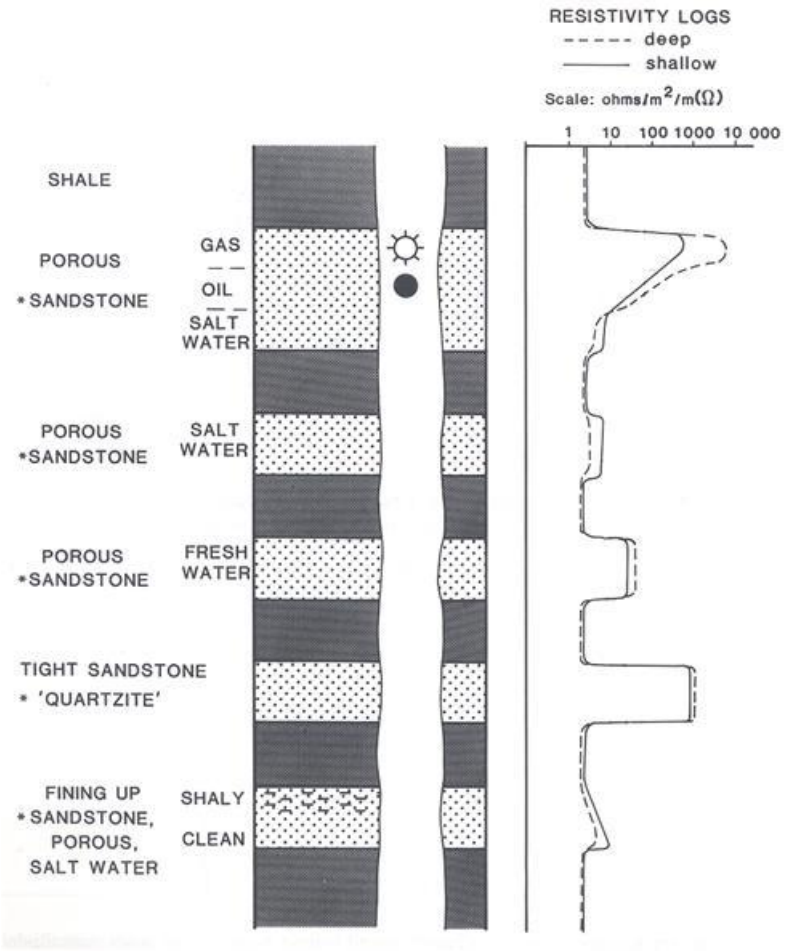

Figure 8.14. Typical responses for the resistivity log. * Sandstone could equally be a clean and porous limestone or dolomite (Rider, 1996).

Gross lithology (*permeable beds*)

Resistivity logs cannot be used as a first order diagnostic of reservoir lithologies, there are no set limits or ranges for the resistivity of individual rock types (sandstone, limestone, dolomite...). However, impermeable beds such as shale, mudstone or tight limestone can be identified if the deep and shallow resistivity curves overlay at the same value. This suggests that the formation is impermeable to the drilling mud, hence invasion effects are not seen (Figure 8.14).

Formation water type, relative to the drilling mud

If a porous formation contains more saline water than the drilling mud the deep resistivity measurement will be lower than the shallow measurement. When the formation contains less saline,

low conductivity water than then drilling mud the deep resistivity measurement will be higher than the shallow measurements (Figure 8.14).

Hydrocarbon

If hydrocarbons are present the resistivity measurements will be higher than in water zones. The deep resistivity will be significantly higher than the shallow measurement (Figure 8.14) – in the uninvaded zone low-non conductive hydrocarbon acts as an insulator within the pore space. Resistivity cannot normally be used to differentiate oil from gas, both are non conductive and so produce similar log responses. In Figure 8.14 the formation water below the hydrocarbon is more saline than the drilling mud as deep resistivity measurement is lower than the shallow measurement.

Resistivity logs can also be used in well correlation exercises, and to identify broad changes in facies associated with differences in mud (shale) volume and porosity.

QUANTITATIVE INTERPRETATION OF THE RESISTIVITY LOGS

As the resistivity logs respond primarily to the presence of conductive fluids contained within the pore space, the main application of resistivity logs is in estimating water and hydrocarbon saturation.

RESISTIVITY INDEX (IR) AND WATER SATURATION

Hydrocarbons are electrical insulators, i.e. non electrical conductors. If present in a formation, hydrocarbon will increase the resistivity. Along with the Formation Resistivity Factor (*F*, Equation 8.4), Archie proposed a second factor called the resistivity index (IR). The resistivity index is the resistivity of a hydrocarbon-bearing rock (R_t) divided by the resistivity of a water-bearing rock (R_o), Equation 8.5 – the resistivity of a formation depends on the ratio of a rock that is fully water-saturated to one that is fully hydrocarbon-saturated.

$$IR = \frac{R_t}{R_o} \qquad \text{(Equation 8.5)}$$

Substituting equation 8.3 for R_o gives equation 8.6.

$$IR = \frac{R_t}{F \times R_w} \qquad \text{(Equation 8.6)}$$

Replacing *F* with equation 8.4 gives equation 8.7. Therefore resistivity index is a product of porosity, resistivity of the formation, and resistivity of the formation water.

$$IR = \frac{\emptyset^m \times R_t}{a \times R_w} \qquad \text{(Equation 8.7)}$$

Archie also showed that the resistivity index is related to water saturation (Equation 8.8), where 'n' is the saturation exponent. This is known as *Archie's Second Law*.

$$IR = \frac{1}{{S_w}^n} \quad \text{(Equation 8.8)}$$

Therefore if we combine equations 8.7 and 8.8 we can see water saturation as a function of porosity, resistivity of the formation, and resistivity of the formation water (Equation 8.9, which can be rearranged to give Equations 8.10 and 8.11). Equation 8.11 is known as the *Archie Saturation Equation*.

$$\frac{1}{{S_w}^n} = \frac{\emptyset^m \times R_t}{a \times R_w} \quad \text{(Equation 8.9)}$$

$${S_w}^n = \frac{a \times R_w}{\emptyset^m \times R_t} \quad \text{(Equation 8.10)}$$

$$S_w = \sqrt[n]{\frac{a \times R_w}{\emptyset^m \times R_t}} \quad \text{(Equation 8.11)}$$

The saturation exponent '*n*' usually varies from 1.8 – 2.5, but is commonly assumed to be 2.0. As outlined previously, '*a*' (the tortuosity factor) and '*m*' (the cementation exponent) can be derived from a plot of porosity against formation resistivity factor. Typical values are presented in Table 8.2, however if specific values are not available for the formation we may assume *m* = 2 and *a* = 1.

a	***m***	**Comments**
1.0	2.0	Carbonates
0.81	2.0	Sandstones (consolidated)
0.62	2.15	Unconsolidated sands
1.65	1.33	Shaly sands
1.45	1.70	Calcareous sands

Table 8.2. Variations in values of *a* and *m* for some reservoir lithologies (after Asquith & Krygowski, 2004).

Porosity must be entered as a fraction (p.u.), not a percentage in the Archie Saturation Equation.

The Archie Equations has the following assumptions:

- Clean formation (Shale volume < 20 %)
- Water saturation is >15 %
- Formation water salinity >20,000 ppm
- Intergranular porosity
- Unimodal pore-throat size distribution
- Water-wet system

- No conductive minerals are present (e.g. pyrite)

Remember, whatever pore space is not filled by water in the uninvaded zone is filled with hydrocarbon. Therefore, hydrocarbon saturation (S_h) = 1 – S_w.

ESTIMATION OF FORMATION WATER RESISTIVITY (R_w)

In mature and producing oil fields formation water resistivity will have been sampled and detailed analyses are available in water catalogues. In exploration wells, R_w can be determined from a sample obtained using extended drill stem tests (DST). However, this may not always be possible and so we must estimate R_w from the wireline log responses. Key methods are:

1) The SP method
2) The Archie method
3) The Ratio method

We have previously described how formation water resistivity can be determined from the SP log (section 3).

The Archie method

Formation resistivity can be calculated by rearranging the Archie Saturation Equation, in a clean (non-shaly) water-bearing formation. Equation 8.10 can be rearranged to give Equation 8.12. In a water-bearing zone there will be no hydrocarbon present and so water saturation equals one. Therefore formation water resistivity can be calculated using equation 8.13.

$$R_w = \frac{{S_w}^n \times \emptyset^m \times R_t}{a} \qquad \text{(Equation 8.12)}$$

$$R_w = \frac{\emptyset^m \times R_t}{a} \qquad \text{(Equation 8.13)}$$

Porosity (in p.u.) can be derived from bulk density log or neutron log (or a combination of the two), and R_t can be read from the deep resistivity log.

The Ratio method

As with the Archie method, in a clean (non-shaly) water-bearing formation, or zone, where the invaded zone is fully saturated with mud filtrate (S_{xo} = 1) and the uninvaded zone is fully saturated with formation water (S_w = 1) the *ratio method* can be used to calculate Rw. As we are looking at a single zone porosity, '*a*' and R_w are assumed to be constant. The ratio of the shallow resistivity measurement (R_{xo}) and the deep resistivity measurement (R_t) will be the same as the ratio of the

resistivity of mud filtrate (R_{mf}) to the resistivity of the formation water (R_w), Equation 8.14. Therefore the resistivity of the formation water can be calculated using Equation 8.15.

$$\frac{R_{xo}}{R_t} = \frac{R_{mf}}{R_w} \quad \text{(Equation 8.14)}$$

$$R_w = R_t \frac{R_{mf}}{R_w} \quad \text{(Equation 8.15)}$$

There may be variations in the R_w values calculated using the SP, Archie and Ratio methods. If this is the case it is suggested that the Archie method be used, as this will always give a water saturation of 1 in the water zone.

DETERMINATION OF MUD FILTRATE SATURATION IN THE FLUSHED ZONE (S_{xo})

The Archie Saturation equation, derived in equations 8.5 – 8.11, can also be applied to the flushed (invaded) zone to estimate the water saturation of the flushed zone (S_{xo}, Equation 8.16). R_w is replaced by R_{mf}, and R_t is replaced by the shallow resistivity measurement (R_{xo}).

$$S_{xo} = \sqrt[n]{\frac{a \times R_{mf}}{\emptyset^m \times R_{xo}}} \quad \text{(Equation 8.16)}$$

Again remember that whatever pore space is not filled by water in the flushed zone is filled with mud filtrate. Therefore, mud filtrate saturation (S_{mf}) = 1 – S_{xo}.

Estimating the fractional volume of mud filtrate in the flushed zone is important as it gives an indication of *hydrocarbon moveability*. A comparison of water saturation in the flushed and uninvaded zones (S_{xo} and S_w, respectively) can be used to determine the bulk-volume fraction of hydrocarbon displaced during invasion. The annulus resistivity profile shown in Figure 8.3 illustrated that as mud filtrate invades the formation it displaces hydrocarbons first, and then formation water. Consequently, water saturation in the flushed zone that originally contained moveable hydrocarbon will be increased ($S_{xo} > S_w$). Equation 8.17 can be used to calculate the moveable oil saturation (MOS), and equation 8.18 provides an estimate of the bulk volume of oil moved during invasion.

$$MOS = S_{xo} - S_w \quad \text{(Equation 8.17)}$$

$$Pore\ fraction\ occupied\ by\ MOS = \emptyset \times (S_{xo} - S_w) \quad \text{(Equation 8.17)}$$

The ratio of water saturation in the uninvaded zone to the flushed zone (S_w / S_{xo}) provides a qualitative index of hydrocarbon moveability (Equation 8.19). If S_w / S_{xo} = 1 then S_w = S_{xo}, and so no hydrocarbons have been moved during invasion. This would suggest that any hydrocarbon present is predominantly residual. Moveable hydrocarbons are indicated by S_w / $S_{xo} \leq 0.7$ in clastic formations, and ≤ 0.6 in carbonate formations.

COMMON ABBREVIATIONS AND SYMBOLS

GENERAL			
a	Tortuosity Factor	POTA	NGR potassium concentration
BHT	Bottom Hole Temperature	PSP	Pseudostatic Spontaneous Potential
BS	Bit Size	R	Resistivity
CALI	Caliper Log	r	Resistance
CBW	Clay Bound Water	RHOB	Bulk Density Log
cm	centimetres	R_i	Transition zone restivity
DRHO	Density correction	R_m	Drilling mud resistivity
DTC	Compressional sonic transit time log	R_{mf}	Mud filtrate resistivity
EFT	Estimated Formation Temperature	R_o	Uninvaded formation resistivity (water bearing)
F	Formation Resistivity Factor	R_s	Shoulder bed resistivity
FVF	Formation Volume Factor	R_t	Uninvaded formation resistivity (hydrocarbon and water bearing)
GR	Gamma Ray Log	R_w	Formation water resistivity
GR_{clean}	Clean Sand GR value	R_{xo}	Flushed zone resistivity
GR_{log}	GR log reading	S_h	Hydrocarbon saturation
GR_{sh}	Shale GR value	SP	Spontaneous Potential
GRV	Gross Rock Volume	SSP	Static Spontaneous Potential
HCIIP	Hydrocarbon initially in place	STOIIP	Stock tank oil initially in place
in.	inches	S_w	Water saturation
IR	Resistivity Index	S_{wi}	Irreducible water saturation
k	Permeability	S_{xo}	Flushed zone water saturation
LWD	Logging While Drilling	THOR	NGR thorium concentration
m	Cementation Exponent	URAN	NGR uranium concentration
MOS	Moveable Oil Saturation	V_{sh}	Volume of shale
MWD	Measurements While Drilling	Δt	Transit time
n	Saturation Exponent	Δt_f	Fluid travel time
NPHI	Neutron Log	Δt_{log}	Transit time measurement
NTG	Net-to-gross	Δt_{ma}	Matrix travel time
Ø	Porosity	ρ_b	Bulk Density reading
$Ø_e$	Effective porosity	ρ_f	Fluid density
ØN	Neutron (porosity) log	ρ_{ma}	Matrix density
$Ø_t$	Total porosity		

UNITS			
API	American Institute of Petroleum (units)	mD	Millidarcy
D	Darcy	ohm.m	Resistivity units
ft	feet	p.u.	porosity units
g/cm^3	Density units	µsec/ft	Sonic travel time units
m	metres	mD	Millidarcy

ELECTICAL LOGS			
a	Tortuosity Factor	ML	Microlog
AIT	Array Induction Tool	MLL	Microlaterolog
CHFR	Cased Hole Formation Resistivity Tool	MSFL	MicroSpherically Focused Log
DIL	Dual Induction Laterolog	*n*	Saturation Exponent
DLL	Dual Laterolog	PL	Proximity Log
HRLA	High Resolution Laterolog Array	R	Resistivity
IDPH	Induction Deep Phasor	R_i	Transition zone restivity
IL	Induction Log	R_m	Drilling mud resistivity
ILD	Deep Induction Log	R_{mf}	Mud filtrate resistivity
ILM	Medium Induction Log	R_o	Uninvaded formation resistivity (water bearing)
IMPH	Induction Medium Phasor	R_s	Shoulder bed resistivity
LL	Laterolog	R_t	Uninvaded formation resistivity (hydrocarbon and water bearing)
LLD	Deep Laterolog	R_w	Formation water resistivity
LLS	Shallow Laterolog	R_{xo}	Flushed zone resistivity
LN	Long Normal	SN	Short Normal
m	Cementation Exponent	SP	Spontaneous Potential

RADIOACTIVE LOGS			
CGR	Computer GR log	PE / PEF	Photoelectric Factor
CNL	Compensated Neutron Log	POTA	NGR potassium concentration
DRHO	Density correction	RHOB	Bulk Density Log
FDT	Formation Density Compensated log	SGR	Standard total GR log
GR	Gamma Ray Log	SNP	Sidewall Neutron Porosity tool
GR_{clean}	Clean Sand GR value	THOR	NGR thorium concentration
GR_{log}	GR log reading	TNPH	Total Neutron Porosity log
GR_{sh}	Shale GR value	URAN	NGR uranium concentration
LDT	Litho-Density log	URAN	Volumetric photoelectric absorption index
NGS	Natural Gamma Ray Spectroscopy	ρ_b	Bulk Density reading
NPHI	Neutron Log	ρ_f	Fluid density
ØN	Neutron (porosity) log	ρ_{ma}	Matrix density

SONIC LOGS			
AST	Array-Sonic Tool	Δt	Transit time
BHC	Borehole Compensated Sonic tool	Δt_f	Fluid travel time
DTC	Compressional sonic transit time log	Δt_{log}	Transit time measurement
LSS	Long-Spaced Sonic tool	Δt_{ma}	Matrix travel time

SELECTED REFERENCES

Text Books

Asquith, G & Krygowski, D. (2004). Basic Well Log Analysis (2nd ed). AAPG Methods in Exploration Series, 16. AAPG, Tulsa, Oklahoma.

Baker Hughes (2011). Log Interpretation Charts. Baker Hughes Inc. Houston, Texas

Baker Hughes (2011). Introduction to Wireline Log Analysis. Baker Hughes Inc., Houston, Texas.

Coates, G.R., Xiao, L. & Prammer, M.G. (1999). NMR Logging Principles and Applications. Haliburton Energy Services, Houston, Texas.

Doveton, J.H. (1994). Geologic Log Analysis Using Computer Methods. AAPG Computer Applications in Geology, 2. AAPG, Tulsa, Oklahoma

Ellis, D.V. & Signer, J.M. (2007). Well Logging for Earth Scientists (2nd ed.). Springer, Netherlands.

Lovell, M. & Parkinson, N. (eds). (2002). Geological Application of Well Logs. AAPG Methods in Exploration Series, 13. AAPG, Tulsa, Oklahoma

Rider, M. (1996). The Geological Interpretation of Well Logs (2nd ed.). Rider-French Consulting Ltd, Scotland.

Rider, M. & Kennedy, M. (2011). The Geological Interpretation of Well Logs (3rd ed.). Rider-French Consulting Ltd, Scotland.

Schlumberger (1991). Log Interpretation Principles / Applications. Schlumberger Wireline & Testing, Houston, Texas.

Schlumberger (2009). Log Interpretation Charts. Schlumberger, Sugar Land, Texas.

Tiab, D. & Donaldson, E. (1996). Petrophysics: theory and practice of measuring reservoir rock and fluid properties. Gulf Publishing Company, Houston.

Theys, P. (1999). Log Data Aquisition and Quality Controls (2nd ed.). Editions Technip, Paris

Journal Articles

Allen, D., et al. (1989). Logging While Drilling. *Oilfield Review*, April, 1989, p 4-17.

Andersen, M.A. (2011). Discovering the Secrets of the Earth. *Oilfield Review*, 23 (1), p. 59-60.

Archie, G.E. (1942). The Electrical Resistivity Log as an aid in determining some reservoir characteristics. *Petroleum Technology*, 5, p. 54-62.

Betts, P. et al. (l 990). Acquiring and interpreting logs in Horizontal wells. *Oilfield Review*, 2 (1), p. 34-51.

Brown, E. & Milne, A. (1990). The Challenge of completing and stimulating horizontal wells. *Oilfield Review*, July, 1990, p. 52-63.

Elliott, H.W. (1983). Some 'Pitfalls' In Log Interpretation. *Log Analyst*, 24, p. 10-24.

Hatton, I.R., Reeder, M., Newman, M. St J. & Roberts, D. (1992). Techniques and applications of petrophysical correlation in submarine fan environments, early Tertiary sequence,North Sea. *IN* Geological Applications of Wireline Logs II, A. Hurst, C.M. Griffiths & P.F. Worthington (eds.), Geol Soc Spec Pub, No 65, p. 21-30.

Hilchie, D.W. (1968). Caliper Logging – theory and practice. *The Log Analyst*, 9 (1), p. 3-12.

Hook, J.R. (2003). An Introduction to Porosity. *Petrophysics*, 44, 205-212.

Jackson, P., Jarrard, R., CJ, P. & Pearce, J. (1995). Resistivity/Porosity/Velocity Relationships from Downhole Logs: an aid for evaluationg pore morphology. *Proceedings of the Ocean Drilling Program, Scientific Results*, 133, p. 661-681.

Jenkins, R.E. (1960). Accuracy of porosity determinations. First SPWLA Logging Symp., Tulsa, Oklahoma.

Meyer, B.L. & Nederlof, M.H. (1984). Identification of source rocks on wireline logs by density/resistivity and sonic transit time/resistivity crossplots. *AAPG Bulletin*, 68, p. 121-29.

Raymer, L.L., Hunt, E.R. & Gardner, G.H.F. (1980). Improved Sonic Transit Time-to-Porosity Transform. *SPWLA Logging Symposium Transactions*, July, 1980.

Simandoux, P. (1963). Mesures dielectriques en milieu poreux, application a mesure saturation en eau: Etude du Comportement des Massifs Argileux: Revue de l'instutu Francais du Petrole, Supplementary Issue (Translated text in SPWLA Reprint Volume, Shaly Sand, July 1982).

Wyllie, M.R.J., Gregory, A.R. & Gardner, G.H.F. (1956). Elastic Wave Velocities in Heterogeneous and Porous Media. *Geophysics*, 21 (1), p. 41-70.

Wyllie, M.R.J., Gregory, A.R. & Gardner, G.H.F. (1958). An Experimental Investigation of Factors Affecting Elastic Wave Velocities in Porous Media. *Geophysics*, 23 (3), p. 459-93.

Worthington, P.E. (1985). The Evolution of Shaly-Sand Concepts in Reservoir Evaluation. *The Log Analyst*, 26 (1), p. 23-40.

Useful websites

The Society of Petrophysical Well Log Analysts (SPWLA)
- General – *www.spwla.org*
- Tool mnemonics – *www.spwla.org/technical/tool-mnemonics*
- Log mnemonics – *www.spwla.org/technical/curve-mnemonics*
- Glossary – *www.fesaus.org/glossary/doku.php*

The London Petrophysical Society
- *www.lps.org.uk*

EXERCISES

Exercise 1 – Gamma Ray

1) Select and mark the shale and clean lines from the GR log.
2) Estimate the fractional volume of shale from this log section.

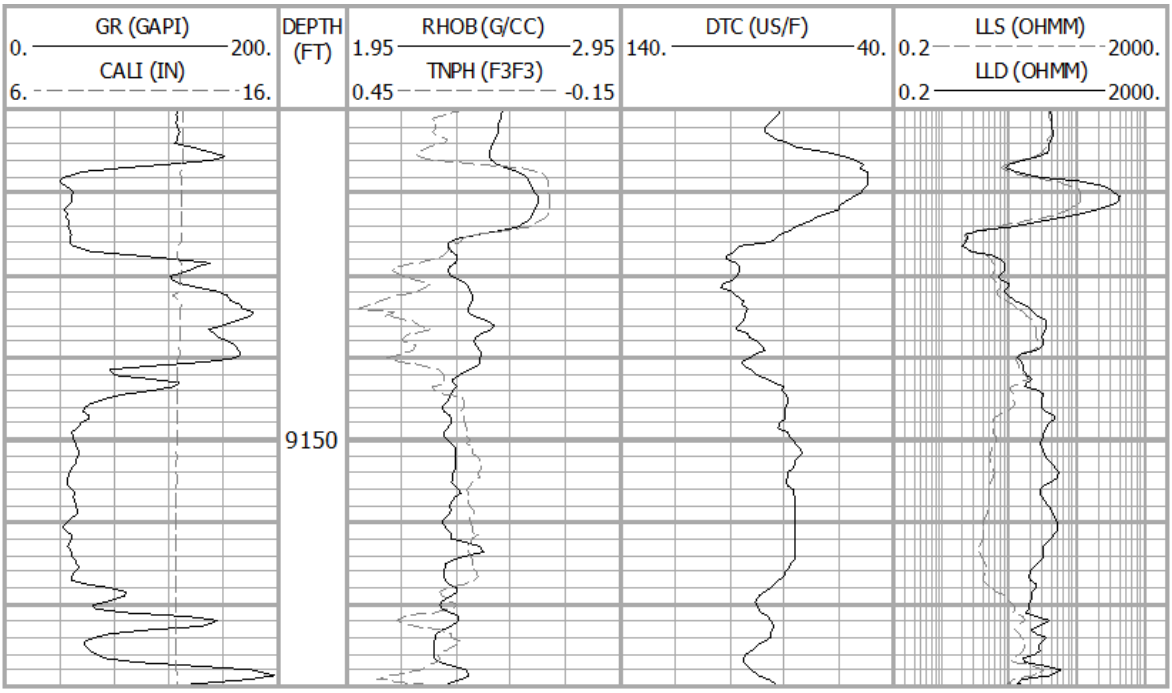

Depth	GR_{log}	GR_{clean}	GR_{shale}	V_{sh}
9120 ft				
9142 ft				
9160 ft				

Exercise 2 – Spontaneous Potential

1) Identify the permeable zones
2) Identify the pore fluids
3) Comment on the nature of the formation water, in terms of contract between R_w and R_{mf}.

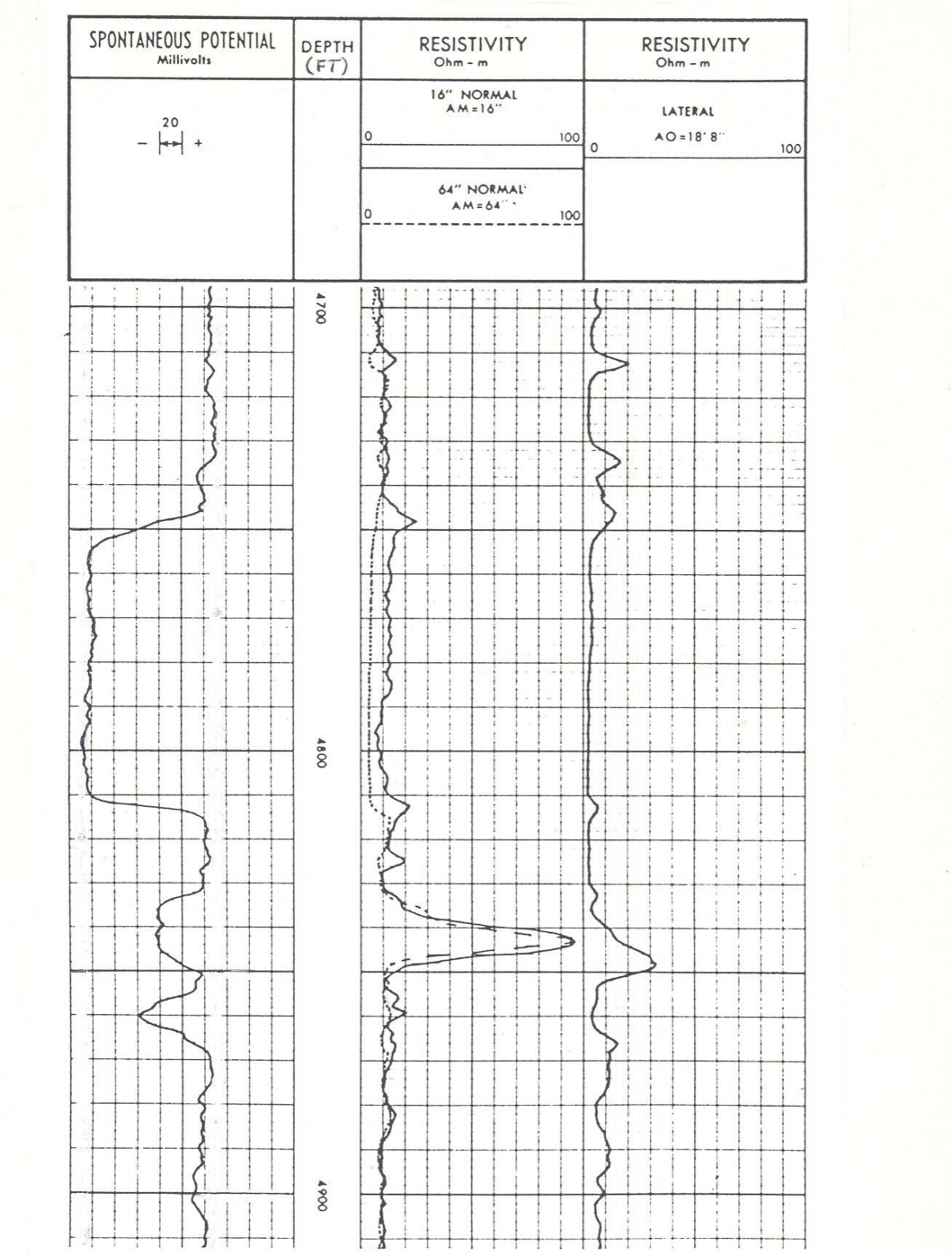

Exercise 3 – Spontaneous Potential

1) Identify the permeable zones
2) Identify the pore fluids
3) Comment on the nature of the formation water, in terms of contract between R_w and R_{mf}.

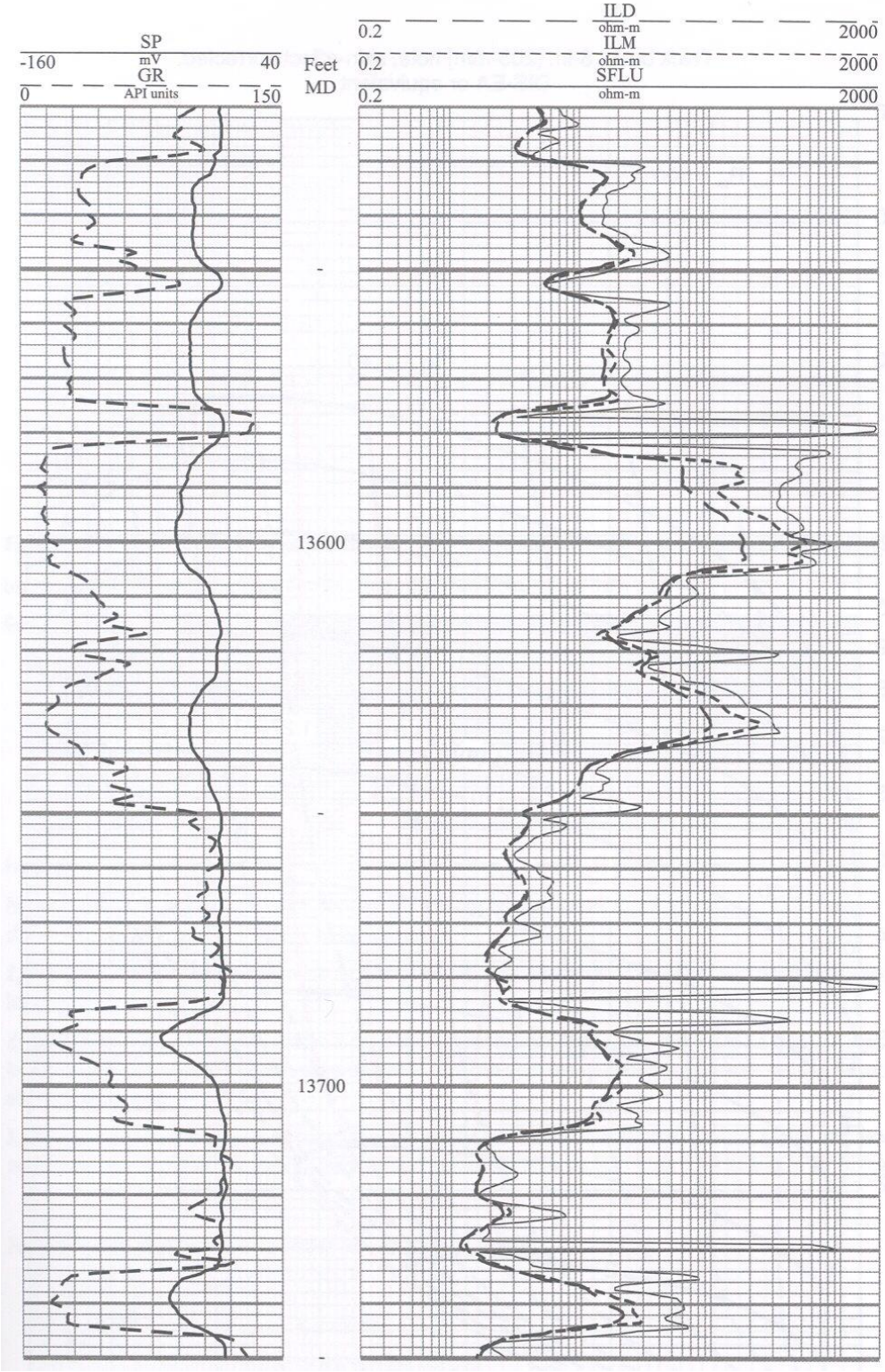

Exercise 4 – Spontaneous Potential

1) Identify the permeable zones
2) Identify the pore fluids
3) Comment on the nature of the formation water, in terms of contract between R_w and R_{mf}.

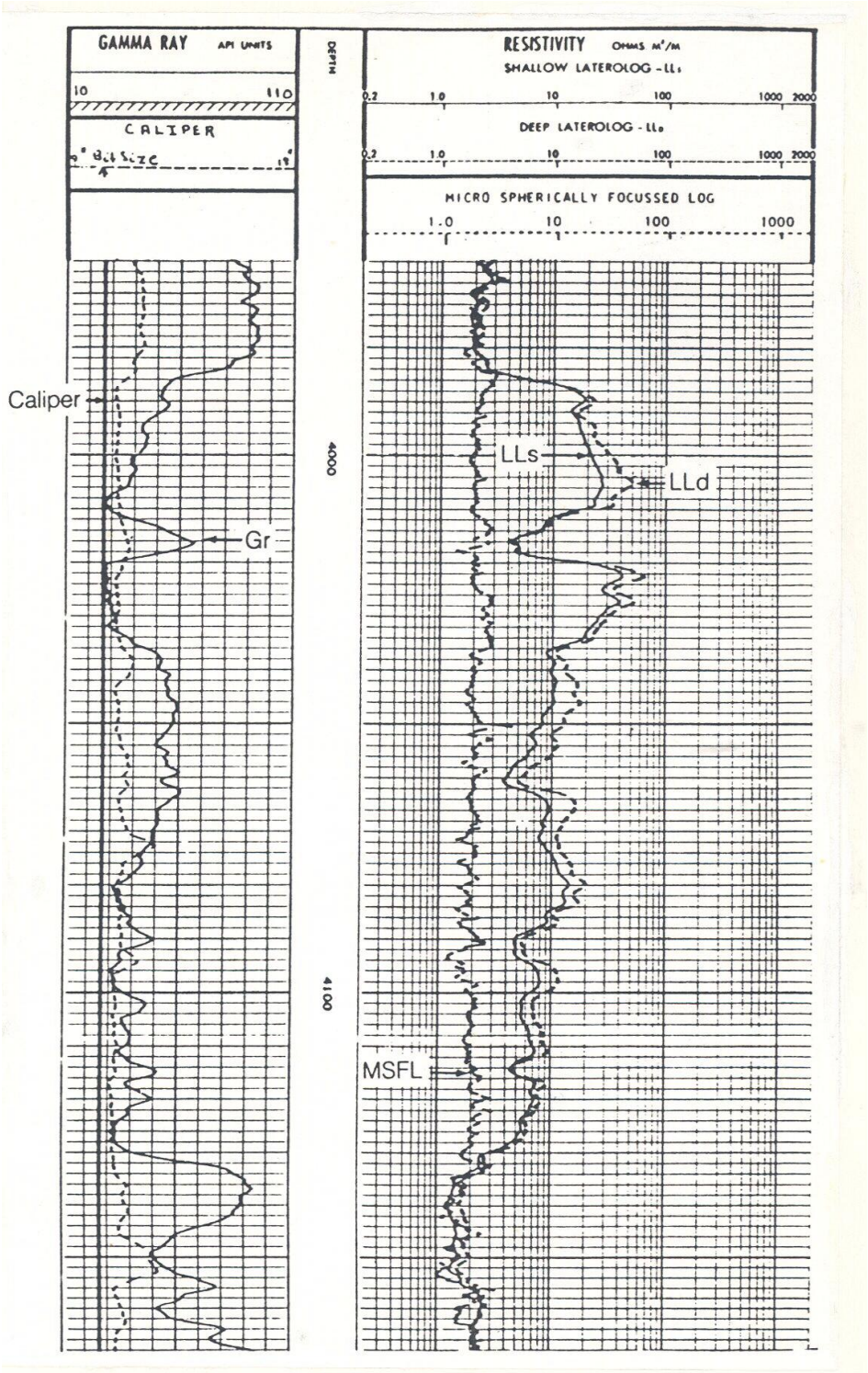

Exercise 5 – Porosity estimation

1) Read the bulk density (RHOB), neutron (TNPH), and sonic (DTC) values from the log suite below, at depths of 9120, 9150, and 9160 ft
2) Assuming that this is from a consolidated sandstone saturated with freshwater, calculate effective porosity using the bulk density, neutron porosity, and sonic logs

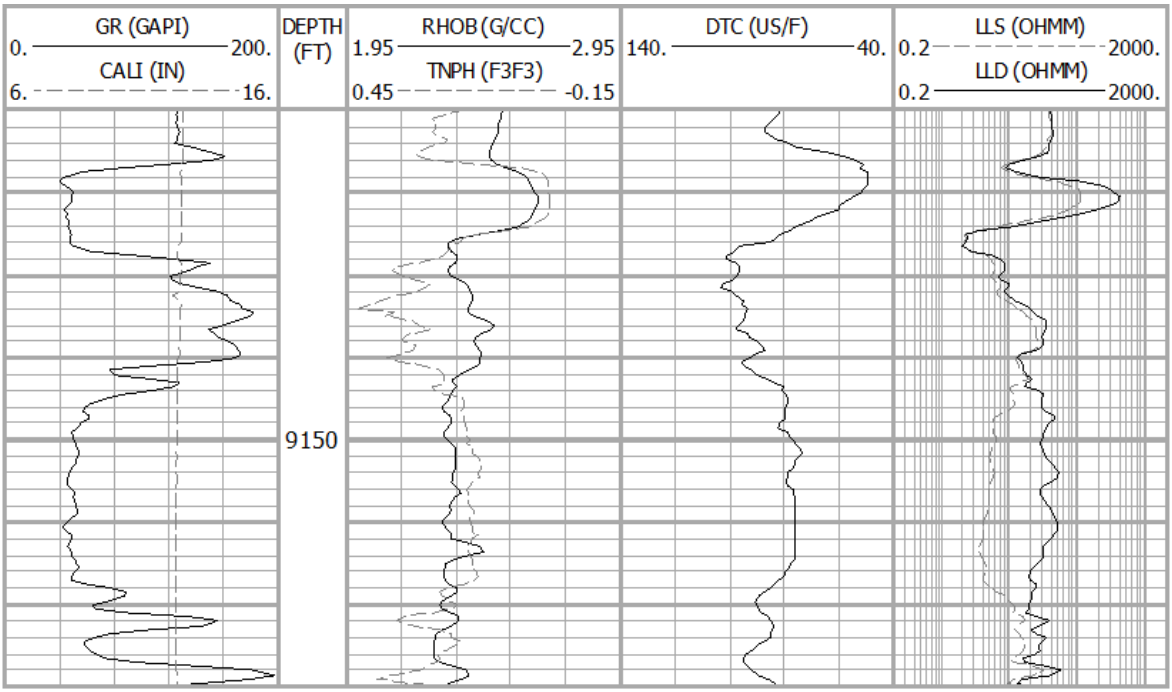

Depth	$RHOB_{log}$	$TNPH_{log}$	DTC_{log}
9120 ft			
9150 ft			
9160 ft			
Matrix value			
Fluid value			

Depth	Ø - Density	Ø - Neutron	Ø - Sonic	Average Ø
9120 ft				
9150 ft				
9160 ft				

Porosity equations;

3) Explain the difference between the three porosity estimates you have calculated.

Exercise 6 – Porosity and Shale Volume from Neutron – Density Crossplots

Determine lithology, porosity, and shale volume for depth intervals 1 – 8

Assume: no hydrocarbons are present, and fluid density is 1.0 g/cm^3

Using the Neutron – Density crossplot provided (take an average reading for each interval to plot).

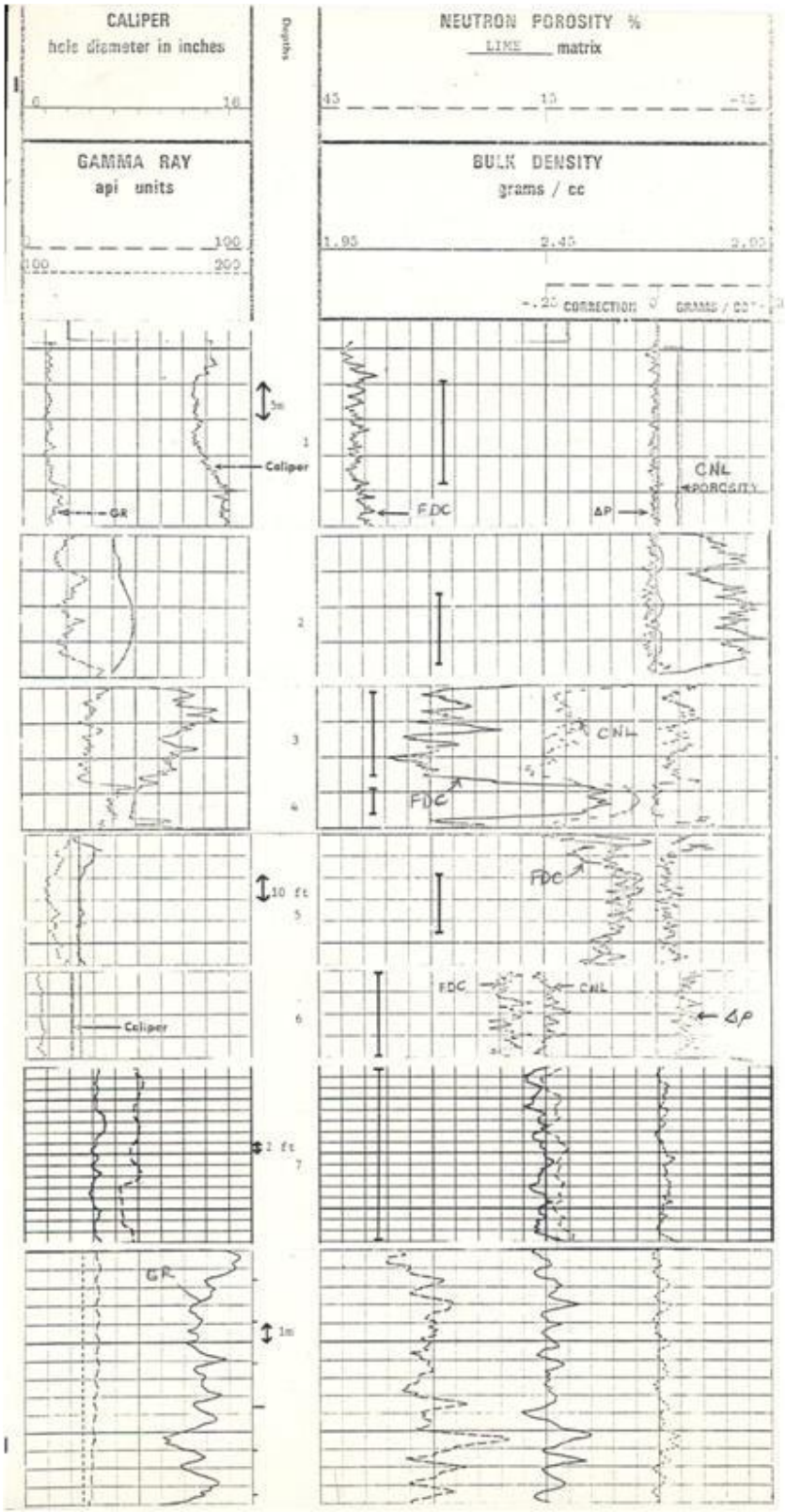

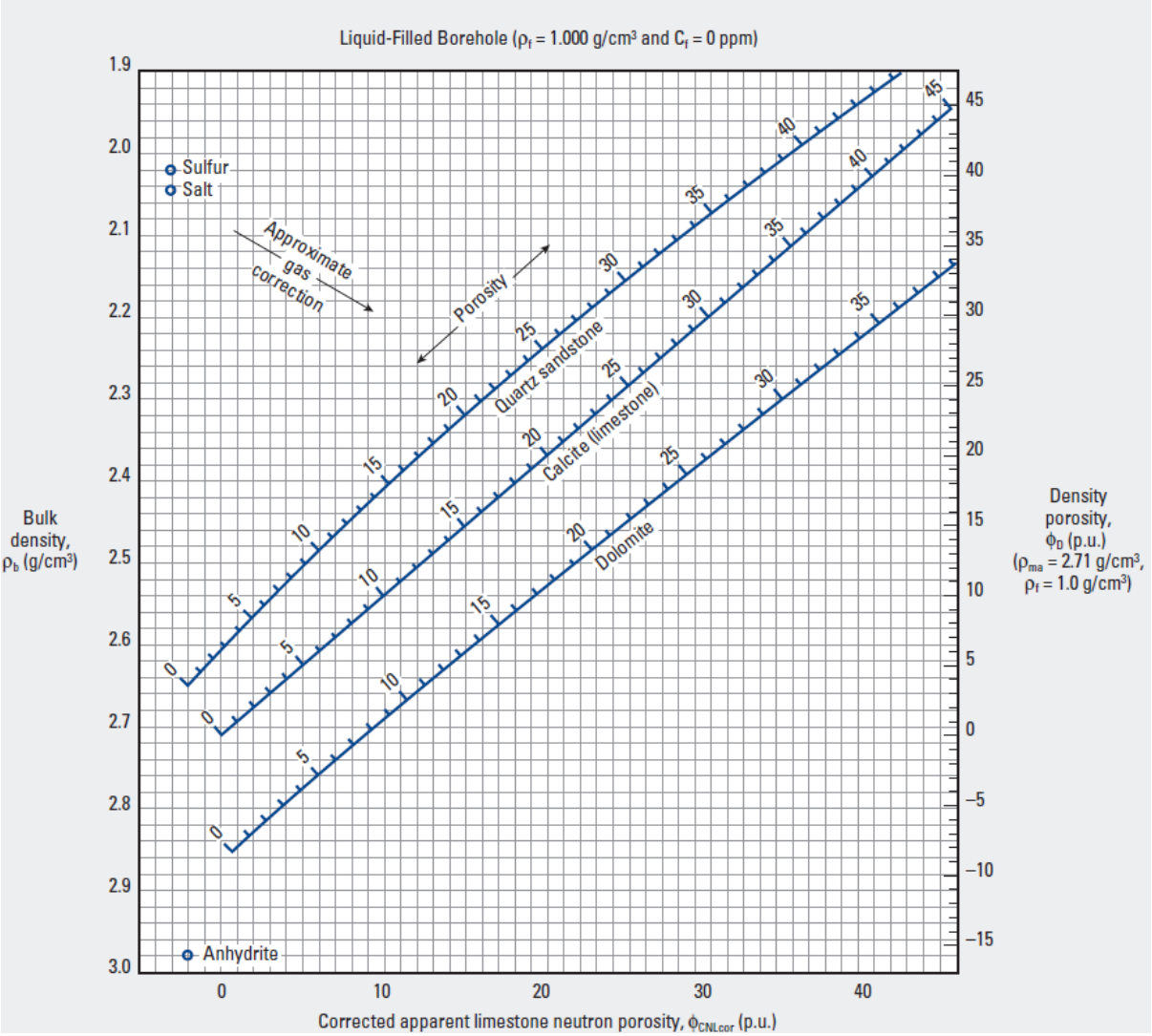
Liquid-Filled Borehole (ρ_f = 1.000 g/cm³ and C_f = 0 ppm)
Sulfur
Salt
Anhydrite
Approximate gas correction
Porosity
Quartz sandstone
Calcite (limestone)
Dolomite
Bulk density, ρ_b (g/cm³)
Density porosity, ϕ_D (p.u.) (ρ_{ma} = 2.71 g/cm³, ρ_f = 1.0 g/cm³)
Corrected apparent limestone neutron porosity, ϕ_{CNLcor} (p.u.)
1.9
2.0
2.1
2.2
2.3
2.4
2.5
2.6
2.7
2.8
2.9
3.0
0
10
20
30
40
45
40
35
30
25
20
15
10
5
0
−5
−10
−15

Exercise 7 – Saturation

1) Enter the relevant porosity values from Exercise 5 into the table below.
2) Record the deep and shallow resistivity readings for the three depths.
3) Calculate Sw and Sxo using the Archie Saturation Equation.
    a. Assume m=n=2 and a=1, Rw = 0.025 ohm.m, Rmf = 0.06 ohm.m
4) Calculate MOS and Sw/Sxo.
5) Comment on your findings.

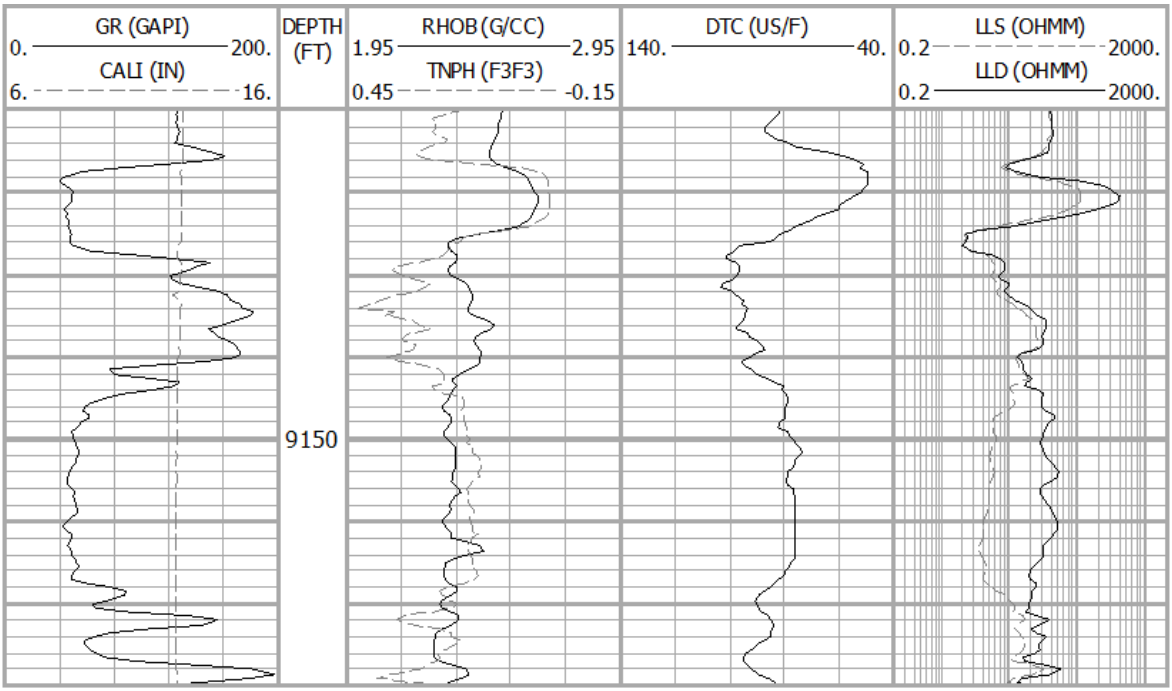

Depth	Average Ø (Exercise 5)	Deep resistivity	Shallow resistivity
9120 ft			
9150 ft			
9160 ft			

Depth	S_w	S_{xo}	MOS	S_w / S_{xo}
9120 ft				
9150 ft				
9160 ft				

Exercise 8 – Estimating Rw and Calculating Sw

1) Identify zone of interest by placing bed boundaries on the log
2) Identify the log curves and indicate what they measure
3) Calculate Rw *(in a water zone, if hydrocarbon is present)*
4) Calculate Sw

Interpretation parameters:

R_m = 0.067 ohm.m @ 67° F
R_{mf} = 0.21 ohm.m @ 65° F
R_{mc}: Not given
BHT: 160° F
Porosity = 21% (core data)
a = 0.81, m=n=2
TD logger: 10,085 ft
Bit size: 8.5in

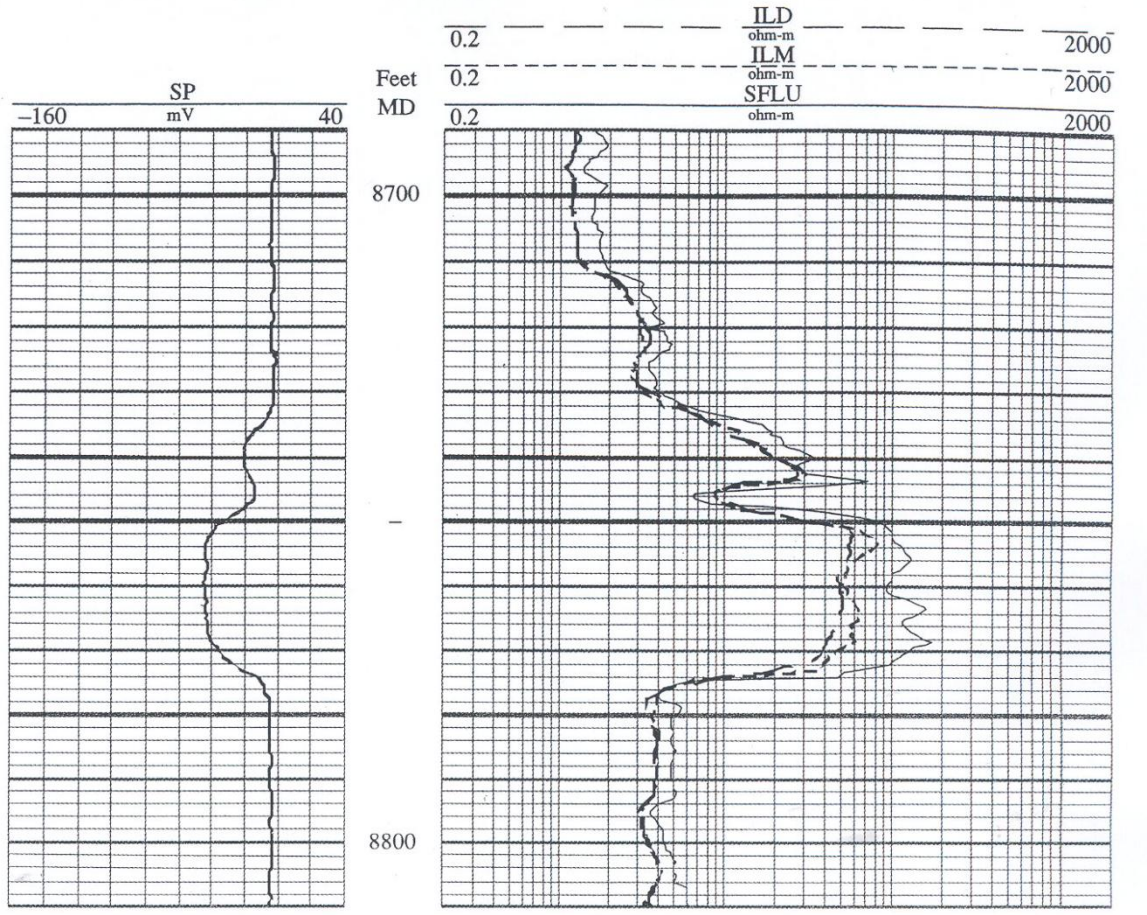

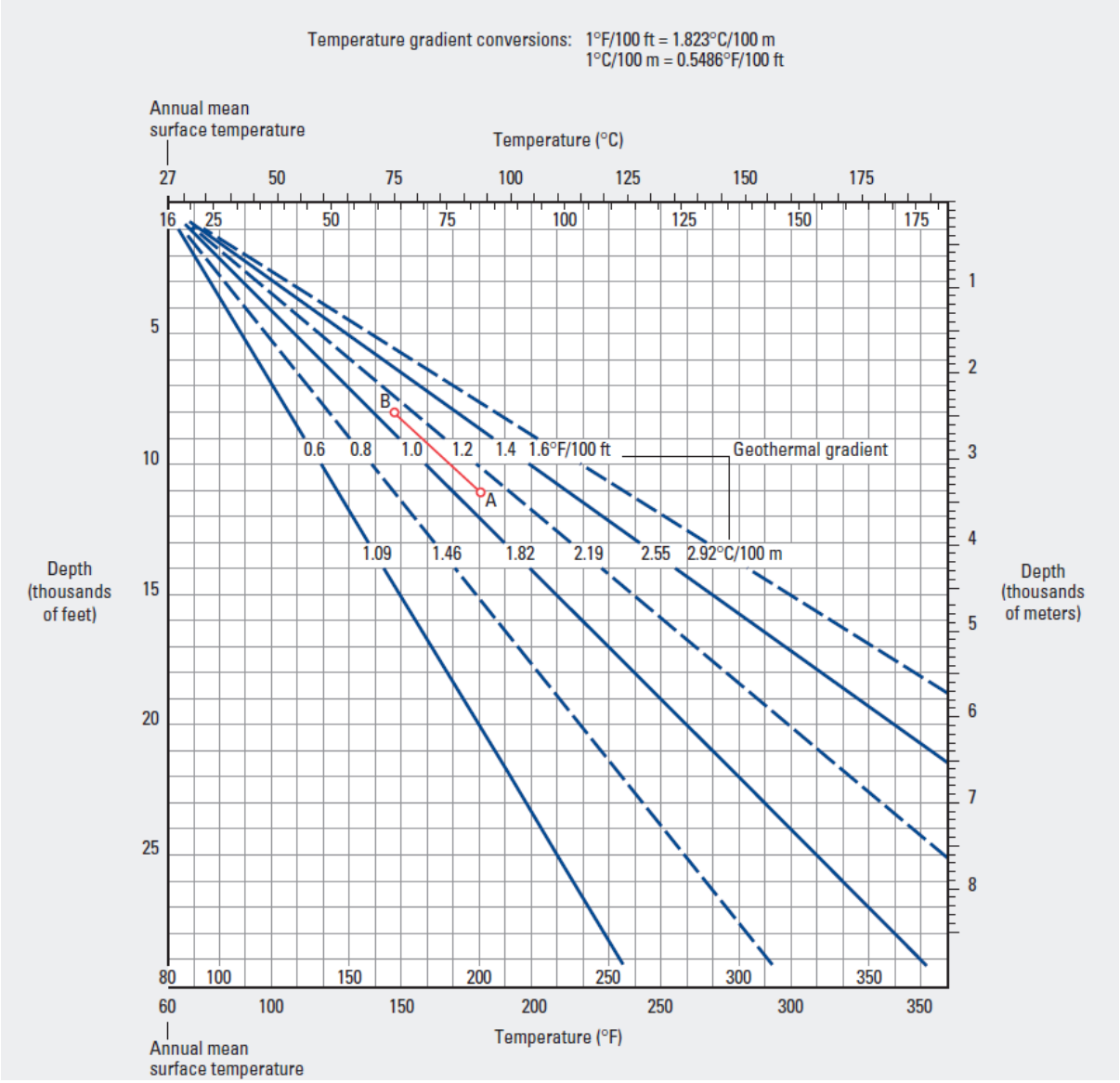

Schlumberger Chart Gen-2

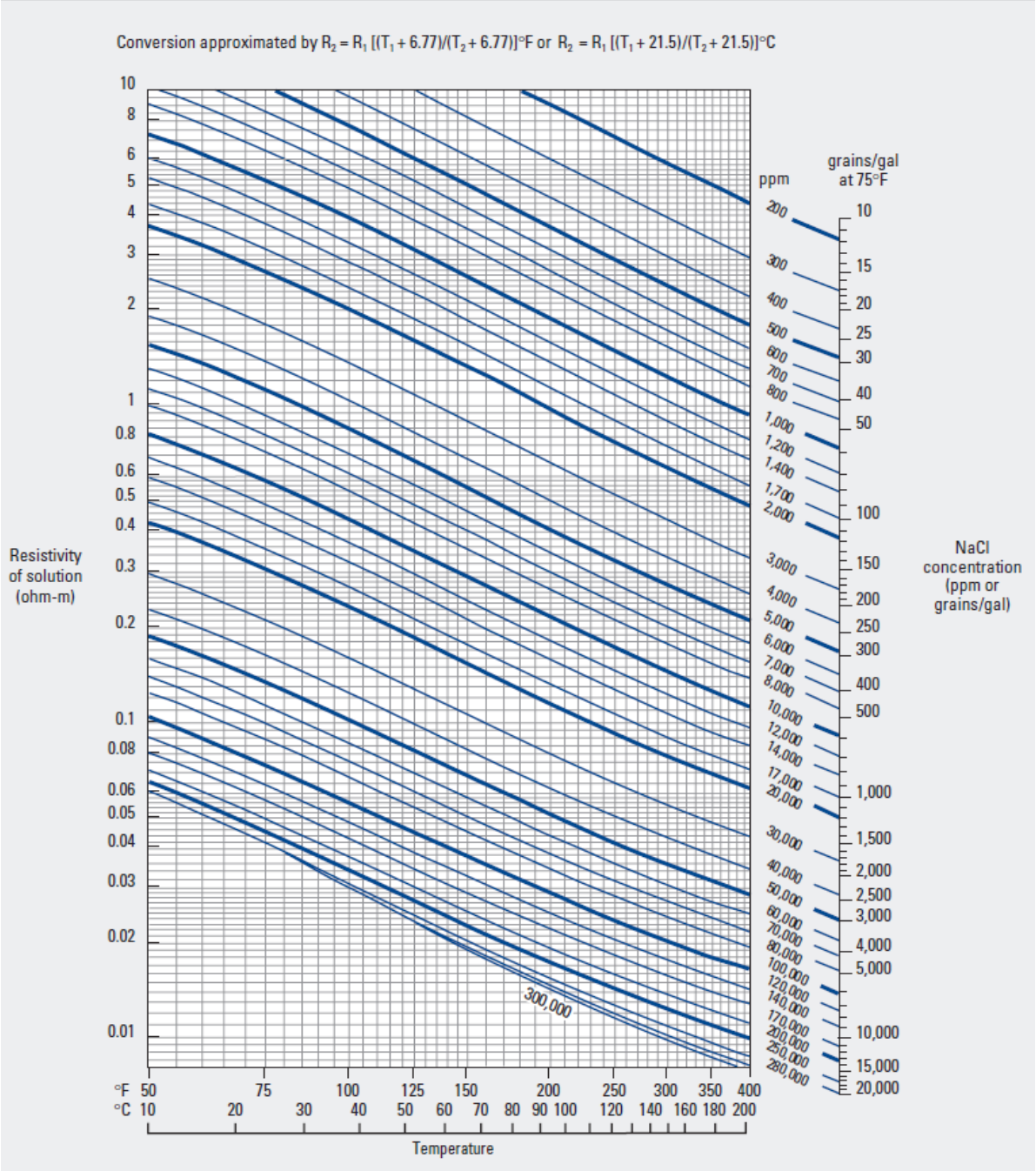

Schlumberger Chart Gen-6

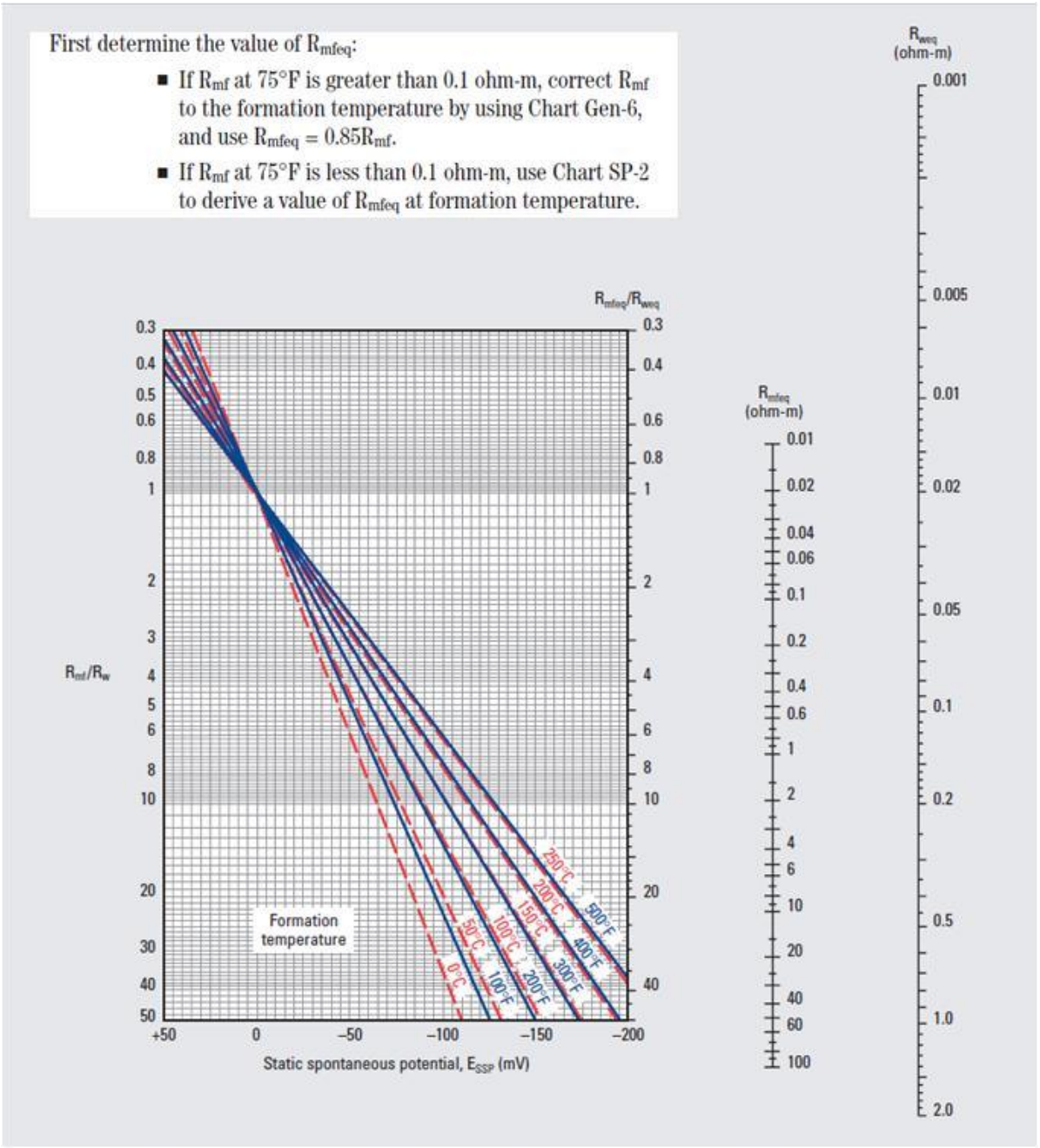

Schlumberger Chart SP-1

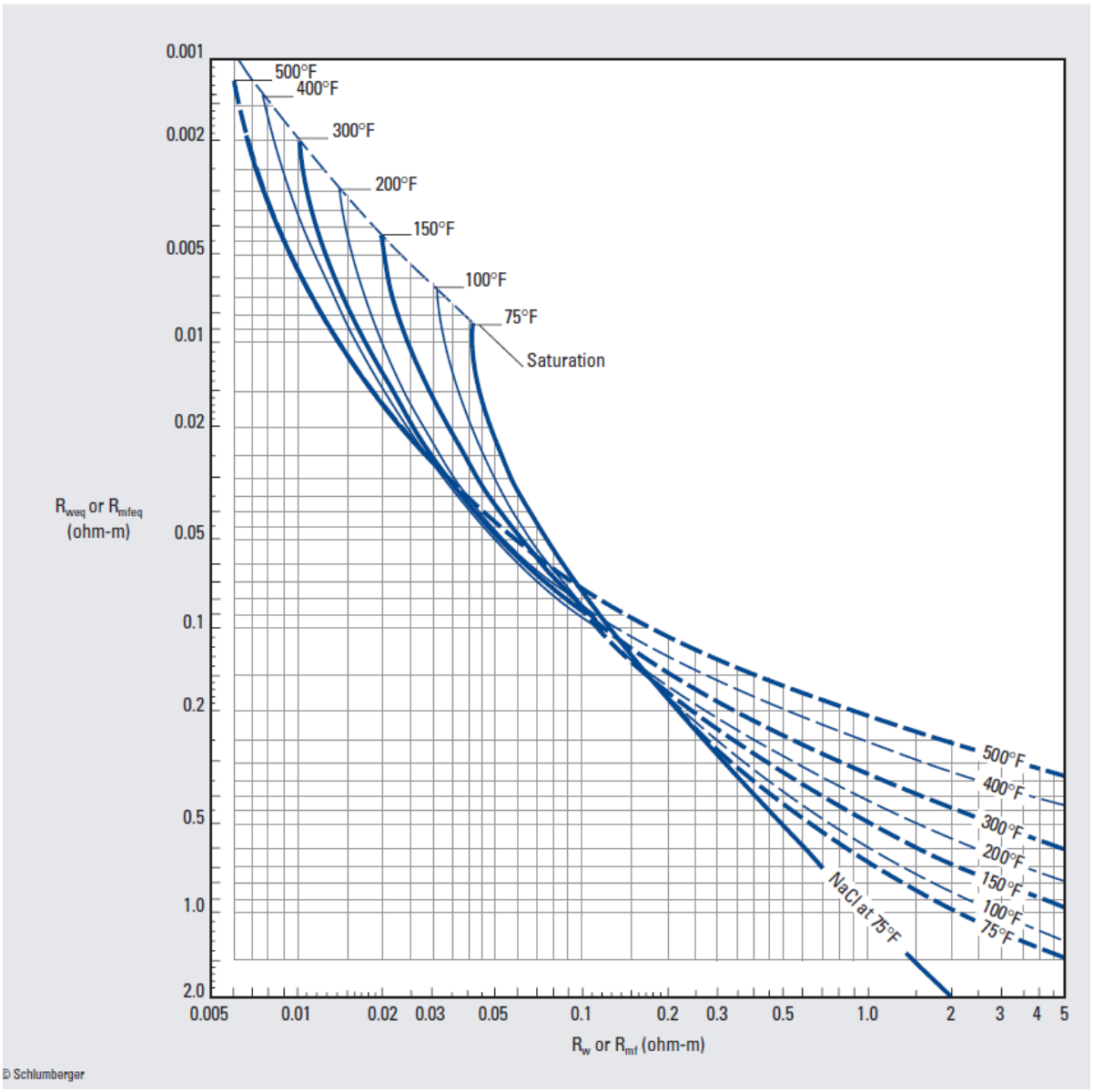

Schlumberger Chart SP-2

Exercise 9 – Full Wireline Log Analysis

Examine the accompanying suite of logs:

A. Qualitative Interpretation

1) Identify permeable zone(s)
2) Identify the lithology of the permeable zone(s)
3) Identify the pore fluid(s)
4) Can you identify any fluid contacts? If so mark them on the logs
5) Are the log readings reliable?

B. Quantitative Interpretation

6) Evaluate the section for shale volume, porosity, water and hydrocarbon saturation
7) Comment on production capability

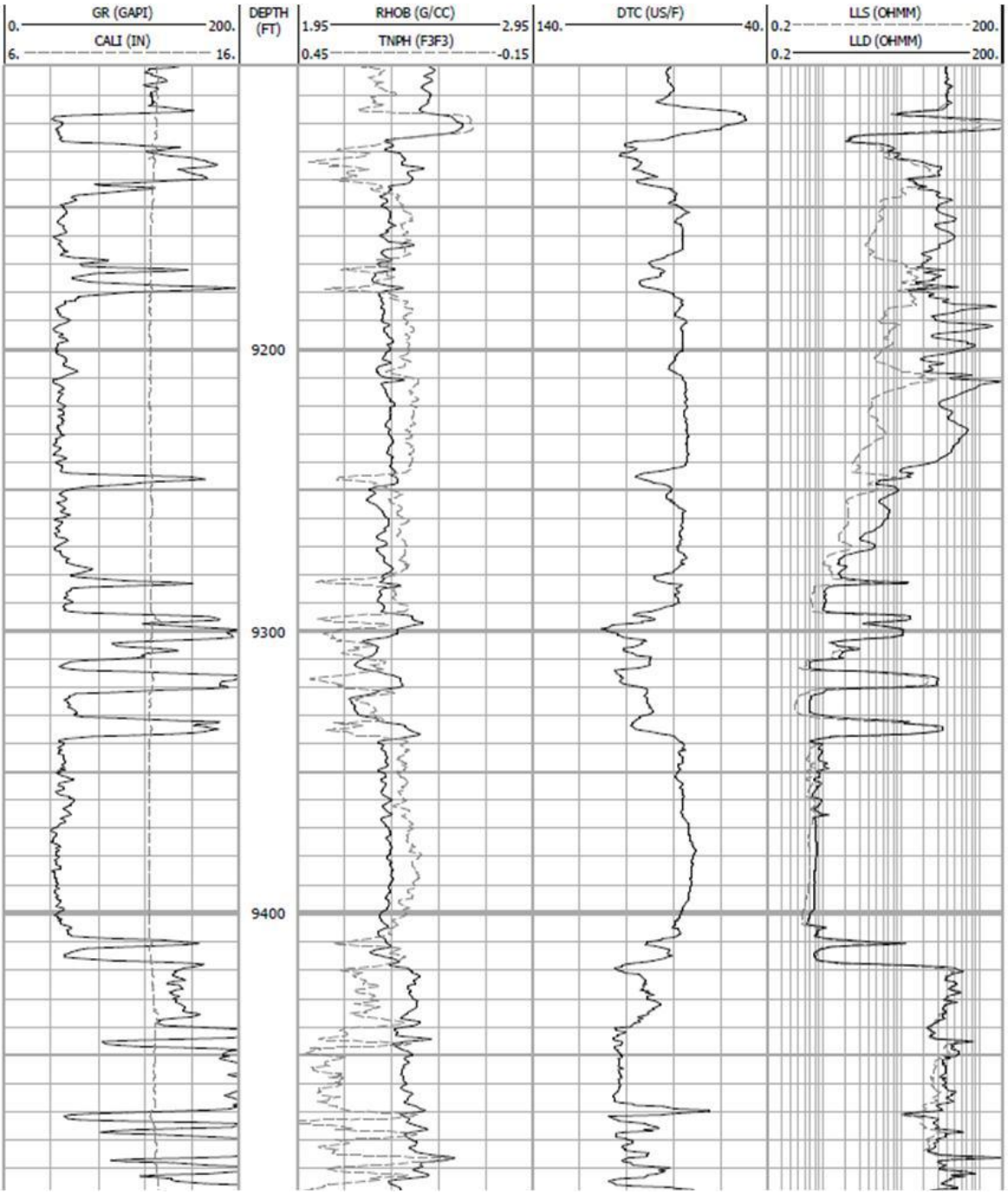

Interpretation parameters:

R_w = 0.045 ohm.m at 195 ^oF

R_{mf} = 0.045 ohm.m at 54 ^oF

Datum temperature = 195 ^oF at 9200 ft

a = 1, m = 1.7, n = 1.9

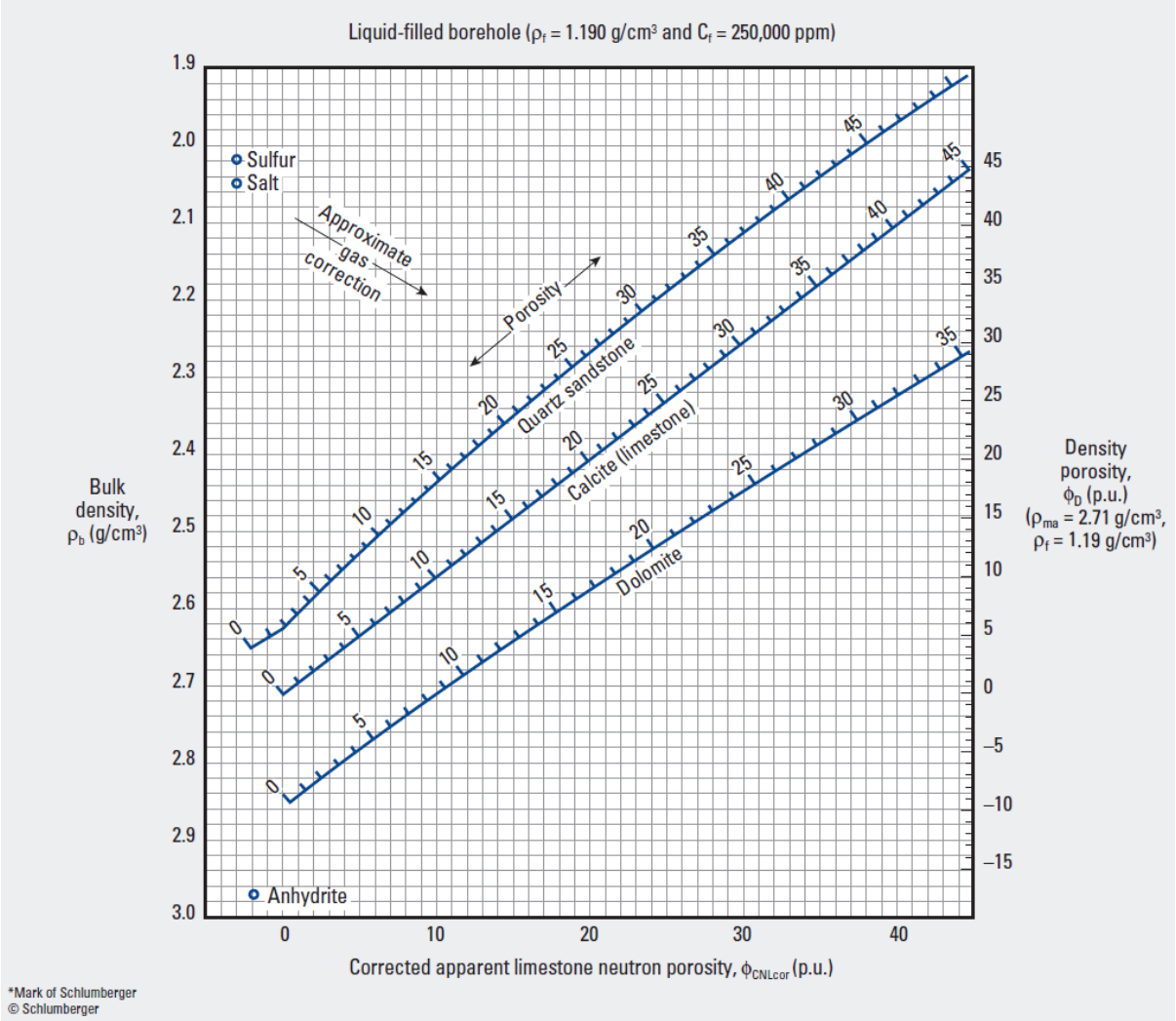
Liquid-filled borehole (ρ_f = 1.190 g/cm³ and C_f = 250,000 ppm)
Sulfur
Salt
Approximate gas correction
Porosity
Quartz sandstone
Calcite (limestone)
Dolomite
Anhydrite
Bulk density, ρ_b (g/cm³)
Density porosity, ϕ_D (p.u.) (ρ_{ma} = 2.71 g/cm³, ρ_f = 1.19 g/cm³)
Corrected apparent limestone neutron porosity, ϕ_{CNLcor} (p.u.)
*Mark of Schlumberger
© Schlumberger

Exercise 10 – Full Wireline Log Analysis 2: Wytch Farm well K-01

Examine the accompanying suite of logs:

A. Qualitative Interpretation

1) Identify permeable zone(s)
    a. Comment on the GR log, remember your observations of the Sherwood Sandstone from the Wessex Basin Field trip...
2) Identify the lithology of the permeable zone(s)
3) Identify the pore fluid(s)
4) Can you identify any fluid contacts? If so mark them on the logs
5) Are the log readings reliable?

B. Quantitative Interpretation

6) Evaluate the section for shale volume, porosity, water and hydrocarbon saturation
7) Can you comment on production capability?

You will be using the data from this well again as part of the Wytch Farm Field Development Project.

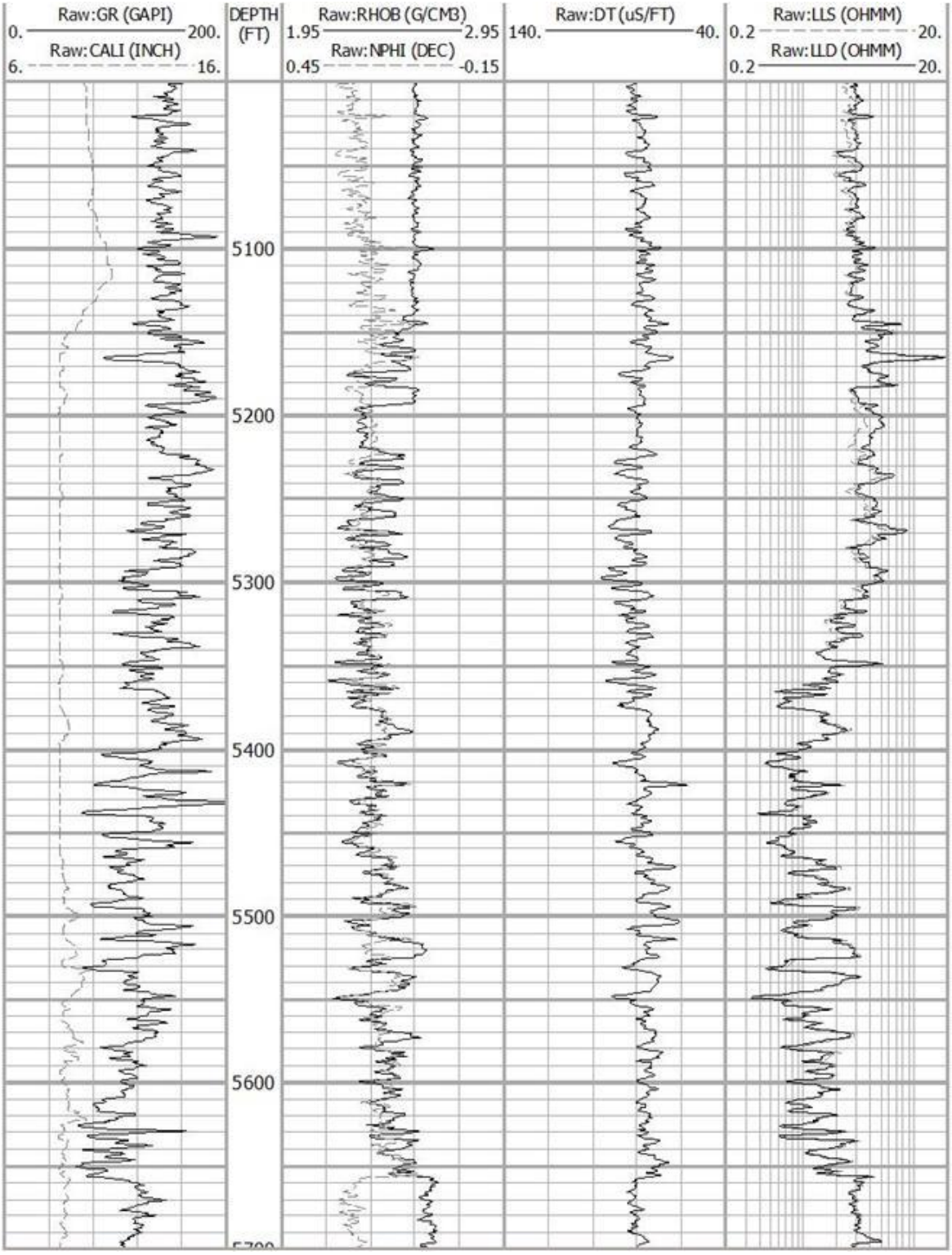

Interpretation parameters:

R_w = 0.025 ohm.m at 150 ^oF

R_{mf} = 0.06 ohm.m at 64.8 ^oF

Datum temperature = 150 ^oF at 5200 ft

a = 0.91, m = 1.8, n = 2

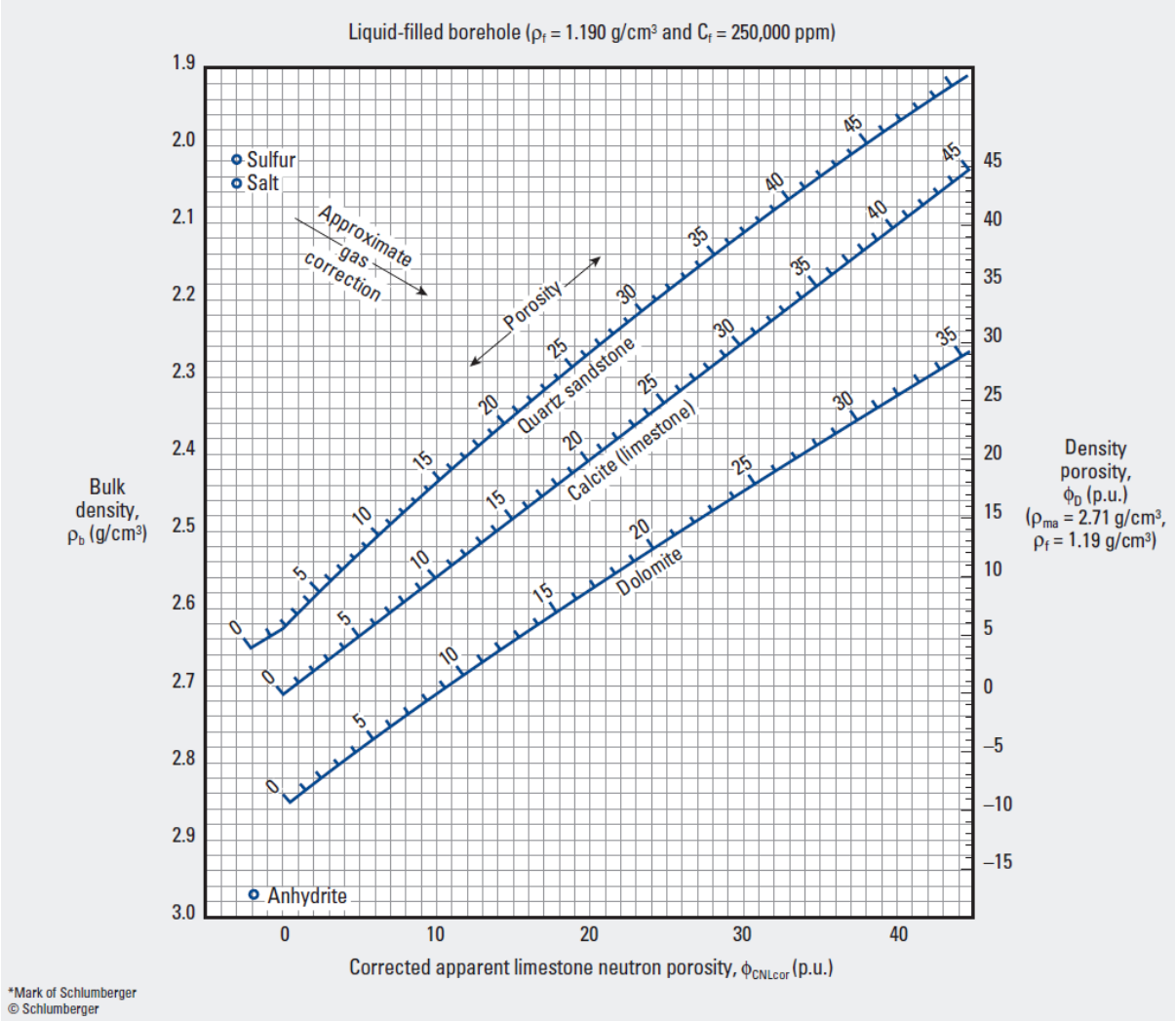
Liquid-filled borehole (ρ_f = 1.190 g/cm³ and C_f = 250,000 ppm)
Sulfur
Salt
Approximate gas correction
Porosity
Quartz sandstone
Calcite (limestone)
Dolomite
Anhydrite
Bulk density, ρ_b (g/cm³)
Density porosity, ϕ_D (p.u.) (ρ_{ma} = 2.71 g/cm³, ρ_f = 1.19 g/cm³)
Corrected apparent limestone neutron porosity, ϕ_{CNLcor} (p.u.)
*Mark of Schlumberger
© Schlumberger

Exercise 11 – Full Wireline Log Analysis: Example Exam Question (2010)

Examine the accompanying suite of logs:

(i) Identify the permeable zone(s)

(ii) Identify the pore fluids

(iii) Can you identify any fluid contacts?

(iv) Can you identify the lithology of the permeable zones with confidence?

(v) Could the GR log be relied on for this purpose?

(vi) The lithology of which zones can you identify with confidence?

(vii) Evaluate the section for porosity, hydrocarbon saturation and production capability.

Interpretation parameters:

Bit size: 8.5 in. Drilling fluid: water based mud Rmf = 0.074 at 67º F

From formation water analysis: Rw = 0.11 at 67º F BHT = 210º F at 3,524m

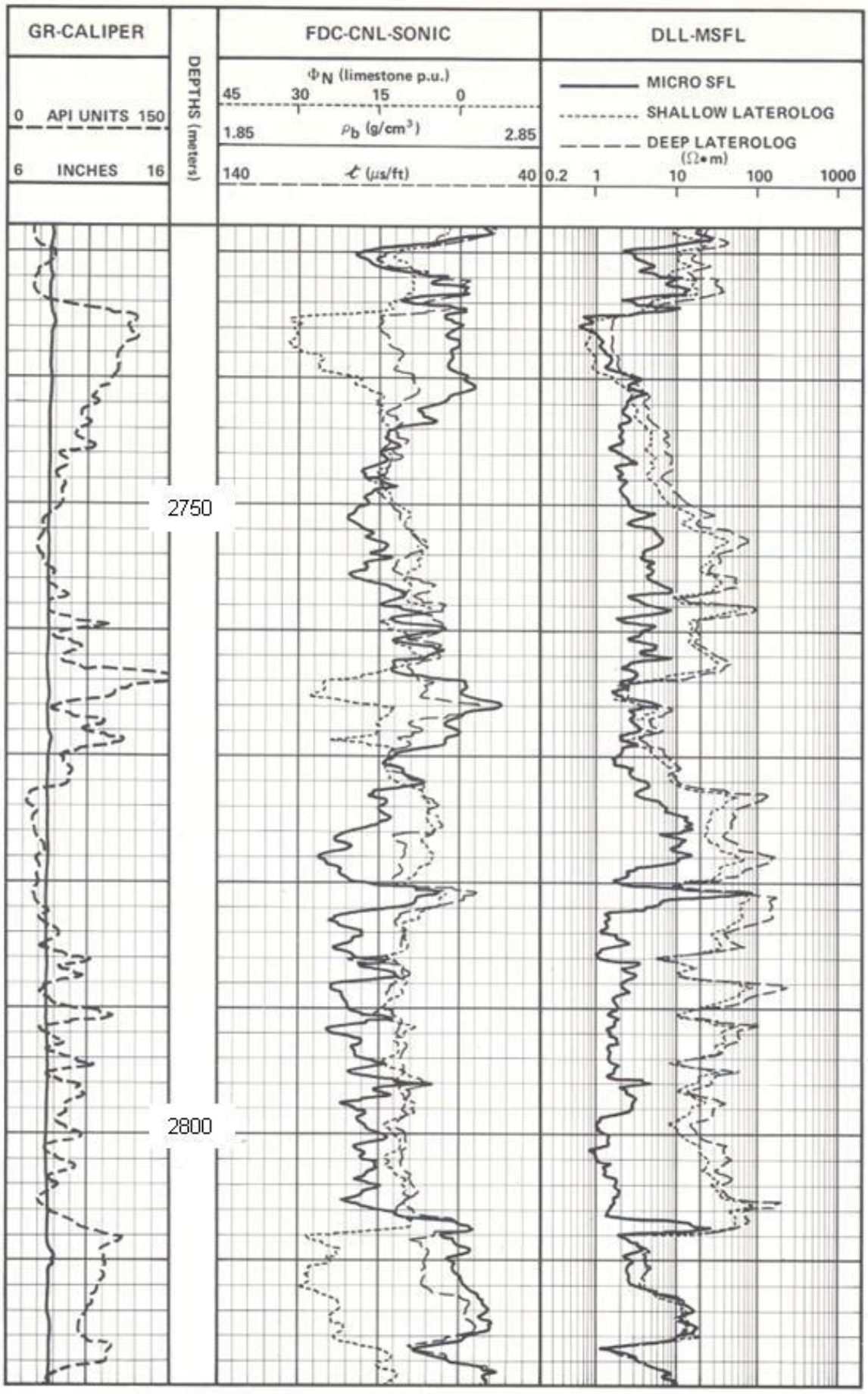
GR-CALIPER
0 API UNITS 150
6 INCHES 16
DEPTHS (meters)
FDC-CNL-SONIC
Φ_N (limestone p.u.)
45 30 15 0
1.85 ρ_b (g/cm^3) 2.85
140 t (μs/ft) 40
DLL-MSFL
MICRO SFL
SHALLOW LATEROLOG
DEEP LATEROLOG
(Ω•m)
0.2 1 10 100 1000
2750
2800

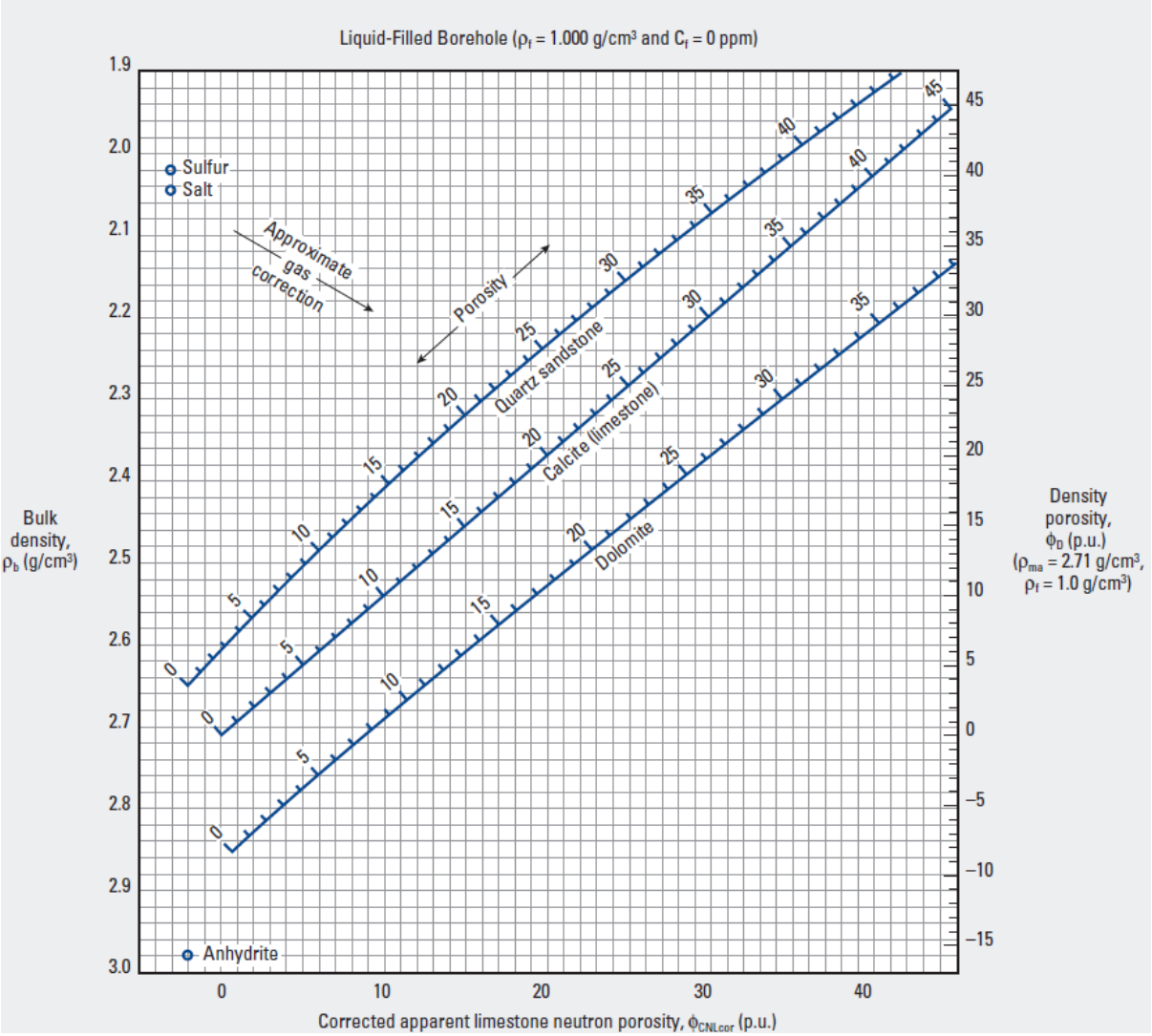
Liquid-Filled Borehole (ρ_f = 1.000 g/cm³ and C_f = 0 ppm)
Sulfur
Salt
Anhydrite
Approximate gas correction
Porosity
Quartz sandstone
Calcite (limestone)
Dolomite
Bulk density, ρ_b (g/cm³)
Density porosity, ϕ_D (p.u.) (ρ_{ma} = 2.71 g/cm³, ρ_f = 1.0 g/cm³)
Corrected apparent limestone neutron porosity, ϕ_{CNLcor} (p.u.)
1.9
2.0
2.1
2.2
2.3
2.4
2.5
2.6
2.7
2.8
2.9
3.0
0
10
20
30
40
45
40
35
30
25
20
15
10
5
0
−5
−10
−15

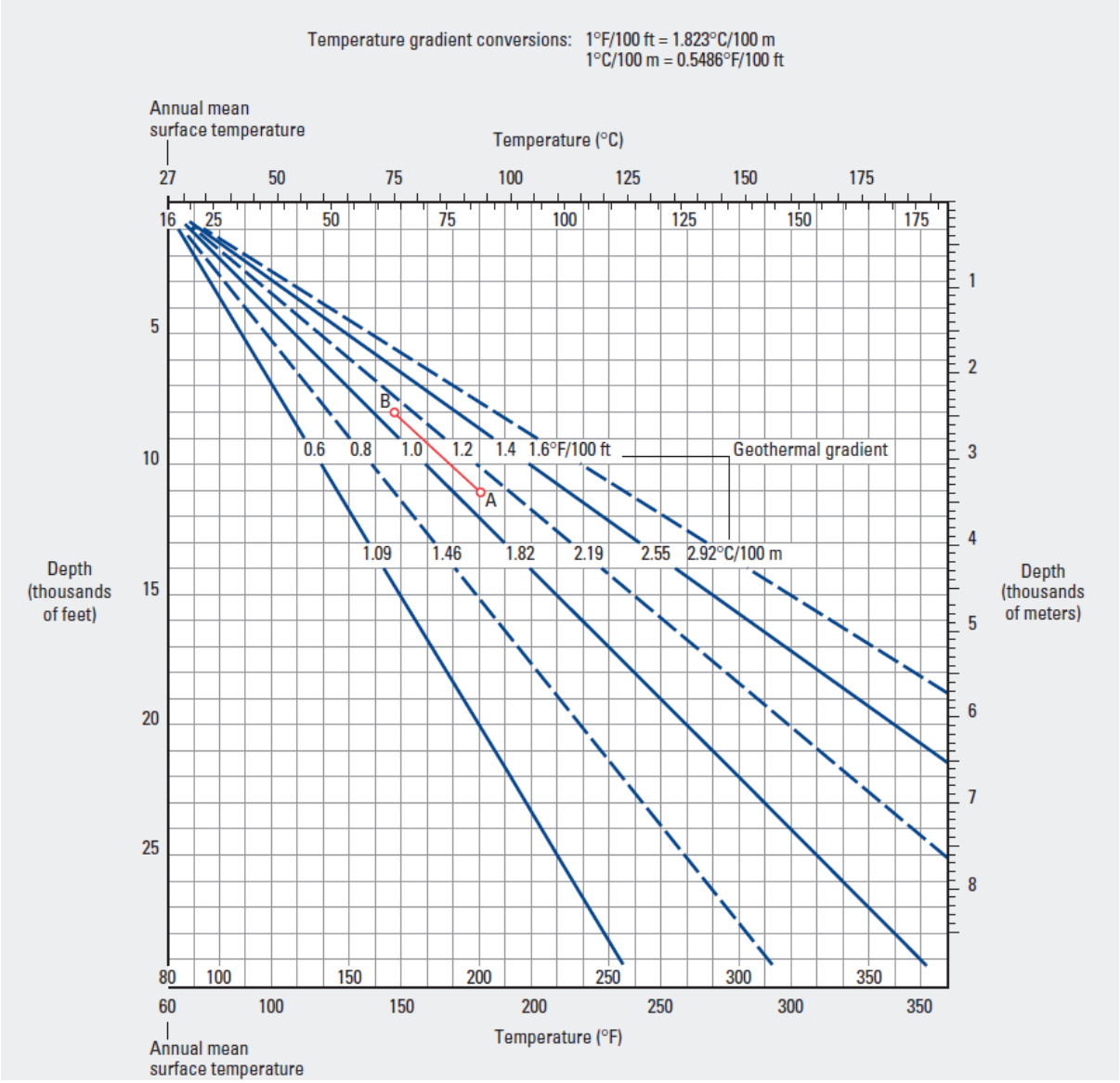

Schlumberger Chart Gen-2

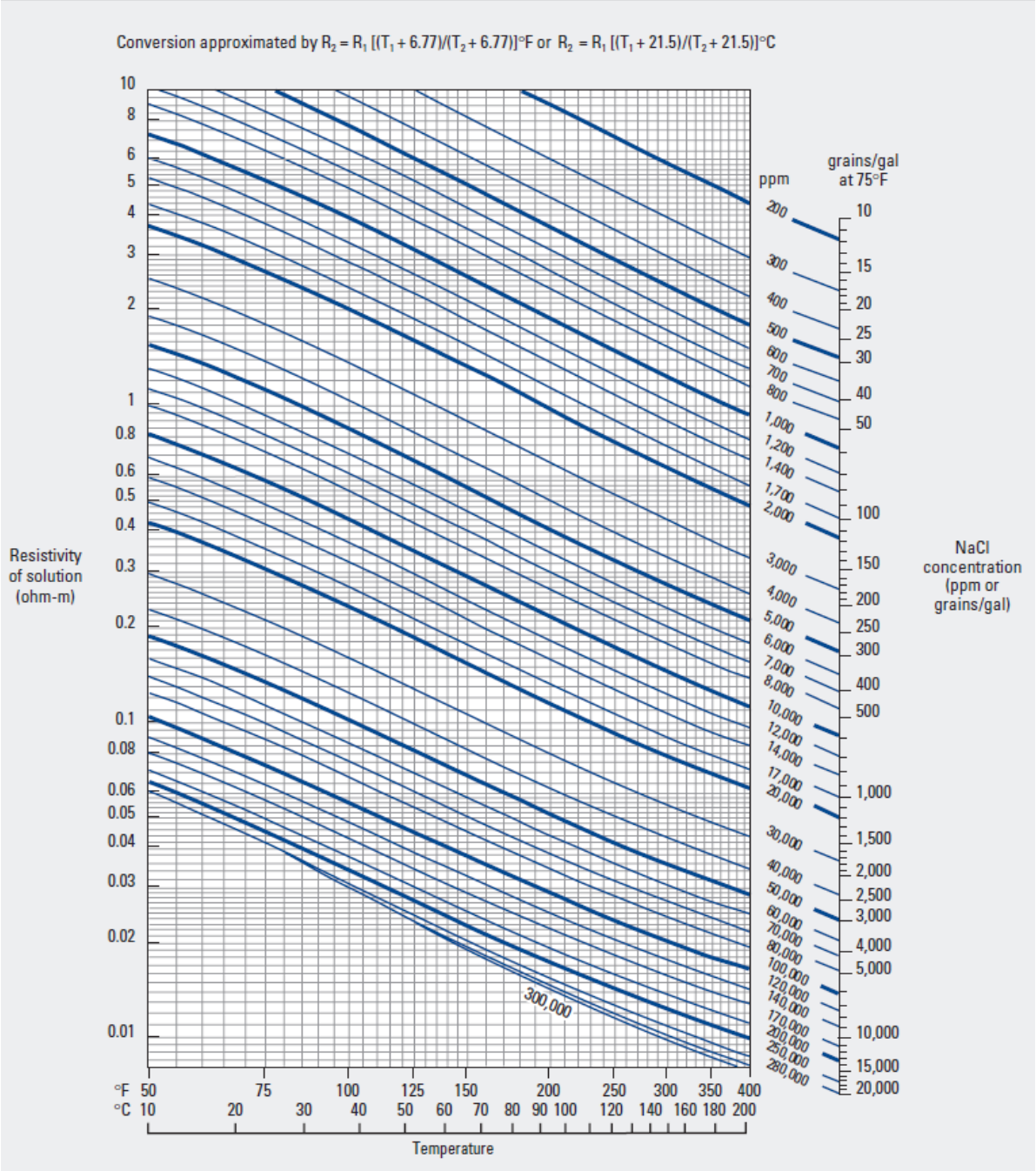

Schlumberger Chart Gen-6